arXiv:cond-mat/9912470v1 [cond-mat.soft] 29 Dec 1999

Stability of Bose-Einstein Condensates Confined in Traps

TAKEYA TSURUMI, HIROFUMI MORISE and MIKI WADATI

Department of Physics, Graduate School of Science, University of Tokyo, Hongo 7-3-1, Bunkyo-ku, Tokyo 113-0033, Japan

Abstract

Bose-Einstein condensation has been realized in dilute atomic vapors. This achievement has generated immerse interest in this field. Presented is a review of recent theoretical research into the properties of trapped dilute-gas Bose-Einstein condensates. Among them, stability of Bose-Einstein condensates confined in traps is mainly discussed. Static properties of the ground state are investigated by use of the variational method. The anlysis is extended to the stability of two-component condensates. Time-development of the condensate is well-described by the Gross-Pitaevskii equation which is known in nonlinear physics as the nonlinear Schrödinger equation. For the case that the inter-atomic potential is effectively attractive, a singularity of the solution emerges in a finite time. This phenomenon which we call collapse explains the upper bound for the number of atoms in such condensates under traps.

Contents

1 Introduction **4**

2 Ginzburg-Pitaevskii-Gross Equation **7**
2.1 Time-independent case 7
2.2 Time-dependent case 11

3 Static Properties of Bose-Einstein Condensates **13**
3.1 Ground state of a Bose-Einstein condensate under axially symmetric magnetic trap 14
3.1.1 Formulation 14
3.1.2 Repulsive case 16
3.1.3 Attractive case 20
3.2 Stability of a two-component Bose-Einstein condensate 24
3.2.1 Formulation 24
3.2.2 $N_1 = N_2$ case 25
3.2.3 Phase diagrams 26
3.2.4 Phase separation 32
3.3 Long-range interacting bosons confined in traps 33
3.3.1 Stability of the ground state 34
3.3.2 Charged bosons confined in ion traps 35
3.4 Summary 36

4 Dynamical Properties of Bose-Einstein Condensates **39**
4.1 Stability of the D-dimensional nonlinear Schrödinger equation under confined potential 39
4.1.1 Repulsive case 40
4.1.2 Attractive case 41
4.2 Collapse of the condensate 48
4.2.1 Time-evolution of the condensate 48
4.2.2 Application to ^{7}Li system 52
4.3 Summary 54

5 Summary and Concluding Remarks **56**

A Bose-Einstein Condensation of a Free Boson Gas Confined in Harmonic Potentials **58**

B Pseudopotential **61**

C The Ground State Energy under the Thomas-Fermi Approximations **65**

Bibliography **68**

Chapter 1

Introduction

The Bose-Einstein condensation (BEC) [1]–[4] is one of the most remarkable phenomena in quantum many-body systems. The condensation is a logical consequence of the Bose-Einstein statistics: a gas of non-interacting bosonic atoms, below a certain temperature, suddenly develops a macroscopic population in the lowest energy quantum mechanical state. However, BEC occurs at such low temperature that the dimensionless phase-space density, $\rho_{\rm ps} \equiv n(\lambda_{\rm db})^3$, is larger than 2.612, where n is the number density of atoms, and $\lambda_{\rm db}$ is the thermal de Broglie wavelength, $\lambda_{\rm db} = h/(2\pi m k_{\rm B} T)^{1/2}$, with h Planck's constant, m the mass of the atom, $k_{\rm B}$ Boltzmann's constant and T the temperature, respectively (see, for instance, [5] as a text book). Accordingly, for many years, BEC had been regarded as a mathematical artifact: In December 1924, Einstein wrote to P. Ehrenfest, 'From a certain temperature on, the molecules "condense" without attractive forces, that is, they accumulate at zero velocity. The theory is pretty, but is there also some truth to it?' [6]. Keesom observed in 1928 the phase transition between He-I (the nomal fluid phase) and He-II (the superfluid phase) in liquid helium, ^{4}He [7]. F. London interpreted this phenomenon as BEC in 1938 [8]. In liquid helium, however, the nature of the BEC transition is difficult to observe clearly because of strong inter-atomic interactions. There exists a non-negligible difference between the observed transition temperature $T_\lambda = 2.18$K and the estimated transition temperature $T_{\rm c} = 3.14$K by an ideal gas approximation. In 1993, the evidence of BEC in a gas of excitons in a semi-conductor host has been observed [9]. Although the interactions in these systems are weak, little information about them is known, and thus it is difficult to understand the net effect of BEC in the exciton gas. In 1970's, efforts started to observe BEC in a dilute vapor of spin-polarized hydrogen [4], whose inter-atomic interaction is sufficiently weak and well understood. However, BEC in the hydrogen gas was not achieved for a long time, because of the existence of inelastic inter-atomic collisions, which cause trap loss and heating.

Recently, combinations of various new technologies developed in atomic physics such as laser cooling and trapping [10], evaporation cooling and magnetic trap have made it possible to increase the phase-space density of a vapor of alkali atoms, and to observe BEC of such atoms in controllable situations. In 1995, BEC was observed in a series of experiments on vapors of ^{87}Rb [11], ^{7}Li [12, 13] and ^{23}Na [14] in which the atoms

were confined in magnetic traps and cooled down to extremely low temperature of the order of $10^{-6} \sim 10^{-7}$K (Table 1.1) [15]–[19]. Rigorously speaking, for an ideal gas of

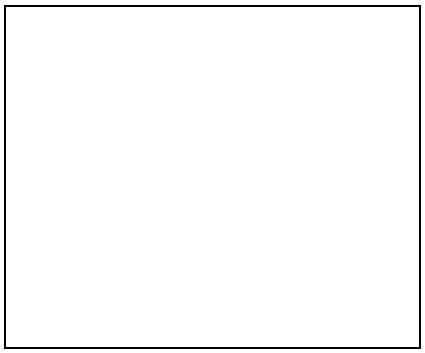

Table 1.1: Experimental values of parameters. a; s-wave scattering length, $T_{\rm c}$; critical temperature, $N_{\rm t}$; the total number of atoms in trap, ω; trap frequency. Note that the total number of the atoms is the sum of normal and condensed ones. The values of $T_{\rm c}$, $N_{\rm t}$ and ω are taken from the reference in the right most column.

N bosonic atoms in a harmonic potential, the condition $n(\lambda_{\rm db})^3 > 2.612$ is replaced by $N(\hbar\bar{\omega})^3/(k_{\rm B}T)^3 > 1.202$ where $\bar{\omega} \equiv (\omega_x\omega_y\omega_z)^{1/3}$ is the geometric mean of the harmonic trap frequencies (Appendix A). In 1998, BEC of spin-polarized hydrogen atoms was finally observed [20]. Now, more than twenty groups have succeeded in observing BEC [21]–[24].

The experimental realization of BEC of alkali-atoms has stimulated experimental and theoretical research in their physical properties. One of the advantages using confined atomic vapors is the various choices of atomic systems. The low energy properties are characterized by the s-wave scattering length a. While ^{87}Rb, ^{23}Na and ^{1}H atoms have positive s-wave scattering lengths [25]–[28], it is known that ^{7}Li and ^{85}Rb atoms have negative s-wave scattering lengths, corresponding to low-energy attractive interactions [25, 29]. In the homogeneous case, it was predicted that the condensate is unstable in three-dimension when the inter-particle interactions are attractive [30]. The stability of the condensate under magnetic trap has been studied numerically and analytically [31]–[51]. The condensate was predicted to be (meta)stable under the magnetic trap, only when the number of atoms is below some critical number. The estimated critical number for ^{7}Li atoms is about 10^3, which agrees with the observed upper bound of the number of atoms in the condensate [13].

The overlapping condensates of the two different spin states of ^{87}Rb in a magnetic trap were observed [52]–[54], which has also stimulated theoretical research of the multi-component condensates [55]–[60]. Because of the repulsive interaction between the condensates and the gravitational force, two condensates were observed to be separated. In the study of dynamics of component separation of this system [54], it was observed that the time-evolution is rather complex; the initial configuration quickly damps out and tends to preserve the total density profile. With respect to damping, effects of the excitations are

not small and it is not yet certain what mechanism is responsible. The time-independence of the total density profile is due to the similarity in intraspecies and interspecies scattering lentghs in ^{87}Rb.

Further, optical trapping of the condensates of ^{23}Na in several hyperfine states was demonstrated [61]. In a magnetic trap, spins of atoms are polarized. Thus, Bose-Einstein condensates are described in terms of scalar wavefunctions (order parameters). In an optical trap, on the other hand, degrees of freedom of atomic spin are recovered, and consequently the condensate wavefunction behaves as spinor. By applying weak magnetic fields with spatial gradient, the degeneracy of the internal degree of freedom is lifted, and the freedom of spin orientation gives the formation of spin domains [62, 63]. The domains can also be easily miscible by turn off the magnetic fields, which is unlike the experiments of ^{87}Rb [52]. For this system, several theoretical works have also been done [64]–[68], where Skirmion [64], spin texture [65], the dynamics of spin mixing [66], spin domain formation [67] and internal vortex structure [68] are studied.

Keeping the developments in mind, we study static and dynamical properties of the Bose-Einstein condensates of atomic gases confined in traps. In Chap. 2, a system of bosons with inter-particle interactions of finite range, trapped in an external potential and at very low temperature, are considered. Applying the pseudopotential method [5, 73] and the mean field approach to the system, the Ginzburg-Pitaevskii-Gross equation [69]–[72] is derived. The time-dependent case, which we call the Gross-Pitaevskii equation, is essentially equivalent to the nonlinear Schrödinger equation. In Chap. 3, by use of the variational approach [32, 33], static properties of the Bose-Einstein condensates are discussed. The ground state properties of a condensate with repulsive or attractive inter-atomic interaction confined in axially symmetric magnetic trap are investigated (Sec. 3.1). The analysis is extended to that of the stability of a two-component Bose-Einstein condensate under magnetic traps, where the possibility of phase separations is also discussed (Sec. 3.2). While the inter-particle interaction is assumed to be of finite range in the first two sections in this chapter, the properties of the Bose-Einstein condensate of long-ranged interacting bosons confined in traps are considered in (and only in) Sec. 3.3. In Chap. 4, dynamical properties of Bose-Einstein condensates are considered. A key idea is the extension of the Zakharov's theory [41]. The stability of the wavefunction of the D-dimensional nonlinear Schrödinger equation with harmonic potential terms is analyzed (Sec. 4.1) and is applied to investigate the instability of condensates with effectively attractive inter-atomic interaction (Sec. 4.2). There, a formula for the critical number of atoms, above which the collapse of the condensate occurs, is derived. The last chapter is devoted to summary and concluding remarks.

Chapter 2

Ginzburg-Pitaevskii-Gross Equation

In this chapter, we present the basic equation to describe Bose-Einstein condensates. In Sec. 2.1, following Ref. [72] based on the Hartree approximation, we derive the Ginzburg-Pitaevskii-Gross equation [69]–[72], which is essentially equivalent to the time-independent nonlinear Schrödinger equation. In Sec. 2.2, we consider the time-dependent case. To derive the equation of motion for the condensate, we begin with the second-quantized formulation. By employing the mean field approach, we obtain the so-called Gross-Pitaevskii equation [70]–[72] or equivalently the (time-dependent) nonlinear Schrödinger equation.

2.1 Time-independent case

We consider N identical bosonic particles with inter-particle interactions of finite range, trapped in an external potential, $V(\boldsymbol{r})$. We assume that the gas is sufficiently dilute and at very low temperature. In such a situation, two-body interaction is dominant and the s-wave part plays a central role. We may replace the scattering from an inter-particle potential of finite range by that from a hard-sphere of diameter a, which is identical to s-wave scattering length in this case. Then, the Hamiltonian operator of the system of hard-spheres can be given in certain approximations, the detail of which we explain in the Appendix B, by the pseudopotential Hamiltonian operator [5, 73],

$$H = \sum_{i=1}^{N} \left(-\frac{\hbar^2}{2m} \Delta_i + V(\boldsymbol{r}_i) \right) + \frac{1}{2} \sum_{i \neq j} U_0 \, \delta(\boldsymbol{r}_i - \boldsymbol{r}_j) \, \frac{\partial}{\partial r_{ij}} \left(r_{ij} \, \cdot \right), \tag{2.1.1}$$

where m is the mass of a bosonic particle, and

$$\Delta_i \equiv \frac{\partial^2}{\partial x_i^2} + \frac{\partial^2}{\partial y_i^2} + \frac{\partial^2}{\partial z_i^2}, \tag{2.1.2}$$

$$r_{ij} \equiv |\boldsymbol{r}_i - \boldsymbol{r}_j|, \tag{2.1.3}$$

$$U_0 \equiv 4\pi\hbar^2 a/m. \tag{2.1.4}$$

The magnetic trap is well approximated by a harmonic potential,

$$V(\boldsymbol{r}) = \frac{m}{2} \left(\omega_x^2 x^2 + \omega_y^2 y^2 + \omega_z^2 z^2 \right), \tag{2.1.5}$$

with $(\omega_x, \omega_y, \omega_z)$ being trap frequencies.

In the ground state of the system, almost all bosons may occupy the lowest single-particle state because of sufficiently weak inter-particle interactions. Thus, following the Hartree approximation, we write the ground state wavefunction, $\Phi_0(\boldsymbol{r}_1, \boldsymbol{r}_2, \cdots, \boldsymbol{r}_N)$, in terms of the product of N single-particle state wavefunctions, $g(\boldsymbol{r})$,

$$\Phi_0(\boldsymbol{r}_1, \boldsymbol{r}_2, \cdots, \boldsymbol{r}_N) = \prod_{i=1}^{N} g(\boldsymbol{r}_i), \tag{2.1.6}$$

where $g(\boldsymbol{r})$ is normalized as

$$\langle g|g\rangle \equiv \int \mathrm{d}\boldsymbol{r}|g(\boldsymbol{r})|^2 = 1, \tag{2.1.7}$$

and thus the norm of the wavefunction Φ_0, defined by $\langle\Phi_0|\Phi_0\rangle$,

$$\langle\Phi_0|\Phi_0\rangle \equiv \int \mathrm{d}\boldsymbol{r}_1 \cdots \int \mathrm{d}\boldsymbol{r}_N |\Phi_0(\boldsymbol{r}_1 \cdots \boldsymbol{r}_N)|^2 = \left(\int \mathrm{d}\boldsymbol{r}|g(\boldsymbol{r})|^2\right)^N, \tag{2.1.8}$$

is equal to unity. From Eqs. (2.1.1) and (2.1.6), we have

$$\begin{aligned}
&\langle\Phi_0|H|\Phi_0\rangle \\
&= \sum_{i=1}^{N} \int \mathrm{d}\boldsymbol{r}_1 \cdots \int \mathrm{d}\boldsymbol{r}_N \Phi_0^* \left(-\frac{\hbar^2}{2m}\Delta_i + V(\boldsymbol{r}_i)\right) \Phi_0 \\
&\quad + \frac{U_0}{2} \sum_{i\neq j} \int \mathrm{d}\boldsymbol{r}_1 \cdots \int \mathrm{d}\boldsymbol{r}_N \Phi_0^* \delta(\boldsymbol{r}_i - \boldsymbol{r}_j) \frac{\partial}{\partial r_{ij}} (r_{ij}\Phi_0) \\
&= N \int \mathrm{d}\boldsymbol{r} g^*(\boldsymbol{r}) \left(-\frac{\hbar^2}{2m}\Delta + V(\boldsymbol{r})\right) g(\boldsymbol{r}) \\
&\quad + \frac{N(N-1)}{2} U_0 \int \mathrm{d}\boldsymbol{r}_1 \int \mathrm{d}\boldsymbol{r}_2 g^*(\boldsymbol{r}_2) g^*(\boldsymbol{r}_1) \delta(\boldsymbol{r}_1 - \boldsymbol{r}_2) \frac{\partial}{\partial r_{12}} \left[r_{12} g(\boldsymbol{r}_1) g(\boldsymbol{r}_2)\right],
\end{aligned} \tag{2.1.9}$$

where the superscript $*$ means the complex conjugate and

$$\Delta \equiv \frac{\partial^2}{\partial x^2} + \frac{\partial^2}{\partial y^2} + \frac{\partial^2}{\partial z^2}. \tag{2.1.10}$$

In Eq. (2.1.9), if the product of two single-state wavefunctions $g(\boldsymbol{r}_1)g(\boldsymbol{r}_2)$ is not singular at $r_{12} = 0$, the operator $(\partial/\partial r_{12})\,(r_{12}\,\cdot)$ can be set equal to unity, which gives

$$\begin{aligned}
\langle\Phi_0|H|\Phi_0\rangle &= N \int \mathrm{d}\boldsymbol{r} g^*(\boldsymbol{r}) \left(-\frac{\hbar^2}{2m}\Delta + V(\boldsymbol{r})\right) g(\boldsymbol{r}) \\
&\quad + \frac{N(N-1)}{2} U_0 \int \mathrm{d}\boldsymbol{r} \int \mathrm{d}\boldsymbol{r}' g^*(\boldsymbol{r}') g^*(\boldsymbol{r}) \delta(\boldsymbol{r} - \boldsymbol{r}')\, g(\boldsymbol{r}) g(\boldsymbol{r}') \\
&= N \int \mathrm{d}\boldsymbol{r} \left[g^*(\boldsymbol{r}) \left(-\frac{\hbar^2}{2m}\Delta + V(\boldsymbol{r})\right) g(\boldsymbol{r}) + \frac{N-1}{2} U_0 \left|g(\boldsymbol{r})\right|^4\right].
\end{aligned} \tag{2.1.11}$$

We minimize the functional $\langle\Phi_0|H|\Phi_0\rangle$ (2.1.11) under the constraint:

$$\langle\Phi_0|\Phi_0\rangle = 1. \tag{2.1.12}$$

To find the constrained extremum of $\langle\Phi_0|H|\Phi_0\rangle$, we set the variation of a functional $\langle\Phi_0|H|\Phi_0\rangle - \mu\langle\Phi_0|\Phi_0\rangle$ equal to zero,

$$\frac{\delta}{\delta g^*(\boldsymbol{r})}\left(\langle\Phi_0|H|\Phi_0\rangle - \mu\left\langle\Phi_0|\Phi_0\right\rangle\right) = 0, \tag{2.1.13}$$

where μ is a Lagrange's multiplier. Substituting Eqs. (2.1.8) and (2.1.11) into Eq. (2.1.13), we obtain

$$-\frac{\hbar^2}{2m}\Delta g(\boldsymbol{r}) + V(\boldsymbol{r})g(\boldsymbol{r}) + (N-1)U_0\left|g(\boldsymbol{r})\right|^2 g(\boldsymbol{r}) = \mu g(\boldsymbol{r}). \tag{2.1.14}$$

Introducing a wavefunction $\Psi(\boldsymbol{r})$,

$$\Psi(\boldsymbol{r}) \equiv N^{1/2} g(\boldsymbol{r}), \tag{2.1.15}$$

we get

$$-\frac{\hbar^2}{2m}\Delta\Psi(\boldsymbol{r}) + V(\boldsymbol{r})\Psi(\boldsymbol{r}) + \left(1-\frac{1}{N}\right)U_0\left|\Psi(\boldsymbol{r})\right|^2\Psi(\boldsymbol{r}) = \mu\Psi(\boldsymbol{r}), \tag{2.1.16}$$

with

$$\langle\Psi|\Psi\rangle \equiv \int \mathrm{d}\boldsymbol{r}|\Psi(\boldsymbol{r})|^2 = N. \tag{2.1.17}$$

The wavefunction Ψ has many names; an order parameter, a macroscopic wavefunction and a Bose-Einstein condensate wavefunction. For sufficiently large N, we can neglect the $1/N$-order term appearing in the left hand side of Eq. (2.1.16). The result is

$$-\frac{\hbar^2}{2m}\Delta\Psi(\boldsymbol{r}) + V(\boldsymbol{r})\psi(\boldsymbol{r}) + U_0\left|\Psi(\boldsymbol{r})\right|^2\Psi(\boldsymbol{r}) = \mu\Psi(\boldsymbol{r}). \tag{2.1.18}$$

We refer to Eq. (2.1.18) as the Ginzburg-Pitaevskii-Gross equation [69]–[72] with an external potential term. This equation may also be referred to as the time-independent nonlinear Schrödinger equation.

From Eqs. (2.1.11) and (2.1.15), the ground state energy of the system, E, is

$$\begin{aligned} E &= N\int \mathrm{d}\boldsymbol{r}\left[\frac{\hbar^2}{2m}\left|\nabla g(\boldsymbol{r})\right|^2 + V(\boldsymbol{r})\left|g(\boldsymbol{r})\right|^2 + (N-1)\frac{U_0}{2}\left|g(\boldsymbol{r})\right|^4\right] \\ &= \int \mathrm{d}\boldsymbol{r}\left[\frac{\hbar^2}{2m}\left|\nabla\Psi(\boldsymbol{r})\right|^2 + V(\boldsymbol{r})\left|\Psi(\boldsymbol{r})\right|^2 + \left(1-\frac{1}{N}\right)\frac{U_0}{2}\left|\Psi(\boldsymbol{r})\right|^4\right], \end{aligned} \tag{2.1.19}$$

which we call the Ginzburg-Pitaevskii-Gross energy functional [69]–[72] with an external potential term. On the other hand, multiplying the both sides of Eq. (2.1.16) by $\Psi^*(\boldsymbol{r})$ and integrating it, we have

$$\begin{aligned} N\mu &= \int \mathrm{d}\boldsymbol{r}\left[\frac{\hbar^2}{2m}\left|\nabla\Psi\right|^2 + V(\boldsymbol{r})\left|\Psi\right|^2 + \left(1-\frac{1}{N}\right)U_0\left|\Psi\right|^4\right] \\ &= E + \left(1-\frac{1}{N}\right)\frac{U_0}{2}\int \mathrm{d}\boldsymbol{r}\left|\Psi\right|^4. \end{aligned} \tag{2.1.20}$$

Another derivation of Eq. (2.1.20) may be instructive. We give a small change to the single-particle wavefunction $g(\boldsymbol{r})$, and denote the resultant by $\tilde{g}(\boldsymbol{r})$,

$$\tilde{g}(\boldsymbol{r}) \equiv (1+\epsilon)^{1/2} g(\boldsymbol{r}), \tag{2.1.21}$$

where ϵ is a sufficiently small constant and $g(\boldsymbol{r})$ satisfies Eqs. (2.1.7) and (2.1.14). Similar to (2.1.21), we also define

$$\tilde{\Psi}(\boldsymbol{r}) \equiv (1+\epsilon)^{1/2} \Psi(\boldsymbol{r}), \tag{2.1.22}$$

where Ψ satisfies Eq. (2.1.16). From the normalization condition of $\Psi(\boldsymbol{r})$ (2.1.17), we have

$$\langle \tilde{\Psi} | \tilde{\Psi} \rangle \equiv \int \mathrm{d}\boldsymbol{r} |\tilde{\Psi}(\boldsymbol{r})|^2 = N + \epsilon\, N. \tag{2.1.23}$$

In (2.1.23), we can regard $\epsilon\, N$ as a virtual change of the number of particles, δN,

$$\delta N \equiv \epsilon\, N. \tag{2.1.24}$$

From (2.1.6) with (2.1.21), we construct a transformed wavefunction of the system, $\tilde{\Phi}_0$,

$$\tilde{\Phi}_0 \equiv \prod_{i=1}^{N} \tilde{g}(\boldsymbol{r}_i), \tag{2.1.25}$$

Then, the norm of the wavefunction $\tilde{\Phi}_0$ is

$$\begin{aligned} \langle \tilde{\Phi}_0 | \tilde{\Phi}_0 \rangle &= \left(\int \mathrm{d}\boldsymbol{r} |\tilde{g}(\boldsymbol{r})|^2 \right)^N \\ &= (1+\epsilon)^N \\ &\approx 1 + \epsilon\, N = 1 + \delta N. \end{aligned} \tag{2.1.26}$$

From (2.1.12) and (2.1.26), we obtain a variation of the norm of Φ_0,

$$\delta \langle \Phi_0 | \Phi_0 \rangle \equiv \langle \tilde{\Phi}_0 | \tilde{\Phi}_0 \rangle - \langle \Phi_0 | \Phi_0 \rangle = \delta N. \tag{2.1.27}$$

The corresponding change of the energy is calculated as follows. By replacing Ψ with $\tilde{\Psi}$ in (2.1.19), we get

$$\int \mathrm{d}\boldsymbol{r} \left[\frac{\hbar^2}{2m} \left| \nabla \tilde{\Psi}(\boldsymbol{r}) \right|^2 + V(\boldsymbol{r}) \left| \tilde{\Psi}(\boldsymbol{r}) \right|^2 + \left(1 - \frac{1}{N} \right) \frac{U_0}{2} \left| \tilde{\Psi}(\boldsymbol{r}) \right|^4 \right] \approx E + \delta E, \tag{2.1.28}$$

where

$$\delta E \equiv \frac{\delta N}{N} \int \mathrm{d}\boldsymbol{r} \left[\frac{\hbar^2}{2m} |\nabla \Psi|^2 + V(\boldsymbol{r}) |\Psi|^2 + \left(1 - \frac{1}{N} \right) U_0 |\Psi|^4 \right]. \tag{2.1.29}$$

Because Ψ satisfies Eq. (2.1.16), the variations δN (2.1.27) and δE (2.1.29) satisfy the extremum condition (2.1.13), and thus we have

$$\delta E - \mu\, \delta N = 0. \tag{2.1.30}$$

Substituting (2.1.29) into (2.1.30), we get

$$\mu = \frac{\delta E}{\delta N} = \frac{1}{N} \int \mathrm{d}\boldsymbol{r} \left[\frac{\hbar^2}{2m} |\nabla \Psi|^2 + V(\boldsymbol{r}) |\Psi|^2 + \left(1 - \frac{1}{N} \right) U_0 |\Psi|^4 \right], \tag{2.1.31}$$

which is the same as (2.1.20). From (2.1.31), it is clear that μ, introduced as a Lagrange's multiplier, has a meaning of the chemical potential of the system.

2.2 Time-dependent case

In this sub-section, we consider the time-dependent case, $\Psi = \Psi(\boldsymbol{r}, t)$. To derive the equation of motion of Ψ, we use the second-quantized formulation. Let $\hat{\Psi}(\boldsymbol{r}, t)$ and $\hat{\Psi}^\dagger(\boldsymbol{r}, t)$ denote the bosonic annihilation and creation operators, respectively. The (equal-time) commutation relations among the operators are

$$\left[\hat{\Psi}(\boldsymbol{r}, t), \hat{\Psi}(\boldsymbol{r}', t)\right] \equiv \hat{\Psi}(\boldsymbol{r}, t)\hat{\Psi}(\boldsymbol{r}', t) - \hat{\Psi}(\boldsymbol{r}', t)\hat{\Psi}(\boldsymbol{r}, t) = 0, \tag{2.2.1}$$

$$\left[\hat{\Psi}(\boldsymbol{r}, t), \hat{\Psi}^\dagger(\boldsymbol{r}', t)\right] = \delta(\boldsymbol{r} - \boldsymbol{r}'), \tag{2.2.2}$$

and the second-quantized Hamiltonian of the system, $\hat{H}$, can be written as

$$\hat{H} \equiv \int \mathrm{d}\boldsymbol{r} \left[\frac{\hbar^2}{2m}\nabla\hat{\Psi}^\dagger \cdot \nabla\hat{\Psi} + V(\boldsymbol{r})\hat{\Psi}^\dagger\hat{\Psi} + \frac{U_0}{2}\hat{\Psi}^\dagger\hat{\Psi}^\dagger\hat{\Psi}\hat{\Psi}\right]. \tag{2.2.3}$$

The time-evolution of the operator $\hat{\Psi}(\boldsymbol{r}, t)$ obeys the Heisenberg equation,

$$\mathrm{i}\hbar\frac{\partial}{\partial t}\hat{\Psi} = \left[\hat{\Psi}, \hat{H}\right]. \tag{2.2.4}$$

Substituting the Hamiltonian (2.2.3) into Eq. (2.2.4) and using the commutation relations (2.2.1) and (2.2.2), we get

$$\mathrm{i}\hbar\frac{\partial}{\partial t}\hat{\Psi} = -\frac{\hbar^2}{2m}\Delta\hat{\Psi} + V(\boldsymbol{r})\hat{\Psi} + U_0\hat{\Psi}^\dagger\hat{\Psi}\hat{\Psi}. \tag{2.2.5}$$

We denote an expectation value by $\langle\,\cdot\,\rangle$. The Heisenberg equation for the bosonic operator (2.2.5) gives

$$\mathrm{i}\hbar\frac{\partial}{\partial t}\left\langle\hat{\Psi}\right\rangle = -\frac{\hbar^2}{2m}\Delta\left\langle\hat{\Psi}\right\rangle + V(\boldsymbol{r})\left\langle\hat{\Psi}\right\rangle + U_0\left\langle\hat{\Psi}^\dagger\hat{\Psi}\hat{\Psi}\right\rangle. \tag{2.2.6}$$

According to the mean field theory [15, 16], we may replace expectation values of the bosonic annihilation and creation operators by the condensate wavefunction $\Psi(\boldsymbol{r}, t)$ and its complex conjugate $\Psi^*(\boldsymbol{r}, t)$ respectively,

$$\left\langle\hat{\Psi}(\boldsymbol{r}, t)\right\rangle = \Psi(\boldsymbol{r}, t), \quad \left\langle\hat{\Psi}^\dagger(\boldsymbol{r}, t)\right\rangle = \Psi^*(\boldsymbol{r}, t). \tag{2.2.7}$$

For the third term in the right hand side of Eq. (2.2.6), we take the following approximation,

$$\left\langle\hat{\Psi}^\dagger\hat{\Psi}\hat{\Psi}\right\rangle \approx \left\langle\hat{\Psi}^\dagger\right\rangle\left\langle\hat{\Psi}\right\rangle\left\langle\hat{\Psi}\right\rangle = |\Psi(\,\boldsymbol{r}, t)|^2\Psi(\boldsymbol{r}, t). \tag{2.2.8}$$

Substituting (2.2.7) and (2.2.8) into Eq. (2.2.6), we have

$$\mathrm{i}\hbar\frac{\partial}{\partial t}\Psi(\boldsymbol{r}, t) = -\frac{\hbar^2}{2m}\Delta\Psi(\boldsymbol{r}, t) + V(\boldsymbol{r})\Psi(\boldsymbol{r}, t) + U_0\left|\Psi(\boldsymbol{r}, t)\right|^2\Psi(\boldsymbol{r}, t), \tag{2.2.9}$$

which is called the Gross-Pitaevskii equation [70]–[72] with an external potential or the (time-dependent) nonlinear Schrödinger equation. The one-dimensional nonlinear Schrödinger equation is known to be integrable and has been studied extensively related to various areas of physics [74, 75]. The equation (2.2.9) can be written in a variational form,

$$\mathrm{i}\hbar\frac{\partial\Psi}{\partial t} = \frac{\delta}{\delta\Psi^*}E[\Psi], \tag{2.2.10}$$

where the functional $E[\,\cdot\,]$ is defined by Eq. (2.1.19) with the $1/N$-order term deleted. We note that, by setting

$$\Psi(\boldsymbol{r},t) = \exp(-\mathrm{i}\,\mu\,t)\,\Psi(\boldsymbol{r}), \tag{2.2.11}$$

in Eq. (2.2.9), we obtain the Ginzburg-Pitaevskii-Gross equation (2.1.18) again.

The existence of non-zero $\Psi(\boldsymbol{r},t) = \left\langle\hat{\Psi}(\boldsymbol{r},t)\right\rangle$ has an important meaning in physics, the breakdown of the gauge symmetry. One of the consequences is that the condensate has a definite phase $\theta(\boldsymbol{r},t)$ as defined by $\Psi(\boldsymbol{r},t) = f(\boldsymbol{r},t)\exp[\mathrm{i}\,\theta(\boldsymbol{r},t)]$ where f and θ are real functions.

Chapter 3

Static Properties of Bose-Einstein Condensates

In this chapter, we consider the static properties of Bose-Einstein condensates. In Sec. 3.1, by using the variational approach, we examine the ground state properties of a Bose-Einstein condensate with repulsive or attractive inter-atomic interaction confined in axially symmetric magnetic trap [44]. Employing a gaussian trial wavefunction to describe the condensate, we derive the minimum conditions of the Ginzburg-Pitaevskii-Gross energy functional (2.1.19). In the repulsive inter-atomic interaction case, it is shown that, if the trap has a high asymmetry and thus the equi-potential surface of the trap is "cigar" or "pancake" shaped, we can assume different approximations to each of axial and transverse directions. We also compare the energy with the one obtained from the Thomas-Fermi approximation [33]. In the attractive interaction case, different from the repulsive case, the energy function has only a local minimum. The local minimum of the energy no longer exists above some critical number of atoms. This can be regarded as a static theory of the collapse. We calculate the critical number for three shapes of the equi-potential surface of the trap: almost sphere, cigar and pancake.

In Sec. 3.2, we extend the analysis in Sec. 3.1 to discuss the stability of a two-component Bose-Einstein condensate under magnetic traps [60]. We first investigate the case where the numbers of two species of atoms are the same. The effect of interspecies interaction on the critical number of atoms is explicitly shown. We also present phase diagrams for various combinations of the scattering lengths. We further develop the variational approach and consider the phase separation of the condensate.

Inter-particle interactions of finite range are well approximated by the delta function. We may think of the long-range interaction like a Coulomb potential, because of the possibility of Bose-Einstein condensation for all bosonic atoms and molecules with and without charges in future. Then, in Sec. 3.3 (and only in this section), we consider the properties of the Bose-Einstein condensate of long-ranged interacting bosons confined in traps. As in Sec. 3.1, we derive the minimum conditions of the energy, and obtain the ground state energy. It is interesting to see that the condensate of long-range interacting bosons under traps is stable both for repulsive and attractive cases.

3.1 Ground state of a Bose-Einstein condensate under axially symmetric magnetic trap

The ground state properties of a Bose-Einstein condensate with repulsive or attractive inter-atomic interaction confined in axially symmetric magnetic trap are studied through the variational approach [44]. It is shown that, if the trap has a high asymmetry and thus the equi-potential surface of the trap is of "cigar" or "pancake" shape, the properties of the condensate are drastically changed from the case of isotropic (spherically symmetric) trap.

3.1.1 Formulation

We consider the ground state properties of a Bose-Einstein condensate confined in axially symmetric magnetic trap,

$$V(\boldsymbol{r}) = \frac{m}{2}(\omega_\perp^2 r_\perp^2 + \omega_z^2 z^2). \tag{3.1.1}$$

Here, the axis of the symmetry is chosen to be the z-axis, and $r_\perp$ denotes the radius of the projection of the position vector $\boldsymbol{r}$ on the xy-plane, m the atomic mass, and ω_z and $\omega_\perp$ the trap (angular) frequencies along the z-axis and in the xy-plane, respectively.

Following Baym and Pethick [33] and Fetter [32] for isotropic case, we employ as the ground state wavefunction a gaussian trial function,

$$\Psi(r_\perp, z) = \left(\frac{N}{\pi^{3/2} d_\perp^2 d_z}\right)^{1/2} \exp[-(r_\perp^2/d_\perp^2 + z^2/d_z^2)/2], \tag{3.1.2}$$

where $d_\perp$ and d_z are variational parameters. The macroscopic wavefunction of the condensate, $\Psi(\boldsymbol{r})$, is assumed to be axially symmetric, as the magnetic trap is. This assumption is reasonable as far as the system is near the ground state. We have normalized the trial function (3.1.2) to the number of the particles in the condensate, N,

$$2\pi \int_0^\infty r_\perp \mathrm{d}r_\perp \int_{-\infty}^\infty \mathrm{d}z |\Psi(r_\perp, z)|^2 = N. \tag{3.1.3}$$

For the weakly interacting system at zero temperature, the number of the non-condensate particles is considered to be negligible. The parameters $d_\perp$ and d_z measure the extent of the wavefunction in the radial and axial directions. If there is no interaction between atoms, the exact ground state wavefunction is obtained by setting $d_\perp$ and d_z equal to characteristic oscillator lenghs, $l_\perp$ and l_z respectively, which are defined by

$$l_\perp \equiv \left(\frac{\hbar}{m\omega_\perp}\right)^{1/2}, \quad l_z \equiv \left(\frac{\hbar}{m\omega_z}\right)^{1/2}. \tag{3.1.4}$$

In the Hartree approximation (see Sec. 2.1), the ground state energy of the system is given by a Ginzburg-Pitaevskii-Gross energy functional [69]–[72] with the harmonic potential

terms,

$$E[\Psi] = \int \mathrm{d}\boldsymbol{r} \left[\frac{\hbar^2}{2m} |\nabla\Psi|^2 + \frac{m}{2}(\omega_\perp^2 r_\perp^2 + \omega_z^2 z^2)|\Psi|^2 + \frac{2\pi\hbar^2 a}{m}|\Psi|^4 \right], \tag{3.1.5}$$

where a is the s-wave scattering length. We note that the minimization of the functional $E - \mu N$, where μ is the chemical potential, gives the Ginzburg-Pitaevskii-Gross equation [69]–[72] with the harmonic potential terms,

$$-\frac{\hbar^2}{2m}\Delta\Psi + \frac{m}{2}(\omega_\perp^2 r_\perp^2 + \omega_z^2 z^2)\Psi + \frac{4\pi\hbar^2 a}{m}|\Psi|^2\Psi = \mu\Psi. \tag{3.1.6}$$

Substituing (3.1.2) into (3.1.5), we obtain

$$E(d_\perp, d_z) = N\left(\frac{\hbar^2}{2md_\perp^2} + \frac{m}{2}\omega_\perp^2 d_\perp^2\right) + \frac{N}{2}\left(\frac{\hbar^2}{2md_z^2} + \frac{m}{2}\omega_z^2 d_z^2\right) + \frac{\hbar^2 a N^2}{(2\pi)^{1/2} m}\frac{1}{d_\perp^2 d_z}. \tag{3.1.7}$$

The kinetic energy and the potential energy are respectively proportional to d^{-2} and d^2. We introduce dimensionless variational parameters

$$s_\perp \equiv l_\perp/d_\perp, \quad s_z \equiv l_z/d_z, \tag{3.1.8}$$

and dimensionless experimental constants

$$\delta \equiv \omega_z/\omega_\perp, \quad G_\perp \equiv (2/\pi)^{1/2} N a/l_\perp. \tag{3.1.9}$$

The constant δ measures the anisotropy of the trap. The constant $G_\perp$ represents the strength of the interaction and is positive (negative) for the repulsive (attractive) interaction case. We may use other constants such as $G_z \equiv (2/\pi)^{1/2} N a/l_z$, but those can be expressed in terms of δ and $G_\perp$. Substituting (3.1.8) and (3.1.9) into (3.1.7) yields

$$E(s_\perp, s_z) = \frac{N\hbar\omega_\perp}{2}\left[(s_\perp^2 + s_\perp^{-2}) + \frac{\delta}{2}(s_z^2 + s_z^{-2}) + \delta^{1/2} G_\perp s_\perp^2 s_z\right]. \tag{3.1.10}$$

We note that the large (small) s corresponds to the contraction (spread) of the condensate. We investigate the existence of a minimum of $E(s_\perp, s_z)$ as a function of the two variational parameters $s_\perp$ and s_z. The minimum conditions,

$$\frac{\partial E}{\partial s_\perp} = 0, \tag{3.1.11}$$

$$\frac{\partial E}{\partial s_z} = 0, \tag{3.1.12}$$

determine the location of the minimum. Substituting (3.1.10) into (3.1.11), we get

$$(s_\perp - s_\perp^{-3}) + \delta^{1/2} G_\perp s_\perp s_z = 0. \tag{3.1.13}$$

Similarly, substitution of (3.1.10) into (3.1.12) gives

$$(s_z - s_z^{-3}) + \delta^{-1/2} G_\perp s_\perp^2 = 0. \tag{3.1.14}$$

We also calculate the second derivatives $\frac{\partial^2 E}{\partial s_\perp^2}$, $\frac{\partial^2 E}{\partial s_z^2}$ and $\frac{\partial^2 E}{\partial s_\perp \partial s_z}$ of $E(s_\perp, s_z)$,

$$\frac{\partial^2 E}{\partial s_\perp^2} = N\hbar\omega_\perp(1 + 3s_\perp^{-4} + \delta^{1/2}G_\perp s_z), \tag{3.1.15}$$

$$\frac{\partial^2 E}{\partial s_z^2} = \frac{\delta}{2}N\hbar\omega_\perp(1 + 3s_z^{-4}), \tag{3.1.16}$$

$$\frac{\partial^2 E}{\partial s_\perp \partial s_z} = \delta^{1/2}N\hbar\omega_\perp G_\perp s_\perp, \tag{3.1.17}$$

from which we have the determinant of the Hessian matrix, Δ,

$$\begin{aligned}\Delta &\equiv \frac{\partial^2 E}{\partial s_\perp^2}\frac{\partial^2 E}{\partial s_z^2} - \left(\frac{\partial^2 E}{\partial s_\perp \partial s_z}\right)^2 \\ &= \delta(N\hbar\omega_\perp)^2\left[(1 + 3s_\perp^{-4} + \delta^{1/2}G_\perp s_z)(1 + 3s_z^{-4})/2 - G_\perp^2 s_\perp^2\right].\end{aligned} \tag{3.1.18}$$

In the following, we deal with the minimum conditions (3.1.13) and (3.1.14) analytically through appropriate approximations depending on the values of δ and $G_\perp$.

3.1.2 Repulsive case

We consider the case where the inter-atomic interaction is repulsive. In this case, the s-wave scattering length a and accordingly the constant $G_\perp$ defined by (3.1.9) are positive. From (3.1.13), we have

$$(s_\perp^4 - 1) = -\delta^{1/2}G_\perp s_\perp^4 s_z < 0. \tag{3.1.19}$$

Then, the parameter $s_\perp$ is smaller than 1 at the minimum point. In a similar manner, we can show from (3.1.14) that s_z is smaller than 1 at the minimum point. Those indicate that a repulsive inter-atomic interaction always acts to expand the condensate size [32]. From (3.1.15), we see that $\frac{\partial^2 E}{\partial s_\perp^2}$ is positive, and by substituting (3.1.13) and (3.1.14) into (3.1.18), we have

$$\Delta = \delta(N\hbar\omega_\perp)^2(3s_\perp^{-4} + s_z^{-4} + 5s_\perp^{-4}s_z^{-4} - 1), \tag{3.1.20}$$

which gives

$$\Delta > \delta(N\hbar\omega_\perp)^2(s_z^{-4} - 1) > 0. \tag{3.1.21}$$

Here, we have used the fact that $s_\perp$ and s_z are smaller than 1. Therefore, we confirm that a point $(s_\perp, s_z)$ which satisfies (3.1.13) and (3.1.14) is indeed a minimum point.

1) Weak interaction approximation

We first consider the case that the third terms in both (3.1.13) and (3.1.14) are negligible, which means the following conditions,

$$s_\perp \sim s_\perp^{-3} \gg \delta^{1/2}G_\perp s_\perp s_z, \quad s_z \sim s_z^{-3} \gg \delta^{-1/2}G_\perp s_\perp^2. \tag{3.1.22}$$

This approximation corresponds to the situation where the inter-atomic interaction is sufficiently weak in both xy- and z-directions. In this case, the approximate solutions of (3.1.13) and (3.1.14) are

$$s_\perp = 1 - \frac{1}{4}\delta^{1/2} G_\perp, \quad s_z = 1 - \frac{1}{4}\delta^{-1/2} G_\perp. \tag{3.1.23}$$

Recall that $s_\perp = s_z = 1$ recovers the exact result for non-interaction case. By substituting (3.1.23) into (3.1.22), we obtain a criterion of the approximation for δ and $G_\perp$,

$$G_\perp \ll \min\{\delta^{-1/2}, \delta^{1/2}\}. \tag{3.1.24}$$

We refer to (3.1.24) as the weak interaction case (region I in Fig. 3.1.1). From (3.1.8), we

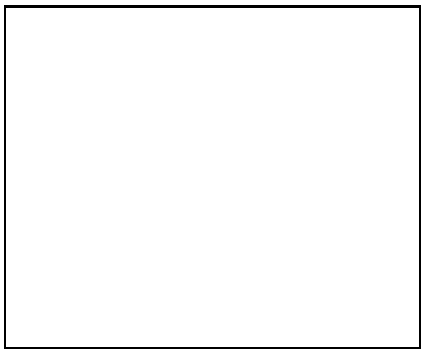

Figure 3.1.1: Approximations for the repulsive inter-atomic interaction: I. weak interaction case (3.1.24), II. strong interaction case (3.1.31), III. intermediate case-1 (3.1.40), IV. intermediate case-2 (3.1.52). The abscissa and ordinate represent the anisotropy of the trap, δ, and the strength of the interaction, $G_\perp$, respectively.

have the original variational parameters as

$$d_\perp = \left(1 + \frac{1}{4}\delta^{1/2} G_\perp\right) l_\perp, \quad d_z = \left(1 + \frac{1}{4}\delta^{-1/2} G_\perp\right) l_z, \tag{3.1.25}$$

which give the aspect ratio of the condensate, $A \equiv d_z/d_\perp$,

$$A = \delta^{-1/2}\left[1 + \frac{1}{4}(\delta^{-1/2} - \delta^{1/2}) G_\perp\right]. \tag{3.1.26}$$

We note that, if $\delta < 1$ ($\delta > 1$), the aspect ratio (3.1.26) is larger (smaller) than that for the non-interaction case, $G_\perp = 0$. The energy E of the condensate (3.1.10) is estimated as

$$E = \frac{N\hbar\omega_\perp}{2}(2 + \delta + \delta^{1/2} G_\perp). \tag{3.1.27}$$

2) Strong interaction approximation

We consider the case that the first terms in both (3.1.13) and (3.1.14) are small. The conditions are

$$s_\perp \ll \delta^{1/2} G_\perp s_\perp s_z \sim s_\perp^{-3}, \quad s_z \ll \delta^{-1/2} G_\perp s_\perp^2 \sim s_z^{-3}. \tag{3.1.28}$$

This is similar to the Thomas-Fermi approximation [33] where the effect of the inter-atomic interaction is assumed to be dominant over the kinetic one. In this case, the approximate solutions of $s_\perp$ and s_z are given by

$$s_\perp = (\delta G_\perp)^{-1/5} \left[1 + \frac{1}{10}(\delta^2 - 3)(\delta G_\perp)^{-4/5}\right], \tag{3.1.29}$$

$$s_z = \delta^{1/2} (\delta G_\perp)^{-1/5} \left[1 - \frac{2}{5}\left(\delta^2 - \frac{1}{2}\right)(\delta G_\perp)^{-4/5}\right]. \tag{3.1.30}$$

By substituting (3.1.29) and (3.1.30) into (3.1.28), we obtain a criterion of the approximation for δ and $G_\perp$,

$$G_\perp \gg \max\{\delta^{-1}, \delta^{3/2}\}. \tag{3.1.31}$$

We call (3.1.31) the strong interaction case (region II in Fig. 3.1.1). The corresponding values of $d_\perp$, d_z, A and E are calculated as

$$d_\perp = (\delta G_\perp)^{1/5} \left[1 - \frac{1}{10}(\delta^2 - 3)(\delta G_\perp)^{-4/5}\right] l_\perp, \tag{3.1.32}$$

$$d_z = \delta^{-1/2} (\delta G_\perp)^{1/5} \left[1 + \frac{2}{5}\left(\delta^2 - \frac{1}{2}\right)(\delta G_\perp)^{-4/5}\right] l_z, \tag{3.1.33}$$

$$A = \delta^{-1} \left[1 + \frac{1}{2}(\delta^2 - 1)(\delta G_\perp)^{-4/5}\right], \tag{3.1.34}$$

$$\begin{aligned} E &= \frac{5N\hbar\omega_\perp}{4}(\delta G_\perp)^{2/5} \left[1 + \frac{2}{5}\left(1 + \frac{\delta^2}{2}\right)(\delta G_\perp)^{-4/5}\right] \\ &= \frac{5}{8\pi^{3/5}} N\hbar\omega_\perp \delta^{2/5} \left(\frac{8\pi N a}{l_\perp}\right)^{2/5} \left[1 + \frac{2}{5}\left(1 + \frac{\delta^2}{2}\right)(\delta G_\perp)^{-4/5}\right]. \end{aligned} \tag{3.1.35}$$

The energy (3.1.35) is equal to Eq. (7) in Ref. [33] to the leading order. It is interesting to compare the leading order term of the energy (3.1.35) with the energy obtained from the three-dimensional Thomas-Fermi approximation (see Appendix C),

$$E_{\rm 3D} = \frac{5}{7}\left(\frac{15g}{8\pi}\right)^{2/5} \left(\frac{m\omega_x^2}{2}\right)^{1/5} \left(\frac{m\omega_y^2}{2}\right)^{1/5} \left(\frac{m\omega_z^2}{2}\right)^{1/5} N^{7/5}. \tag{3.1.36}$$

We see that both of which are proportional to $N^{7/5}$.

3) Mixed approximations

In both weak and strong interaction cases, we have treated similarly the two minimum conditions, (3.1.13) and (3.1.14). However, there exist situations where we can give different approximations to each condition.

First, we consider the case that the third term in (3.1.13) and the first term in (3.1.14) are small, satisfying

$$s_\perp \sim s_\perp^{-3} \gg \delta^{1/2} G_\perp s_\perp s_z, \quad s_z \ll \delta^{-1/2} G_\perp s_\perp^2 \sim s_z^{-3}. \tag{3.1.37}$$

This implies that the effect of the inter-atomic interaction is negligible in xy-direction, but important in z-direction like the Thomas-Fermi approximation. In this case, $s_\perp$ and s_z are approximated as

$$s_\perp = 1 - \frac{1}{4}(\delta G_\perp)^{2/3}, \tag{3.1.38}$$

$$s_z = (\delta^{-1/2} G_\perp)^{-1/3} \left[1 - \frac{1}{3}(\delta^{-1/2} G_\perp)^{-4/3} + \frac{1}{6}(\delta G_\perp)^{2/3}\right]. \tag{3.1.39}$$

By use of (3.1.38) and (3.1.39) in (3.1.37), a criterion of the approximation is given by

$$\delta^{1/2} \ll G_\perp \ll \delta^{-1}, \tag{3.1.40}$$

which requires

$$\delta \ll 1. \tag{3.1.41}$$

Therefore, this approximation is allowed only when the equi-potential surface is elongated in the z-direction and thus "cigar" shaped. We call (3.1.40) the intermediate case-1 (region III in Fig. 3.1.1). Correspondingly, the original parameters $d_\perp$ and d_z, the aspect ratio A and the energy E are calculated as

$$d_\perp = \left[1 + \frac{1}{4}(\delta G_\perp)^{2/3}\right] l_\perp, \tag{3.1.42}$$

$$d_z = (\delta^{-1/2} G_\perp)^{1/3} \left[1 + \frac{1}{3}(\delta^{-1/2} G_\perp)^{-4/3} - \frac{1}{6}(\delta G_\perp)^{2/3}\right] l_z, \tag{3.1.43}$$

$$A = \delta^{-1/2}(\delta^{-1/2} G_\perp)^{1/3} \left[1 + \frac{1}{3}(\delta^{-1/2} G_\perp)^{-4/3} - \frac{5}{12}(\delta G_\perp)^{2/3}\right] \gg 1, \tag{3.1.44}$$

$$E = \frac{N\hbar\omega_\perp}{2}\left[2 + \frac{3}{2}(\delta G_\perp)^{2/3}\right]. \tag{3.1.45}$$

The energy can be rewritten as

$$E = N\hbar\omega_\perp + \frac{3\cdot 2^{1/3}}{8\pi}(m\omega_\perp g/\hbar)^{2/3}\left(\frac{m\omega_z^2}{2}\right)^{1/3} N^{5/3}, \tag{3.1.46}$$

where

$$g \equiv 4\pi\hbar^2 a/m. \tag{3.1.47}$$

The first term is the ground state energy of two-dimensional harmonic oscillators. We note that the second term is proportional to $N^{5/3}$, in the same way as the energy obtained from the one-dimensional Thomas-Fermi approximation (see Appendix C),

$$E_{1\mathrm{D}} = \frac{3}{5}\left(\frac{3g}{4}\right)^{2/3}\left(\frac{m\omega^2}{2}\right)^{1/3} N^{5/3}. \tag{3.1.48}$$

Second, we consider the opposite case; the first term in (3.1.13) and the third term in (3.1.14) can be treated perturbatively, which means the following conditions,

$$s_\perp \ll \delta^{1/2} G_\perp s_\perp s_z \sim s_\perp^{-3}, \quad s_z \sim s_z^{-3} \gg \delta^{-1/2} G_\perp s_\perp^2. \tag{3.1.49}$$

In this case, the effect of the inter-atomic interaction is dominant in xy-direction but negligible in z-direction. The parameters $s_\perp$ and s_z are given by

$$s_\perp = (\delta^{1/2}G_\perp)^{-1/4}\left[1+\frac{1}{16}(\delta^{-3/2}G_\perp)^{1/2}-\frac{1}{4}(\delta^{1/2}G_\perp)^{-1}\right], \tag{3.1.50}$$

$$s_z = 1-\frac{1}{4}(\delta^{-3/2}G_\perp)^{1/2}. \tag{3.1.51}$$

Substitution of (3.1.50) and (3.1.51) into (3.1.49) gives a criterion of the approximation for δ and $G_\perp$ as

$$\delta^{-1/2} \ll G_\perp \ll \delta^{3/2}, \tag{3.1.52}$$

which requires

$$\delta \gg 1. \tag{3.1.53}$$

Therefore, this approximation is allowed only when the equi-potential surface of the trap is an extremely flat spheroid, like a "pancake". The condition (3.1.52) is referred to as the intermediate case-2 (region IV in Fig. 3.1.1). The expressions of $d_\perp$, d_z, A and E are given by

$$d_\perp = (\delta^{1/2}G_\perp)^{1/4}\left[1-\frac{1}{16}(\delta^{-3/2}G_\perp)^{1/2}+\frac{1}{4}(\delta^{1/2}G_\perp)^{-1}\right]l_\perp, \tag{3.1.54}$$

$$d_z = \left[1+\frac{1}{4}(\delta^{-3/2}G_\perp)^{1/2}\right]l_z, \tag{3.1.55}$$

$$A = \delta^{-1/2}(\delta^{1/2}G_\perp)^{-1/4}\left[1+\frac{5}{16}(\delta^{-3/2}G_\perp)^{1/2}-\frac{1}{4}(\delta^{1/2}G_\perp)^{-1}\right] \ll 1, \tag{3.1.56}$$

$$\begin{aligned} E &= \frac{N\hbar\omega_z}{2}\left[1+2(\delta^{-3/2}G_\perp)^{1/2}\right] \\ &= \frac{N\hbar\omega_z}{2}+\frac{1}{2^{1/4}\pi^{3/4}}\left(\frac{m\omega_\perp^2}{2}\right)^{1/2}\left(\frac{m\omega_z}{\hbar}\right)^{1/4}g^{1/2}N^{3/2}, \end{aligned} \tag{3.1.57}$$

with g defined by (3.1.47). We note that the second term in the last expression of (3.1.57) is proportional to $N^{3/2}$, just like the two-dimensional Thomas-Fermi approximation energy (see Appendix C),

$$E_{\rm 2D} = \frac{2}{3}\left(\frac{2}{\pi}\right)^{1/2}\left(\frac{m\omega_x^2}{2}\right)^{1/4}\left(\frac{m\omega_y^2}{2}\right)^{1/4}g^{1/2}N^{3/2}, \tag{3.1.58}$$

while the first term is the ground state energy of one-dimensional harmonic oscillators.

3.1.3 Attractive case

We investigate the case that the inter-atomic interaction is effectively attractive; the s-wave scattering length a and accordingly the constant $G_\perp$ defined by (3.1.9) are assumed to be negative. There, the energy function (3.1.10) has only a local minimum, different from the previous section [32]. Since $G_\perp$ is negative, we have from (3.1.13)

$$(s_\perp^4-1) = -\delta^{1/2}G_\perp s_\perp^4 s_z > 0, \tag{3.1.59}$$

which shows that $s_\perp$ is larger than 1 at the minimum point. Similarly, s_z is larger than 1 at the minimum point. We thus observe that an attractive inter-atomic interaction works to shrink the condensate size [32].

By use of the minimum condition (3.1.13) in (3.1.15), we find that $\frac{\partial^2 E}{\partial s_\perp^2}$ is always positive at a local minimum point,

$$\frac{\partial^2 E}{\partial s_\perp^2} = 4N\hbar\omega_\perp s_\perp^{-4} > 0. \tag{3.1.60}$$

If $G_\perp$ is sufficiently small, the minimization of the energy (3.1.10) is attained at $(s_\perp, s_z) \approx (1, 1)$, and we see that, by substituting $s_\perp \approx 1$ and $s_z \approx 1$ into (3.1.20), the determinant of the Hessian matrix Δ is positive at this point. However, it can be shown that Δ becomes zero for some value of $G_\perp$, at which the local minimum of the energy disappears, leading to the instability of the condensate. This instability will be discussed in Chap. 4 as a dynamical problem. The critical value of $G_\perp$ is determined by taking the value of Δ at the minimum point to be zero,

$$\Delta = \delta(N\hbar\omega_\perp)^2(3s_\perp^{-4} + s_z^{-4} + 5s_\perp^{-4}s_z^{-4} - 1) = 0, \tag{3.1.61}$$

with the minimum conditions (3.1.13) and (3.1.14). From (3.1.13), (3.1.14) and (3.1.61), we get a set of three equations which determine the stability condition,

$$(s_\perp^4 + 5)(s_\perp^4 - 3)(s_\perp^4 - 1)^2 = (8\delta)^2 s_\perp^4, \tag{3.1.62}$$

$$s_z^4 = \frac{s_\perp^4 + 5}{s_\perp^4 - 3}, \tag{3.1.63}$$

$$G_\perp = -\delta^{-1/2} s_z^{-1}(1 - s_\perp^{-4}). \tag{3.1.64}$$

We can solve (3.1.62) analytically for $s_\perp^4$. However, the expression is too complicated to get useful information. In the following, we investigate Eqs. (3.1.62)– (3.1.64), by using some approximations to them.

1) Almost spherical trap

Here we consider the case that the trap is almost spherically symmetric, namely

$$\delta \equiv \omega_z/\omega_\perp = 1 + \epsilon, \quad |\epsilon| \ll 1. \tag{3.1.65}$$

In this case, Eq. (3.1.62) and then Eq. (3.1.63) are approximately solved as

$$s_\perp = 5^{1/4}\left(1 + \frac{\epsilon}{9}\right), \quad s_z = 5^{1/4}\left(1 - \frac{2\epsilon}{9}\right). \tag{3.1.66}$$

From (3.1.66), we get the expressions of the original variational parameters,

$$d_\perp = 5^{-1/4}\left(1 - \frac{\epsilon}{9}\right) l_\perp, \quad d_z = 5^{-1/4}\left(1 + \frac{2\epsilon}{9}\right) l_z, \tag{3.1.67}$$

which give the aspect ratio $A = d_z/d_\perp$,

$$A = 1 - \frac{\epsilon}{6}. \tag{3.1.68}$$

Using (3.1.66) in (3.1.64), we obtain the critical value of $G_\perp$, denoted by $G_{\perp,\mathrm{c}}$,

$$G_{\perp,\mathrm{c}} = -\frac{4}{5^{5/4}}\left(1-\frac{\epsilon}{6}\right). \tag{3.1.69}$$

The result agrees with the one obtained by Fetter (Eq. (7) in Ref. [32]), to the leading order. Further, by substituting (3.1.9) into (3.1.69), we have the critical number of particles, N_c, at which the condensate becomes unstable,

$$N_\mathrm{c} = \frac{2^{3/2}\pi^{1/2}}{5^{5/4}}\frac{l_\perp}{|a|}\left(1-\frac{\epsilon}{6}\right) = 0.671\frac{l_\perp}{|a|}\left(1-\frac{\epsilon}{6}\right) = \frac{2^{3/2}\pi^{1/2}}{5^{5/4}}\frac{l_\perp^{2/3}l_z^{1/3}}{|a|}. \tag{3.1.70}$$

We also calculate the (locally) minimized energy at $G_\perp = G_{\perp,\mathrm{c}}$, defined as E_c,

$$E_\mathrm{c} = \frac{5^{1/2}}{2}\left(1+\frac{\epsilon}{3}\right)N\hbar\omega_\perp = \frac{5^{1/2}}{2}N\hbar\omega_\perp^{2/3}\omega_z^{1/3}. \tag{3.1.71}$$

In an experiment for ^{7}Li [12], the values of frequencies ω_z and $\omega_\perp$ were $\omega_z/2\pi \approx 117\,\mathrm{Hz}$ and $\omega_\perp/2\pi \approx 163\,\mathrm{Hz}$. The s-wave scattering length of ^{7}Li was observed to be $a = -27.3a_0$ where a_0 is the Bohr radius [29]. Using the data in the formula (3.1.70), we have $N_\mathrm{c} = 1450$. This value agrees with the experimental result, $N_\mathrm{c} = 650 \sim 1300$ [13].

2) Cigar shaped trap

We consider the case that the equi-potential surface of the magnetic trap is "cigar" shaped,

$$\delta = \epsilon \ll 1. \tag{3.1.72}$$

In this case, Eqs. (3.1.62) and (3.1.63) are approximately solved to give

$$s_\perp = 3^{1/4}\left(1+\frac{\epsilon^2}{2}\right), \quad s_z = \left(\frac{4}{3}\right)^{1/4}\epsilon^{-1/2}\left(1+\frac{3\epsilon^2}{16}\right). \tag{3.1.73}$$

From (3.1.73), we get $d_\perp$, d_z and A as follows,

$$d_\perp = 3^{-1/4}\left(1-\frac{\epsilon^2}{2}\right)l_\perp, \quad d_z = \left(\frac{3}{4}\right)^{1/4}\left(1-\frac{3\epsilon^2}{16}\right)l_\perp, \tag{3.1.74}$$

$$A = \left(\frac{3}{2}\right)^{1/2}\left(1+\frac{5\epsilon^2}{16}\right). \tag{3.1.75}$$

We observe that d_z is about the order of $l_\perp$ rather than l_z, and accordingly the aspect ratio of the condensate A is about the unity. It is intriguing that, near $G_\perp = G_{\perp,\mathrm{c}}$, the condensate shape does not reflect the anisotropy of the trap, which is assumed to be highly elongated in z-direction.

From (3.1.64) and (3.1.73), we obtain $G_{\perp,\mathrm{c}}$,

$$G_{\perp,\mathrm{c}} = -\frac{2^{1/2}}{3^{3/4}}\left(1+\frac{13\epsilon^2}{16}\right), \tag{3.1.76}$$

and then the critical number of particles $N_{\rm c}$,

$$N_{\rm c} = \frac{\pi^{1/2}}{3^{3/4}} \left(1 + \frac{13\epsilon^2}{16}\right) \frac{l_\perp}{|a|} = 0.778 \left(1 + \frac{13\epsilon^2}{16}\right) \frac{l_\perp}{|a|}. \tag{3.1.77}$$

This critical number is larger than the one obtained in the almost spherical case (3.1.70), if we use the same $l_\perp$ and a in both cases. The critical (locally) minimized energy $E_{\rm c}$ is obtained as

$$E_{\rm c} = \frac{3^{1/2}}{2} \left(1 - \frac{7\epsilon^2}{24}\right) N\hbar\omega_\perp. \tag{3.1.78}$$

3) Pancake shaped trap

We consider the opposite case to the previous one; the equi-potential surface of the trap is an extremely flat spheroid, like a "pancake", namely

$$\delta = \epsilon^{-1} \gg 1 \quad (\epsilon \ll 1). \tag{3.1.79}$$

In this case, the approximate solutions of Eqs. (3.1.62) and (3.1.63) are

$$s_\perp = 4^{1/4}\epsilon^{-1/6}, \quad s_z = 1 + \frac{\epsilon^{2/3}}{2}. \tag{3.1.80}$$

From (3.1.80), we get

$$d_\perp = 4^{-1/4}\epsilon^{1/6} l_\perp = 4^{-1/4}\epsilon^{-1/3} l_z, \quad d_z = \left(1 - \frac{\epsilon^{2/3}}{2}\right) l_z, \tag{3.1.81}$$

$$A = 4^{1/4} \left(1 - \frac{\epsilon^{2/3}}{2}\right) \epsilon^{1/3}. \tag{3.1.82}$$

Note that $d_\perp$ is the order of $\epsilon^{1/6} l_\perp$ or equivalently $\epsilon^{-1/3} l_z$, meaning that $d_\perp$ is much larger than l_z but much smaller than $l_\perp$. On the other hand, d_z remains the order of l_z. Therefore, the aspect ratio $A = d_z/d_\perp$, which is the order of $\epsilon^{1/3}$, is much larger than the ratio between the characteristic oscillator lengths, $l_z/l_\perp = \epsilon^{1/2}$. We observe again that the condensate shape near the instability is not highly anisotropic.

Substitution of (3.1.80) into (3.1.64) gives

$$G_{\perp,{\rm c}} = -\epsilon^{1/2} \left(1 - \frac{3}{4}\epsilon^{2/3}\right), \tag{3.1.83}$$

from which we get

$$N_{\rm c} = \frac{\pi^{1/2}}{2^{1/2}} \left(1 - \frac{3}{4}\epsilon^{2/3}\right) \frac{l_z}{|a|} \approx 1.25 \left(1 - \frac{3}{4}\epsilon^{2/3}\right) \frac{l_z}{|a|}. \tag{3.1.84}$$

We see that the critical number (3.1.84) is larger than the ones obtained in the previous cases (3.1.70) and (3.1.77), if we set l_z in (3.1.84) equal to $l_\perp$ in (3.1.70) and (3.1.77), for a fixed a. The critical minimized energy $E_{\rm c}$ is calculated as

$$E_{\rm c} = \frac{1}{2}(1 + \epsilon^{4/3}) N\hbar\omega_z. \tag{3.1.85}$$

3.2 Stability of a two-component Bose-Einstein condensate

The stability of a two-component Bose-Einstein condensate is an interesting subject experimentally and theoretically. Using the variational method, we investigate the stable and unstable conditions as functions of the particle numbers and the s-wave scattering lengths [60]. We find that interaction between the different species of atoms (simply, interspecies interaction) has significant effects on the stability of each condensate. We also consider the phase separation of the condensate.

3.2.1 Formulation

We consider a two-component Bose-Einstein condensate in isotropic harmonic trap potentials. We denote by m_i, ω_i, N_i, and a_{ii} the mass, the trap frequency, the number of atoms, and the s-wave scattering length of the i-th component respectively. The energy functional of the macroscopic wavefunctions $\Psi_i(\boldsymbol{r})$, which are normalized to N_i, can be written as

$$\begin{aligned} E[\Psi_1,\Psi_2] &= \int \mathrm{d}\boldsymbol{r}\left[\sum_{i=1,2}\left(\frac{\hbar^2}{2m_i}|\nabla\Psi_i(\boldsymbol{r})|^2+V_i(r)|\Psi_i(\boldsymbol{r})|^2\right)\right. \\ &+ \left.\sum_{i=1,2}\frac{2\pi\hbar^2 a_{ii}}{m_i}|\Psi_i(\boldsymbol{r})|^4+\frac{2\pi\hbar^2 a_{12}}{m_{12}}|\Psi_1(\boldsymbol{r})|^2|\Psi_2(\boldsymbol{r})|^2\right], \end{aligned} \tag{3.2.1}$$

where $V_i(r)$ $(i=1,2)$ stand for the isotropic potentials,

$$V_i(r)=\frac{1}{2}m_i\omega_i^2 r^2. \tag{3.2.2}$$

Minimizing the energy functional (3.2.1) with (3.2.2) gives the Ginzburg-Pitaevskii-Gross equation for binary mixtures of the condensates under magnetic traps. The last term in (3.2.1) represents the interactions between the species-1 and the species-2 atoms, whose strength is proportional to the s-wave scattering length a_{12} between them and is anti-proportional to the reduced mass $m_{12}=m_1m_2/(m_1+m_2)$. The positive (negative) value of a_{ij} means the effectively repulsive (attractive) interaction. To perform variational calculations, we use trial functions of the gaussian form

$$\Psi_i(r)=N_i^{\frac{1}{2}}\pi^{-\frac{3}{4}}d_i^{-\frac{3}{2}}\exp\left(-\frac{r^2}{2d_i^2}\right). \tag{3.2.3}$$

The parameter d_i measures the extent of spreading of $\Psi_i(r)$. By substituting (3.2.3) into (3.2.1), one gets the energy as a function of variational parameters d_1 and d_2

$$\begin{aligned} E(d_1,d_2) &= \sum_i\frac{3}{4}N_i\left(\frac{\hbar^2}{m_i}d_i^{-2}+m_i\omega_i^2d_i^2\right)+\sum_i\frac{2\pi\hbar^2a_{ii}}{m_i}(2\pi)^{-\frac{3}{2}}N_i^2d_i^{-3} \\ &+ \frac{2\pi\hbar^2a_{12}}{m_{12}}\pi^{-\frac{3}{2}}N_1N_2\left(d_1^2+d_2^2\right)^{-\frac{3}{2}}. \end{aligned} \tag{3.2.4}$$

To investigate the effects of all the inter-atomic interactions as rigorous as possible, we concentrate on a case where $m_1 = m_2 = m$ and $\omega_1 = \omega_2 = \omega$. We introduce the dimensionless energy ε, scattering length α_{ij}, and width parameter λ_i as

$$\varepsilon = \frac{E}{\hbar\omega}, \;\; \alpha_{ij} = \frac{a_{ij}}{l}, \;\; \lambda_i = \frac{d_i}{l}, \tag{3.2.5}$$

where $l = \sqrt{\hbar/(m\omega)}$ (the characteristic oscillator length). Using ε, α_{ij}, and λ_i instead of E, a_{ij}, and d_i, we rewrite (3.2.4) as

$$\varepsilon = \frac{3}{4}\sum_i N_i(\lambda_i^{-2} + \lambda_i^2) + \frac{1}{\sqrt{2\pi}}\sum_i N_i^2\alpha_{ii}\lambda_i^{-3} + \frac{4}{\sqrt{\pi}}N_1N_2\alpha_{12}(\lambda_1^2 + \lambda_2^2)^{-\frac{3}{2}}. \tag{3.2.6}$$

With respect to the global properties of the function $\varepsilon = \varepsilon(\lambda_1, \lambda_2)$, we remark the following:
(i) A global maximum does not exist because $\varepsilon \to \infty$ as $\lambda_1, \lambda_2 \to \infty$.
(ii) The existence of a minimum depends on the signs of the scattering lengths α_{ij}.
The energy $\varepsilon = \varepsilon(\lambda_1, \lambda_2)$ takes a local minimum when λ_1 and λ_2 satisfy

$$\frac{\partial\varepsilon}{\partial\lambda_1} = 0 \;\; : \;\; 1 - \lambda_1^{-4} - \sqrt{\frac{2}{\pi}}N_1\alpha_{11}\lambda_1^{-5} - \frac{8}{\sqrt{\pi}}N_2\alpha_{12}(\lambda_1^2 + \lambda_2^2)^{-\frac{5}{2}} = 0, \tag{3.2.7}$$

$$\frac{\partial\varepsilon}{\partial\lambda_2} = 0 \;\; : \;\; 1 - \lambda_2^{-4} - \sqrt{\frac{2}{\pi}}N_2\alpha_{22}\lambda_2^{-5} - \frac{8}{\sqrt{\pi}}N_1\alpha_{12}(\lambda_1^2 + \lambda_2^2)^{-\frac{5}{2}} = 0, \tag{3.2.8}$$

and the eigenvalues of the Hessian matrix are positive:

$$\Delta \equiv \frac{\partial^2\varepsilon}{\partial\lambda_1^2}\frac{\partial^2\varepsilon}{\partial\lambda_2^2} - \left(\frac{\partial^2\varepsilon}{\partial\lambda_1\partial\lambda_2}\right)^2 > 0, \;\; \frac{\partial^2\varepsilon}{\partial\lambda_1^2} > 0. \tag{3.2.9}$$

Therefore we can examine the existence of a stable state with gaussian wavefunctions using (3.2.7)–(3.2.9). We analyze these conditions for various physical situations described by α_{ij} and N_i, as follows.

3.2.2 $N_1 = N_2$ case

We begin with the case where $N_1 = N_2 = N$ and $\alpha_{11} = \alpha_{22} = \alpha$. We have set $\alpha_{11} = \alpha_{22}$ to express the results in analytic forms. The conditions (3.2.7) and (3.2.8) give

$$\lambda_1 = \lambda_2, \quad \lambda_1^5 - \lambda_1 = \sqrt{\frac{2}{\pi}}N(\alpha + \alpha_{12}). \tag{3.2.10}$$

Figure 3.2.1 illustrates the stable region for α, α_{12} and N, where (λ_1, λ_2) satisfy (3.2.9) and (3.2.10). The unstable region implies the instability (collapse) of the condensates. From the analysis of the boundary curve, we obtain a critical number $N_c(= N_{1c} = N_{2c})$, which gives an upper limit to the number of atoms, and the parameter $\lambda_c(= \lambda_{1c} = \lambda_{2c})$,

$$N_c = -\frac{2\sqrt{2\pi}}{5^{\frac{5}{4}}}\frac{1}{\alpha + \alpha_{12}}, \;\; \lambda_c = 5^{-\frac{1}{4}} \;\; (\alpha_{12} < 0, \;\; \alpha + \alpha_{12} < 0), \tag{3.2.11}$$

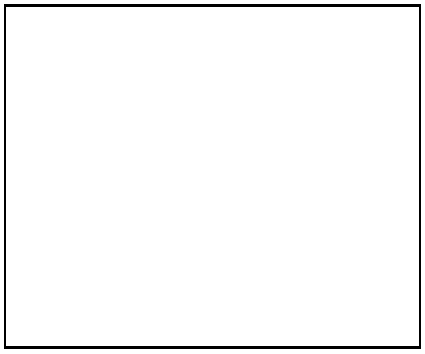

Figure 3.2.1: Stability of the two-component condensate: $N_1 = N_2$ case for (a) $\alpha > 0$, (b) $\alpha < 0$. The boundaries of stable and unstable regions (the solid lines) are determined by Eqs. (3.2.9) and (3.2.10). The dashed lines are discussed in 3.2.4.

$$N_c = \frac{2\sqrt{2\pi}}{5^{\frac{5}{4}}}|\alpha|^{-1}\left(1+4\frac{\alpha_{12}}{|\alpha|}\right)^{\frac{1}{4}}, \quad \lambda_c = 5^{-\frac{1}{4}}\left(1+4\frac{\alpha_{12}}{|\alpha|}\right)^{\frac{1}{4}} \quad (\alpha_{12} > 0, \ \ \alpha < 0). \quad (3.2.12)$$

The conditions (3.2.11) and (3.2.12) are worth to be discussed. First, if there is no interaction between two species of atoms, that is, $\alpha_{12} \equiv 0$, we recover $N_c = 2\sqrt{2\pi}/5^{\frac{5}{4}}|\alpha|$ for the one-component case [32]. Recall that the isotropic limit of (3.1.70) gives this N_c. Second, when the interspecies interaction is effectively attractive (repulsive), that is, $\alpha_{12} < 0$ ($\alpha_{12} > 0$), the critical number of atoms N_c is reduced (enhanced). Thirdly, it is remarkable that the instability occurs even for $\alpha > 0$ if $\alpha_{12} < -\alpha$.

3.2.3 Phase diagrams

We construct phase diagrams for N_1 and N_2: find the boundary line $N_2 = f(N_1)$ which divides N_1N_2-plane into stable and unstable regions. In other words, we pursue the maximum of N_2 as a function of N_1.

1) $\alpha_{11} > 0$, $\alpha_{22} > 0$

This case corresponds to a situation that both intraspecies interactions are repulsive. If interspecies interaction is not strongly attractive, the condensate is stable for any N_1 and N_2 because of their intraspecies repulsions. Therefore we consider here the case $\alpha_{12} < 0$ and $|\alpha_{12}|$ is sufficiently large. We also consider the case that $\{N_1, N_2\}$, $\{\lambda_1, \lambda_2\}$, and $\{\alpha_{11}, \alpha_{22}, |\alpha_{12}|\}$ are sets of the same order quantities. We represent as N, λ and α the quantities which are the same order as $\{N_1, N_2\}$, $\{\lambda_1, \lambda_2\}$ and $\{\alpha_{11}, \alpha_{22}, |\alpha_{12}|\}$ respectively. We start from the following assumption for (N_1, N_2) on the boundary $N_2 = f(N_1)$ and other variables, and we check the validity of the assumption at the end.

The assumption: on the boundary, $f(N_1)/N_1$ remains finite as N_1 tends to infinity, and λ_1 and λ_2 do not get too large when $N_1, N_2 \gg 1$, so as to satisfy

$$1 \approx O(\lambda^{-4}) \ll O(N\alpha\lambda^{-5}). \quad (3.2.13)$$

This assumption is reasonable since we expect that the attractive interspecies interaction suppresses the growth of λ as N gets large.

Under the assumption (3.2.13), neglecting the first and second terms in (3.2.7) and (3.2.8), we obtain the ratios N_2/N_1 and λ_2/λ_1 in the case $\alpha_{12} < -\sqrt{\alpha_{11}\alpha_{22}}$,

$$\frac{N_2}{N_1} = \gamma \equiv \frac{|\alpha_{12}|}{\alpha_{22}} \left(1 \pm \sqrt{1 - \left(\frac{\alpha_{11}\alpha_{22}}{|\alpha_{12}|^2} \right)^{\frac{2}{5}}} \right)^{\frac{5}{2}}, \tag{3.2.14}$$

$$\frac{\lambda_2}{\lambda_1} = \beta \equiv \left(\frac{|\alpha_{12}|^2}{\alpha_{11}\alpha_{22}} \right)^{\frac{1}{5}} \left(1 \pm \sqrt{1 - \left(\frac{\alpha_{11}\alpha_{22}}{|\alpha_{12}|^2} \right)^{\frac{2}{5}}} \right). \tag{3.2.15}$$

Equation (3.2.14) determines asymptotic lines of the boundary curve for sufficiently large N_1 and N_2. Here we remark that $\partial\varepsilon/\partial\lambda_i = 0$ do not give a useful information about the boundary line (or the critical number), but with the approximation used here, $\partial\varepsilon/\partial\lambda_i = 0$ imply $\Delta = 0$. That is the reason why the ratio $f(N_1)/N_1$ has been pursued in (3.2.14). To calculate λ_1 (not λ_2/λ_1), we must take account of terms in the first order which are neglected here. By substituting $\lambda_2/\lambda_1 = \beta(1+\delta)$ and $N_2/N_1 = \gamma(1+\epsilon)$, where $|\delta|, |\epsilon| \ll 1$, into (3.2.7), (3.2.8) and $\Delta = 0$, we obtain

$$\lambda_1 = 5^{-\frac{1}{4}} \left(\frac{\alpha_{11}\beta^3 + \alpha_{22}\gamma}{\alpha_{11}\beta^7 + \alpha_{22}\gamma} \right)^{\frac{1}{4}}. \tag{3.2.16}$$

This shows that λ_1 is a quantity of $O(1)$ and therefore the assumption (3.2.13) is confirmed.

Next we consider the case of small N_1. For simplicity, we consider the case where $\alpha_{11} = \alpha_{22} = \alpha$. The boundary curve $N_2 = f(N_1)$ passes through $(N_1, N_2) = (N_c, N_c)$, where $N_c = 2\sqrt{2\pi}/5^{\frac{5}{4}}(|\alpha_{12}| - \alpha)$ (3.2.11). We examine the behavior of the boundary curve in a neighborhood of this point. We substitute $N_i = N_c + \delta N_i$ and $\lambda_i = \lambda_c + \delta\lambda_i$ into $\partial\varepsilon/\partial\lambda_i = 0$ and $\Delta = 0$. The zeroth order terms give $\lambda_c = 5^{-\frac{1}{4}}$ and the first order terms give

$$\begin{aligned} \frac{|\alpha_{12}|}{|\alpha_{12}| - \alpha}(\delta\lambda_1 - \delta\lambda_2) &= \frac{1}{\sqrt{2\pi}}(\alpha\delta N_1 + \alpha_{12}\delta N_2) \\ &= -\frac{1}{\sqrt{2\pi}}(\alpha_{12}\delta N_1 + \alpha\delta N_2). \end{aligned} \tag{3.2.17}$$

Therefore, we get

$$\frac{\mathrm{d}N_2}{\mathrm{d}N_1} = -1 \quad \text{at} \quad (N_1, N_2) = (N_c, N_c). \tag{3.2.18}$$

Figure 3.2.2 illustrates the phase diagram based on the above discussion. We see that the large attractive interspecies interaction overcomes the repulsive intraspecies interaction and leads to the collapse. We expect the similar tendencies for $\alpha_{11} \neq \alpha_{22}$.

2) $\alpha_{11} < 0$, $\alpha_{22} < 0$

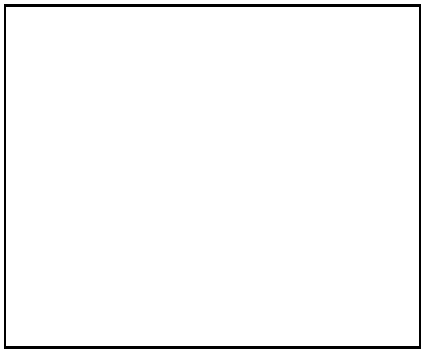

Figure 3.2.2: Phase diagram for $\alpha_{11} = \alpha_{22} \equiv \alpha > 0$ and $\alpha_{12} < -\alpha$.

This case corresponds to a situation that both intraspecies interactions are attractive. The curve $N_2 = f(N_1)$ intersects with the N_2-axis at $(N_1, N_2) = (0, N_{2c}^{(0)})$, where $N_{2c}^{(0)} = 2\sqrt{2\pi}/5^{\frac{5}{4}}|\alpha_{22}|$ is obtained from the one-component theory. We first consider the behavior of $N_2 = f(N_1)$ near this point. Setting $\lambda_i^{(0)} = \lim_{N_1 \to 0} \lambda_i$ and substituting $\lambda_i = \lambda_i^{(0)} + \delta\lambda_i$ into (3.2.7), (3.2.8) and $\Delta = 0$, one gets from the zeroth order terms

$$1 - {\lambda_1^{(0)}}^{-4} - 2^{\frac{9}{2}} \frac{\alpha_{12}}{|\alpha_{22}|} \left(5^{\frac{1}{2}} {\lambda_1^{(0)}}^2 + 1\right)^{-\frac{5}{2}} = 0, \tag{3.2.19}$$

$$\lambda_2^{(0)} = 5^{-\frac{1}{4}}, \tag{3.2.20}$$

and from the first order terms

$$\frac{\mathrm{d}N_2}{\mathrm{d}N_1} = 2^{\frac{5}{2}} \frac{\alpha_{12}}{|\alpha_{22}|} \left(5^{\frac{1}{2}} {\lambda_1^{(0)}}^2 + 1\right)^{-\frac{5}{2}} = \frac{1 - {\lambda_1^{(0)}}^{-4}}{4} \quad \text{at} \quad (N_1, N_2) = (0, N_{2c}^{(0)}), \tag{3.2.21}$$

where $\lambda_1^{(0)}$ is determined by (3.2.19).

Next, in the case $\alpha_{11} = \alpha_{22} = \alpha < 0$, we consider the neighborhood of the point $(N_1, N_2) = (N_c, N_c)$, where N_c is given by (3.2.11) and (3.2.12). If $\alpha_{12} < 0$, N_c is the same as the case where $\alpha > 0$ and $\alpha_{12} < -\alpha$. Therefore,

$$\frac{\mathrm{d}N_2}{\mathrm{d}N_1} = -1 \quad \text{at} \quad (N_1, N_2) = (N_c, N_c). \tag{3.2.22}$$

In the case $\alpha_{12} > 0$, substituting $N_i = N_c + \delta N_i$ and $\lambda_i = \lambda_c + \delta\lambda_i$ into (3.2.7), (3.2.8) and $\Delta = 0$ gives

$$\begin{aligned} \frac{\alpha_{12}}{\alpha}(-\delta\lambda_1 - \delta\lambda_2) &= \frac{1}{\sqrt{2\pi}}(\alpha\delta N_1 + \alpha_{12}\delta N_2) \\ &= \frac{1}{\sqrt{2\pi}}(\alpha_{12}\delta N_1 + \alpha\delta N_2). \end{aligned} \tag{3.2.23}$$

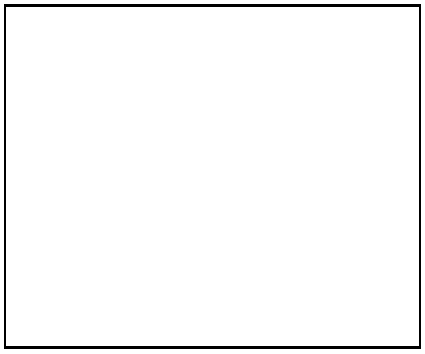

Figure 3.2.3: Phase diagram for $\alpha_{11} = \alpha_{22} \equiv \alpha < 0$. (a) $\alpha_{12} > 0$, (b) $\alpha < \alpha_{12} < 0$, (c) $\alpha_{12} < \alpha < 0$.

Thus, we get

$$\frac{\mathrm{d}N_2}{\mathrm{d}N_1} = 1 \quad \text{at} \quad (N_1, N_2) = (N_c, N_c). \tag{3.2.24}$$

Figure 3.2.3 illustrates the phase diagrams for various α_{12}. We can see that the repulsive (attractive) interspecies interaction enlarges (narrows) the stable region.

3) $\alpha_{11} > 0$, $\alpha_{22} < 0$

In this case, the species-1 atoms have repulsive interactions and the species-2 atoms have attractive interactions. In a neighborhood of $(N_1, N_2) = (0, 2\sqrt{2\pi}/5^{\frac{5}{4}}|\alpha_{22}|)$, the behavior of the boundary $N_2 = f(N_1)$ is the same as that in the previous case. We investigate here $\lim_{N_1 \to \infty} f(N_1)$. First we assume N_2 is sufficiently smaller than N_1. Setting $N_2 = 0$ in (3.2.7) and (3.2.8) gives

$$\lambda_1^5 - \lambda_1 - \sqrt{\frac{2}{\pi}} N_1 \alpha_{11} = 0, \tag{3.2.25}$$

$$1 - \lambda_2^{-4} - \frac{8}{\sqrt{\pi}} N_1 \alpha_{12} (\lambda_1^2 + \lambda_2^2)^{-\frac{5}{2}} = 0. \tag{3.2.26}$$

As seen from the condition (3.2.25), the width λ_1 gets larger as N_1 increases because of the repulsive intraspecies interaction. If $\alpha_{12} < 0$ (attractive interspecies interaction), we have $\lambda_2 < 1$ from (3.2.26) and $\lambda_2 \ll \lambda_1$ is satisfied. This condition is also satisfied for positive and small α_{12}. When $1 \ll \lambda_1$, $\lambda_2 \ll \lambda_1$, and $N_2 \ll N_1$, one gets from (3.2.7) and (3.2.8)

$$1 - \sqrt{\frac{2}{\pi}} N_1 \alpha_{11} \lambda_1^{-5} = 0, \tag{3.2.27}$$

$$1 - \lambda_2^{-4} - \sqrt{\frac{2}{\pi}} N_2 \alpha_{22} \lambda_2^{-5} - \frac{8}{\sqrt{\pi}} N_1 \alpha_{12} \lambda_1^{-5} = 0. \tag{3.2.28}$$

Since

$$\frac{\partial^2 \varepsilon}{\partial \lambda_1^2} = \frac{3}{2} N_1 \left(1 + 4 \sqrt{\frac{2}{\pi}} N_1 \alpha_{11} \lambda_1^{-5} \right) = \frac{15}{2} N_1 > 0, \tag{3.2.29}$$

and

$$\frac{\partial^2 \varepsilon}{\partial \lambda_1 \partial \lambda_2} = \frac{60}{\sqrt{\pi}} N_1 N_2 \alpha_{12} \lambda_1^{-6} \lambda_2 \approx 0, \tag{3.2.30}$$

we can use $\partial^2 \varepsilon / \partial \lambda_2^2 = 0$ instead of $\Delta = 0$. The condition $\partial^2 \varepsilon / \partial \lambda_2^2 = 0$ gives

$$1 + 3\lambda_2^{-4} + 4\sqrt{\frac{2}{\pi}} N_2 \alpha_{22} \lambda_2^{-5} - \frac{8}{\sqrt{\pi}} N_1 \alpha_{12} \lambda_1^{-5} = 0. \tag{3.2.31}$$

From (3.2.27), (3.2.28) and (3.2.31), we obtain the critical number of N_2,

$$N_{2c} = \frac{2\sqrt{2\pi}}{5^{\frac{5}{4}}} \frac{1}{|\alpha_{22}|} \left(1 - \frac{2^{\frac{5}{2}} \alpha_{12}}{\alpha_{11}} \right)^{-\frac{1}{4}}. \tag{3.2.32}$$

This implies that N_{2c} is independent of N_1 and thus $\lim_{N_1 \to \infty} N_{2c}/N_1 = 0$.

If α_{12} is positive and large enough, we expect that the species-2 condensate broadens in its size and N_{2c}/N_1 does not converge to zero as N_1 tends to infinity. We can pursue N_{2c} for a fixed large N_1 without using $\Delta = 0$ directly, as follows. We assume $\lambda_2^4 \gg 1$ for sufficiently large α_{12} and obtain from Eqs. (3.2.7) and (3.2.8)

$$1 = \sqrt{\frac{2}{\pi}} N_1 \alpha_{11} \lambda_1^{-5} + \frac{8}{\sqrt{\pi}} N_2 \alpha_{12} \left(\lambda_1^2 + \lambda_2^2 \right)^{-\frac{5}{2}}, \tag{3.2.33}$$

$$1 = \sqrt{\frac{2}{\pi}} N_2 \alpha_{22} \lambda_2^{-5} + \frac{8}{\sqrt{\pi}} N_1 \alpha_{12} \left(\lambda_1^2 + \lambda_2^2 \right)^{-\frac{5}{2}}. \tag{3.2.34}$$

Equations (3.2.33) and (3.2.34) give a relation for N_2/N_1 as a function of the ratio $\beta = \lambda_2/\lambda_1$,

$$\frac{N_2}{N_1} = \gamma(\beta) \equiv \frac{-\alpha_{11} + \alpha_{12} \left(\frac{1+\beta^2}{2} \right)^{-\frac{5}{2}}}{|\alpha_{22}| \beta^{-5} + \alpha_{12} \left(\frac{1+\beta^2}{2} \right)^{-\frac{5}{2}}}. \tag{3.2.35}$$

Figure 3.2.4 illustrates a function $\gamma(\beta)$ in (3.2.35). In the region $\beta \sim 0$, $\gamma(\beta) \sim \{(-\alpha_{11} + 2^{\frac{5}{2}} \alpha_{12})/|\alpha_{22}|\} \beta^5$. Therefore when $\alpha_{12} > 2^{-\frac{5}{2}} \alpha_{11}$, the maximum of $\gamma(\beta)$ determines the critical number of N_2. Explicit form of $\max_\beta \gamma(\beta)$ can be given in two special cases where $\zeta \equiv 2^{\frac{5}{2}} \alpha_{12}/\alpha_{11}$ is $1+$ and ∞.

(i) Setting $\zeta = 1 + \epsilon$ and expanding in ϵ give

$$\frac{N_{2c}}{N_1} = \max_\beta \gamma(\beta) \simeq \left(\frac{2}{7} \right)^{\frac{7}{2}} \frac{\alpha_{11}}{|\alpha_{22}|} \epsilon^{\frac{7}{2}}. \tag{3.2.36}$$

(ii) Supposing ζ is large and expanding in $1/\zeta$ give

$$\frac{N_{2c}}{N_1} = \max_\beta \gamma(\beta) \simeq 1 - \frac{1}{\zeta} \left\{ 1 + \left(\frac{|\alpha_{22}|}{\alpha_{11}} \right)^{\frac{2}{7}} \right\}^{\frac{7}{2}}. \tag{3.2.37}$$

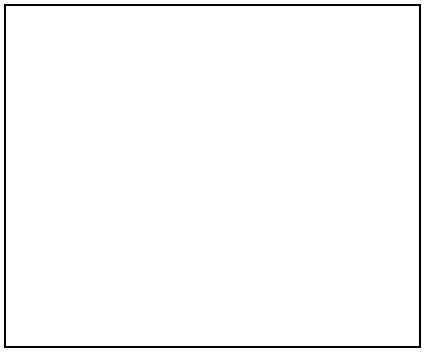

Figure 3.2.4: Function $\gamma(\beta)$ defined in (3.2.35). We set $\alpha_{11} : \alpha_{22} : \alpha_{12} = 1 : -4 : 2^{-\frac{3}{2}}$.

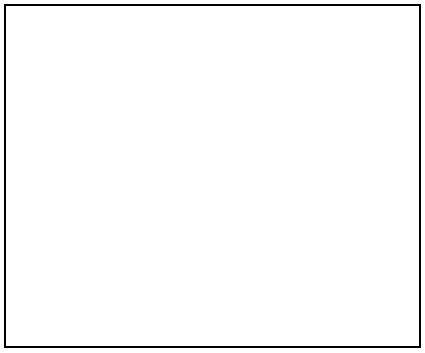

Figure 3.2.5: $\lim_{N_1 \to \infty} f(N_1)/N_1$ as a function of $2^{\frac{5}{2}}\alpha_{12}/\alpha_{11}$. We set $\alpha_{11} : \alpha_{22} = 1 : -4$.

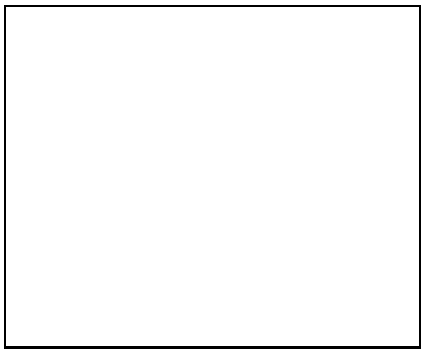

Figure 3.2.6: Phase diagram for $\alpha_{11} > 0$ and $\alpha_{22} < 0$. (a) $\alpha_{12} > 2^{-\frac{5}{2}}\alpha_{11}$, (b) $0 < \alpha_{12} < 2^{-\frac{5}{2}}\alpha_{11}$, (c) $\alpha_{12} < 0$.

Summarizing the above discussion, $\lim_{N_1\to\infty} f(N_1)/N_1$ as a function of $2^{\frac{5}{2}}\alpha_{12}/\alpha_{11}$ is illustrated in Fig. 3.2.5.

Figure 3.2.6 shows phase diagrams for various α_{12}. If $\alpha_{12} > 2^{-\frac{5}{2}}\alpha_{11}$, N_{2c} gets large proportional to N_1 by enlarging the width λ_2. On the other hand, in the case $\alpha_{12} < 2^{-\frac{5}{2}}\alpha_{11}$, the extent of the species-2 condensate remains small because of the attractive intraspecies interaction and its critical number converges to a finite number as N_1 increases.

3.2.4 Phase separation

In the experiments of two-component BEC [52]–[54], phase separation due to the gravitation and the repulsive interspecies interaction was observed. In this sub-section, we discuss the possibility of phase separation caused by the latter. For simplicity, we consider the case where

$$N_1 = N_2 \equiv N,\ \ a_{11} = a_{22} \equiv a,\ \ \omega_x = \omega_y \equiv \omega_\perp,\ \ \omega_z = \delta\omega_\perp. \tag{3.2.38}$$

First, we assume that the anisotropic parameter δ satisfies $\delta \geq 1$ (pancake-like trap). To discuss a possibility of phase separation, we generalize the trial functions into

$$\Psi_i(\boldsymbol{r}) = N^{\frac{1}{2}}\pi^{-\frac{3}{4}}(d_x d_y d_z)^{-\frac{1}{2}} \exp\left(-\frac{x^2}{2d_x^2} - \frac{y^2}{2d_y^2} - \frac{z^2}{2d_z^2}\right)\left(P_0 \pm \sqrt{2}P_1\frac{x}{d_x}\right). \tag{3.2.39}$$

Here $+$ $(-)$ corresponds to $i = 1$ $(i = 2)$, and real parameters P_0 and P_1 satisfy the relation $P_0^2 + P_1^2 = 1$, which is required by the normalization condition,

$$\int \mathrm{d}\boldsymbol{r}|\Psi_\mathrm{i}(\boldsymbol{r})|^2 = \mathrm{N}. \tag{3.2.40}$$

The non-zero value of P_1 detects the phase separation. Substitution of the trial functions (3.2.39) into (3.2.1) gives the energy as a function of the parameters d_x, d_y, d_z and P_1. In terms of dimensionless variables,

$$\varepsilon = \frac{E}{\hbar\omega_\perp},\ \ \alpha = \frac{a}{l_\perp},\ \ \alpha_{12} = \frac{a_{12}}{l_\perp},\ \ \lambda_x = \frac{d_x}{l_\perp},\ \ \lambda_y = \frac{d_y}{l_\perp},\ \ \lambda_z = \frac{d_z}{l_z}, \tag{3.2.41}$$

where $l_\perp = \sqrt{\hbar/(m\omega_\perp)}$, $l_z = \sqrt{\hbar/(m\omega_z)}$, the energy becomes

$$\begin{aligned}\varepsilon \ \ = \ \ & \frac{N}{2}\Big[(1+2P_1^2)(\lambda_x^2+\lambda_x^{-2}) + \lambda_y^2 + \lambda_y^{-2} + \delta(\lambda_z^2+\lambda_z^{-2}) \\ & +2\sqrt{\frac{2}{\pi}}\lambda_x^{-1}\lambda_y^{-1}\lambda_z^{-1}\delta^{1/2}\left\{\alpha N\left(-\frac{5}{4}P_1^4 + P_1^2 + 1\right)\right. \\ & \left.+\alpha_{12}N\left(\frac{11}{4}P_1^4 - 3P_1^2 + 1\right)\right\}\Big].\end{aligned} \tag{3.2.42}$$

The necessary condition for phase separation is

$$\frac{\partial\varepsilon}{\partial P_1^2} = 0,\ \ \frac{\partial\varepsilon}{\partial\lambda_k} = 0 \ \text{ at } \ 0 < P_1^2 \leq 1, \lambda_k > 0 \ \ (k = x, y, z). \tag{3.2.43}$$

Thus, the conditions:

$$\left.\frac{\partial\varepsilon}{\partial P_1^2}\right|_{P_1^2=0}=0,\quad \left.\frac{\partial\varepsilon}{\partial\lambda_k}\right|_{P_1^2=0}=0\ \ (k=x,y,z), \tag{3.2.44}$$

give the boundary curve of phase separation. Solving (3.2.44) gives

$$\lambda_x=\lambda_y=\left(\frac{2\alpha_{12}}{\alpha_{12}-\alpha}\right)^{\frac{1}{4}},\ \ \lambda_z=\delta^{\frac{1}{2}}\sqrt{\frac{2}{\pi}}N(\alpha_{12}-\alpha), \tag{3.2.45}$$

$$N=\frac{\sqrt{\pi}}{2}\frac{\sqrt{\alpha+\alpha_{12}+\sqrt{(\alpha+\alpha_{12})^2+8\delta^2\alpha_{12}(\alpha_{12}-\alpha)}}}{\delta(\alpha_{12}-\alpha)^{\frac{5}{4}}(2\alpha_{12})^{\frac{1}{4}}}. \tag{3.2.46}$$

If α_{12} is larger than α and N is larger than the value (3.2.46), phase separation occurs.

Second, we consider the case, $\delta<1$ (cigar-like trap). Using trial functions

$$\Psi_i(\boldsymbol{r})=N^{\frac{1}{2}}\pi^{-\frac{3}{4}}(d_xd_yd_z)^{-\frac{1}{2}}\exp\left(-\frac{x^2}{2d_x^2}-\frac{y^2}{2d_y^2}-\frac{z^2}{2d_z^2}\right)\left(P_0\pm\sqrt{2}P_1\frac{z}{d_z}\right), \tag{3.2.47}$$

we can calculate the critical number of phase separation,

$$N=\frac{\sqrt{2\pi}}{4}\frac{\delta^{\frac{3}{2}}(\alpha+\alpha_{12})+\sqrt{\delta^3(\alpha+\alpha_{12})^2+8\delta\alpha_{12}(\alpha_{12}-\alpha)}}{(\alpha_{12}-\alpha)^{\frac{5}{4}}(2\alpha_{12})^{\frac{3}{4}}}. \tag{3.2.48}$$

In the limit $\delta\to 1$, (3.2.46) and (3.2.48) coincide. The boundary curves of the phase separation for this case are shown in Fig. 3.2.1 (the dashed lines). We see that the larger interspecies interaction causes phase separation for the smaller number of particles.

3.3 Long-range interacting bosons confined in traps

Throughout this paper except this section, we consider a system of neutral bosonic atoms under magnetic traps. The interaction between neutral atoms is well approximated by the delta function, $V(\boldsymbol{r})=g\,\delta(\boldsymbol{r})$. We may think of the other limit, that is, the long-range interaction like a Coulomb potential, $V(\boldsymbol{r})=g/|\boldsymbol{r}|$. In principle, we believe that the Bose-Einstein condensation occurs for all bosonic atoms and molecules with and without charges.

In this section, we consider the properties of the Bose-Einstein condensate of long-ranged interacting bosons confined in traps. The problem is rather academic, but turns out to be quite interesting: The condensates in the short-ranged and long-ranged cases have different properties.

3.3.1 Stability of the ground state

We again start from the Ginzburg-Pitaevskii-Gross energy functional,

$$E[\Psi] = \int \mathrm{d}\boldsymbol{r} \left[\frac{\hbar^2}{2m} |\nabla\Psi|^2 + \frac{1}{2} m\omega^2 r^2 |\Psi|^2 \right] + \frac{1}{2} \int \mathrm{d}\boldsymbol{r} \int \mathrm{d}\boldsymbol{r}' \, U(\boldsymbol{r}-\boldsymbol{r}') \, |\Psi(\boldsymbol{r})|^2 \, |\Psi(\boldsymbol{r}')|^2 \,, \tag{3.3.1}$$

where the trap is assumed to be an isotropic harmonic potential, and

$$U(\boldsymbol{r}) = g/\,|\boldsymbol{r}|\,. \tag{3.3.2}$$

The coupling constant g can be positive or negative in this sub-section.

We assume that the ground state wavefunction $\Psi(\boldsymbol{r})$ depends only on $r = |\boldsymbol{r}|$. With this assumption and an integral formula for a fixed $\boldsymbol{r}$,

$$\int_0^\pi \sin\theta \, \mathrm{d}\theta \left(r^2 + r'^2 - 2rr'\cos\theta \right)^{-1/2} = \begin{cases} 2/r & (\text{for } r' < r) \\ 2/r' & (\text{for } r' > r), \end{cases} \tag{3.3.3}$$

the last term in (3.3.1) is written as

$$\frac{g}{2} \int \mathrm{d}\boldsymbol{r} \int \mathrm{d}\boldsymbol{r}' \, \frac{1}{|\boldsymbol{r}-\boldsymbol{r}'|} \, |\Psi(\boldsymbol{r})|^2 \, |\Psi(\boldsymbol{r}')|^2 = 16\pi^2 g \int_0^\infty \mathrm{d}r \, r^2 \, |\Psi(\boldsymbol{r})|^2 \int_r^\infty \mathrm{d}r' \, r' \, |\Psi(\boldsymbol{r}')|^2 \,. \tag{3.3.4}$$

We calculate the ground state energy by the variational method. As a trial function, we choose

$$\Psi(\boldsymbol{r}) = C \exp\left(-\frac{r^2}{2d^2} \right), \tag{3.3.5}$$

where C and d are real constants to be determined. The particle number N and the ground state energy are calculated as

$$N = C^2 \pi^{3/2} d^3, \tag{3.3.6}$$

$$E = \frac{3\pi^{3/2}\hbar^2 C^2}{4m} d + \frac{3\pi^{3/2} m\omega^2 C^2}{4} d^5 + \frac{\sqrt{2}}{2} \pi^{5/2} g \, C^4 d^5. \tag{3.3.7}$$

By use of (3.3.6), we eliminate the normalization constant C in (3.3.7). The result is

$$E(d) = \frac{3\hbar^2 N}{4md^2} + \frac{3m\omega^2 N d^2}{4} + \frac{N^2 g}{(2\pi)^{1/2} d}. \tag{3.3.8}$$

It is convenient to introduce a dimensionless parameter λ,

$$\lambda \equiv d/d_0, \tag{3.3.9}$$

where $d_0 \equiv [\hbar/(m\omega)]^{1/2}$. Then, (3.3.8) is rewritten as

$$E(\lambda) = \frac{1}{2} N\hbar\omega \left[\frac{3}{2}(\lambda^{-2} + \lambda^2) + \sigma\lambda^{-1} \right], \tag{3.3.10}$$

where

$$\sigma \equiv \sqrt{\frac{2}{\pi}}\,\frac{Ng}{\hbar\omega}\left(\frac{m\omega}{\hbar}\right)^{1/2}. \tag{3.3.11}$$

We can show that $E(\lambda)$ has an absolute minimum irrespective of the sign of σ, that is, the condensate of long-range interacting bosons under harmonic traps is stable both for repulsive and attractive interactions.

It is interesting to compare the above result with that for the delta function case. The same calculation with $U(\boldsymbol{r}) = g\,\delta(\boldsymbol{r})$ gives

$$E_{\rm d}(\lambda) = \frac{1}{2}N\hbar\omega\left[\frac{3}{2}(\lambda^{-2}+\lambda^{2}) + \sigma_{\rm d}\lambda^{-3}\right], \tag{3.3.12}$$

$$\sigma_{\rm d} \equiv \sqrt{\frac{2}{\pi}}\,\frac{mgN}{4\pi\hbar^{2}}\left(\frac{m\omega}{\hbar}\right)^{1/2}. \tag{3.3.13}$$

A clear difference between (3.3.10) and (3.3.12) is the λ-dependence of the interaction term. The powers of λ, λ^{-1} in (3.3.10) and λ^{-3} in (3.3.12), are easily understood from the scaling property of the interaction potential $U(\boldsymbol{r})$ under the transformation $\boldsymbol{r} \to \lambda\boldsymbol{r}$. In the case of the long-range interaction, the kinetic term proportional to λ^{-2} is dominant over the interaction term proportional to λ^{-1} as $\lambda \to 0$. This explains why the collapse of the condensate does not occur for the long-range interacting bosons confined in traps.

3.3.2 Charged bosons confined in ion traps

We consider the Bose-Einstein condensate of charged bosons confined in ion traps. Based on the results obtained in the sub-section 3.3.1, we further examine the ground state energy. Setting $g = e^{2}$, e being the electric charge, we have

$$E(\lambda) = \frac{1}{2}N\hbar\omega\left[\frac{3}{2}(\lambda^{-2}+\lambda^{2}) + \sigma_{\rm e}\lambda^{-1}\right], \tag{3.3.14}$$

where

$$\sigma_{\rm e} \equiv \sqrt{\frac{2}{\pi}}\,\frac{Ne^{2}}{\hbar\omega}\left(\frac{m\omega}{\hbar}\right)^{1/2}. \tag{3.3.15}$$

We note that $\sigma_{\rm e}$ is positive.

We minimize $E(\lambda)$ with respect to λ. The condition, $\partial E/\partial\lambda = 0$, gives

$$3\lambda^{4} - 3 - \sigma_{\rm e}\lambda = 0. \tag{3.3.16}$$

For a weak interaction case where $\sigma_{\rm e}$ is small, the approximate solution of (3.3.16) is $\lambda \approx 1 + (\sigma/12)$. Using this in (3.3.14), we obtain

$$E = \frac{3}{2}N\hbar\omega\left(1 + \frac{\sigma_{\rm e}}{3}\right). \tag{3.3.17}$$

In the non-interaction limit $\sigma_{\rm e} \to 0$, the exact result $E = 3N\hbar\omega/2$ for harmonic oscillators is recovered.

For a strong interaction case, $\sigma_{\rm e} \gg 1$, (3.3.16) is approximately solved to have

$$\lambda = 3^{-1/3}\sigma_{\rm e}^{1/3} + \sigma_{\rm e}^{-1}. \tag{3.3.18}$$

Then, the ground state energy is obtained as

$$E = \frac{1}{4}3^{4/3}N\hbar\omega\sigma_{\rm e}^{2/3} + \frac{1}{4}3^{5/3}N\hbar\omega\sigma_{\rm e}^{-2/3}. \tag{3.3.19}$$

The dominant term in (3.3.19) shows the N-dependence of the energy explicitly as

$$E = \frac{3^{4/3}2^{2/3}}{4(2\pi)^{1/3}}m^{1/3}\omega^{2/3}e^{4/3}N^{5/3}. \tag{3.3.20}$$

This result corresponds to the Thomas-Fermi approximation in the sense that the kinetic energy is negligible. There should be no confusion with the formula (C.6) where the interaction is the delta function type.

3.4 Summary

We have investigated the static properties of Bose-Einstein condensates. In Sec. 3.1, we have studied the ground state properties of a Bose-Einstein condensate with repulsive or attractive inter-atomic interaction confined in axially symmetric magnetic trap. The gaussian trial wavefunction has two variational parameters which are determined by minimum conditions of the Ginzburg-Pitaevskii-Gross energy functional with harmonic potential terms. For the repulsive case (sub-section 3.1.2), we find four situations according to which terms appearing in (3.1.13) and (3.1.14) can be neglected in a first approximation. The approximation conditions in each situation are summarized in Fig. 3.1.1 with the anisotropy parameter of the trap $\delta = \omega_z/\omega_\perp$ and the relative strength of the inter-atomic interaction $G_\perp = (2/\pi)^{1/2}Na(m\omega_\perp/\hbar)^{1/2}$. For all cases, we can estimate the variational parameters $s_\perp$ and s_z or equivalently $d_\perp$ and d_z, the aspect ratio of the condensate $A = d_z/d_\perp$ and the energy E at the minimum point. In the cases *1)* and *2)*, we have used common approximations to both of the two minimum conditions (3.1.13) and (3.1.14). For the case that the inter-atomic interaction is sufficiently weak (resp. strong) in both xy- and z-directions, the approximation condition is given by (3.1.24) (resp. (3.1.31)) corresponding to the region I, the weak interaction case (resp. the region II, the strong interaction case). The energy (3.1.35) and the one obtained from the three-dimensional Thomas-Fermi approximation have the same N-dependence, proportinal to $N^{7/5}$. It is interesting that, when the anisotropy parameter δ is much larger or smaller than unity, there exist cases where we can give different description to each direction. In the case *3)*, we have first considered the case that the effect of the inter-atomic interaction is negligible in xy-direction but important in z-direction. This occurs when the trap is cigar-shaped. The approximation condition is obtained as (3.1.40), corresponding to the region III, the intermediate case-1. The energy (3.1.46) consists of two parts. The first term describes the two-dimensional

harmonic oscillator. The N-dependence of the second term is $N^{5/3}$ which is the same for the one-dimensional Thomas-Fermi approximation. Next, we have considered the case that the effect of the inter-atomic interaction is dominant in xy-direction but negligible in z-direction. This is realized when the trap is pancake-shaped. We obtain the approximation condition as (3.1.52), corresponding to the region IV, the intermediate case-2. We find here that the second term in the energy (3.1.57) is proportional to $N^{3/2}$, as the energy obtained from the two-dimensional Thomas-Fermi approximation. To summarize, in the above results, the N-dependence of the energy is consistent with the geometrical shape of the condensate and the dimensionality of the Thomas-Fermi approximation. For the attractive case (sub-section 3.1.3), the energy function (3.1.10) has only a local (not an absolute) minimum. As we expect, the local minimum of the energy disappears for some critical value of $G_\perp$, which implies the instability (collapse) of the condensate. By setting the value of the determinant of the Hessian matrix Δ at the minimum point to be zero (3.1.61) with the minimum conditions (3.1.13) and (3.1.14), we calculate the critical value $G_{\perp,\mathrm{c}}$ and obtain the critical number of particles N_c. First, for the case that the trap is nearly spherical, N_c is estimated as (3.1.70), which is essentially the same as the one obtained by Fetter [32]. Next, for the cigar-shaped trap, N_c, estimated as (3.1.77), is larger than the critical number for the nearly spherical trap. The aspect ratio of the condensate A at $G_\perp = G_{\perp,\mathrm{c}}$ (3.1.75) is the order of unity. Similarly, for the pancake-shaped trap, we obtain the critical number as (3.1.84), which is larger than the ones for the nearly spherical and the cigar-shaped traps.

In Sec. 3.2, we have investigated the stability of a two-component Bose-Einstein condensate. For various choices of "dimensionless" s-wave scattering lengths α_{ij}, we have constructed the phase diagram in N_1N_2-plane where N_i is the number of species-i ($i = 1, 2$) atoms. Recall that α_{ij} is related to the s-wave scattering length a_{ij} by (3.2.5). We summarize the salient points of the results, paying attention to the collapse.
1) $a_{11} > 0, a_{22} > 0$. A sufficiently strong attractive interaction between the different species can overcome repulsive interactions within each condensate, which leads to their collapse.
2) $a_{11} < 0, a_{22} < 0$. A repulsive (attractive) interaction between the different species makes the critical number of atoms larger (smaller) than the one for one-component case.
3) $a_{11} > 0, a_{22} < 0$. For a sufficiently strong repulsive interspecies interaction, the critical number of species-2 atoms, N_{2c}, increases as the number of species-1 atoms, N_1. For an attractive interspecies interaction, N_{2c} decreases and approaches a finite value as N_1 increases.

A basic assumption of our analysis has been the gaussian trial functions (3.2.3). While the gaussian ansatz is reasonable for the coexisting condensates in magnetic traps, there is no guarantee that (3.2.3) exhausts all the possible stable states. Thus, in the subsection 3.2.4, we have modified the trial functions, and discussed the possibility of the phase separations. In the pancake trap case, we generalize the trial functions into (3.2.39), and obtain the critical number of atoms (3.2.46), above which the phase separation occurs. In the cigar trap case, the trial functions are modified as (3.2.47), and the critical number of atoms for the phase separation is (3.2.48). The boundary curves of the phase separation in the isotropic limit are plotted by the dashed lines in Fig. 3.2.1.

In Sec. 3.3, we have considered the properties of the Bose-Einstein condensate of long-ranged interacting bosons confined in traps. As in the other sections in this chapter, we have chosen a gaussian function (3.3.5) as a trial function, and obtained the energy function (3.3.10). The energy (3.3.10) has an absolute minimum irrespective of the sign of the strength of the interaction, σ, and therefore the condensate of long-range interacting bosons under traps is stable. By use of the minimum conditions of the energy (3.3.16), we have investigated the ground state energy. For the weak interation case, the energy (3.3.17) is approximately equal to that for harmonic oscillators. For the strong interaction case, the leading term of the energy is proportional to $N^{5/3}$. The results obtained in this sub-section may give useful information, when the Bose-Einstein condensation for bosonic ions under ion traps will be observed in future.

Chapter 4

Dynamical Properties of Bose-Einstein Condensates

In this chapter, we investigate the dynamical properties of Bose-Einstein condensates. In Sec. 4.1, we first investigate the stability of the wavefunction of the D-dimensional nonlinear Schrödinger equation with harmonic potential terms [76]. For the repulsive case, we prove that the wavefunction is absolutely stable. For the attractive case, by extending the Zakharov's theory [77, 78], we show that the singularity of the wavefunction surely emerges in a finite time when the total energy of the system is negative, and even when the energy is positive, the wavefunction collapses in a finite time for a certain class of the initial conditions. In Sec. 4.2, based on the results obtained in Sec. 4.1, we investigate the dynamics of the condensates analytically, and prove that the singularity of solution emerges in a finite time when the total energy of the system is both negative and positive [41]–[43]. In the analysis, the initial wavefunction is assumed to be gaussian with two parameters. We present a formula for the critical number of atoms. Further, by improving our analysis quantitatively, we apply it to the assembly of ^{7}Li atoms. Then, within a reasonable parameter region, the estimated critical number for ^{7}Li atoms is comparable with the upper bound for the number of atoms in the recent experiment of BEC.

4.1 Stability of the D-dimensional nonlinear Schrödinger equation under confined potential

We investigate the stability of the wavefunction of the D-dimensional nonlinear Schrödinger equation with harmonic potential terms. The analysis in this section is a mathematical introduction to the problem of the collapse of the condensate in Sec. 4.2.

Let $x \equiv (x_1, x_2, \cdots, x_D)$ be a point on a D-dimensional Euclidian space $\mathbf{R}^D$. As usual, time is denoted by t. Then the equation for the wavefunction $\phi(x,t)$ is expressed as

$$2\mathrm{i}\frac{\partial \phi}{\partial t} = -\Delta\phi + V(x)\phi + g|\phi|^2\phi. \tag{4.1.1}$$

Here $\Delta \equiv \sum_{n=1}^{D} \partial^2/\partial x_n^2$ is the D-dimensional Laplace operator, $g = \pm 1$, and

$$V(x) = \sum_{n=1}^{D} \nu_n^2 x_n^2, \quad \nu_n > 0. \tag{4.1.2}$$

The coupling constant $g = +1$ ($g = -1$) represents the repulsive (attractive) self-interaction. The numerical factors in (4.1.1) with (4.1.2) are chosen for convenience.

Equation (4.1.1) without external potential ($V(x) = 0$) has been studied by many researchers [77]–[86]. Zakharov [77] and Zakharov and Synakh [78] studied the multi-dimensional nonlinear Schrödinger equation ($D = 2, 3$) for the attractive case ($g = -1$) as models of Langmuir waves in plasma and light waves in nonlinear media. They showed that, when the total energy of the system is negative, the singularity surely emerges in the wavefunction in a finite time. The phenomenon is termed the collapse. Weinstein [80] derived the condition that the collapse occurs even when the energy of the system is positive. Then, it is extremely interesting to examine how the condition obtained by Weinstein is changed when the harmonic potential terms (4.1.2) are added.

4.1.1 Repulsive case

We deal with the repulsive case, namely $g = +1$, and show that the wavefunction $\phi(x, t)$ in Eq. (4.1.1) is absolutely stable for $D \geq 1$, when the wavefunction is confined in the harmonic potential (4.1.2).

Equation (4.1.1) has two constants of motion,

$$N = \int |\phi|^2 \mathrm{d}x, \tag{4.1.3}$$

$$H = \int \left(|\nabla\phi|^2 + V(x)|\phi|^2 + \frac{g}{2}|\phi|^4 \right) \mathrm{d}x, \tag{4.1.4}$$

corresponding to the conservations of particle number N and energy H, respectively. Here and hereafter, $\mathrm{d}x = \mathrm{d}x_1 \cdots \mathrm{d}x_D$. We define a norm, $\| \cdot \|_p$, as

$$\|F\|_p \equiv \left(\int_{\mathbf{R}^D} |F(x)|^p \mathrm{d}x \right)^{1/p}. \tag{4.1.5}$$

For $g = +1$, (4.1.4) with (4.1.2) reads

$$\begin{aligned} H &= \int \left(|\nabla\phi|^2 + \sum_{n=1}^{D} \nu_n^2 x_n^2 |\phi|^2 + \frac{1}{2}|\phi|^4 \right) \mathrm{d}x \\ &= \|\nabla\phi\|_2^2 + \sum_{n=1}^{D} \nu_n^2 \|x_n\phi\|_2^2 + \frac{1}{2}\|\phi\|_4^4. \end{aligned} \tag{4.1.6}$$

Because the third term in the second line of Eq. (4.1.6) is positive, we have inequalities,

$$H > \|\nabla\phi\|_2^2 + \sum_{n=1}^{D} \nu_n^2 \|x_n\phi\|_2^2 \geq \|\nabla\phi\|_2^2 + \Lambda^2 \|x\phi\|_2^2, \tag{4.1.7}$$

where the constant Λ is the smallest among $\{\nu_n\}$,

$$\Lambda \equiv \min(\{\nu_n\}). \tag{4.1.8}$$

Further, by applying the Cauchy-Schwarz inequality (the uncertainty relation in physics),

$$\|\nabla\phi\|_2^2 \, \|x\phi\|_2^2 \geq \left(D\|\phi\|_2^2/2\right)^2 = (DN/2)^2, \tag{4.1.9}$$

to (4.1.7), we obtain

$$H > \|\nabla\phi\|_2^2 + (\Lambda DN/2)^2 \|\nabla\phi\|_2^{-2} \geq \Lambda DN. \tag{4.1.10}$$

From (4.1.10), we see that $\|\nabla\phi\|_2$ is bounded, and thus the wavefunction $\phi(x,t)$ is absolutely stable for the repulsive case.

4.1.2 Attractive case

Next, we consider the attractive case, $g = -1$. To investigate the time-evolution of the wavefunction $\phi(x,t)$, we introduce the expectation value of the square of the radius, $|x|^2 = x_1^2 + x_2^2 + \cdots + x_D^2$, with respect to ϕ,

$$\langle |x|^2(t) \rangle \equiv \|x\phi(t)\|_2^2 = \int |x|^2 |\phi(x,t)|^2 \mathrm{d}x. \tag{4.1.11}$$

The role of this quantity, which should be positive by definition, is fundamental in the Zakharov's theory of the stability [77, 78]. From (4.1.1) and (4.1.11), we get

$$\begin{aligned} \frac{\mathrm{d}}{\mathrm{d}t}\langle |x|^2 \rangle &= \frac{1}{\mathrm{i}} \int (\phi^* x \cdot \nabla\phi - \phi \, x \cdot \nabla\phi^*) \, \mathrm{d}x \\ &= 2 \, \mathrm{Im} \int \phi^* x \cdot \nabla\phi \, \mathrm{d}x, \end{aligned} \tag{4.1.12}$$

where the superscript $*$ means the complex conjugate. By differentiating (4.1.12) with respect to t and using Eq. (4.1.1) again, we obtain [34]

$$\frac{\mathrm{d}^2}{\mathrm{d}t^2}\langle |x|^2 \rangle = 2H - \int (2V(x) + x \cdot \nabla V(x)) |\phi|^2 \mathrm{d}x - \frac{1}{2}(D-2) \, \|\phi\|_4^4. \tag{4.1.13}$$

Substitution of (4.1.2) into (4.1.13) yields the equation of motion for $\langle |x|^2 \rangle$,

$$\frac{\mathrm{d}^2}{\mathrm{d}t^2}\langle |x|^2 \rangle = 2H - 4\Lambda^2 \langle |x|^2 \rangle - f(t), \tag{4.1.14}$$

where

$$f(t) \equiv 4 \sum_{n=1}^{D} (\nu_n^2 - \Lambda^2) \|x_n \phi(t)\|_2^2 + \frac{1}{2}(D-2) \, \|\phi(t)\|_4^4, \tag{4.1.15}$$

with Λ being defined by (4.1.8). Note that $f(t) \geq 0$, if $D \geq 2$. A general solution of the differential equation (4.1.14) is

$$\langle |x|^2 \rangle = \frac{H}{2\Lambda^2} + A\sin(2\Lambda t + \theta_0) - \frac{1}{2\Lambda}\int_0^t f(u)\sin[2\Lambda(t-u)]\mathrm{d}u, \tag{4.1.16}$$

where A and θ_0 are constants. Without loss of generality, we assume that

$$A > 0, \quad 0 \leq \theta_0 < 2\pi. \tag{4.1.17}$$

For the later convenience, we define a function, $l(\theta)$,

$$l(\theta) \equiv \frac{H}{2\Lambda^2} + A\sin\theta, \tag{4.1.18}$$

with

$$\theta \equiv 2\Lambda t + \theta_0. \tag{4.1.19}$$

Then, (4.1.16) becomes

$$\langle |x|^2 \rangle = l(\theta(t)) - \frac{1}{2\Lambda}\int_0^t f(u)\sin[2\Lambda(t-u)]\mathrm{d}u. \tag{4.1.20}$$

The constants A and θ_0 are related to the initial conditions of the wavefunction. Using (4.1.11) and (4.1.16) in (4.1.20), we get

$$\begin{aligned} \langle |x|^2 \rangle|_{t=0} &= \int |x|^2 |\phi_0(x)|^2 \mathrm{d}x \\ &= l(\theta_0) = \frac{H}{2\Lambda^2} + A\sin\theta_0, \end{aligned} \tag{4.1.21}$$

where

$$\phi_0(x) \equiv \phi(x, t=0). \tag{4.1.22}$$

Differentiation of (4.1.16) with respect to t gives

$$\frac{\mathrm{d}}{\mathrm{d}t}\langle |x|^2 \rangle = 2\Lambda A\cos(2\Lambda t + \theta_0) - \int_0^t f(u)\cos[2\Lambda(t-u)]\mathrm{d}u. \tag{4.1.23}$$

Then, from (4.1.12) and (4.1.23), we get

$$\begin{aligned} \left.\frac{\mathrm{d}}{\mathrm{d}t}\langle |x|^2 \rangle\right|_{t=0} &= \frac{1}{\mathrm{i}}\int (\phi_0^* x \cdot \nabla\phi_0 - \phi_0\, x \cdot \nabla\phi_0^*)\,\mathrm{d}x \\ &= 2\Lambda A\cos\theta_0. \end{aligned} \tag{4.1.24}$$

Solving (4.1.21) and (4.1.24), we obtain

$$A = \left[\left(\langle |x|^2 \rangle|_{t=0} - \frac{H}{2\Lambda^2}\right)^2 + \left(\frac{1}{2\Lambda}\left.\frac{\mathrm{d}}{\mathrm{d}t}\langle |x|^2 \rangle\right|_{t=0}\right)^2\right]^{1/2}, \tag{4.1.25}$$

$$\sin\theta_0 = \left(\langle|x|^2\rangle|_{t=0} - \frac{H}{2\Lambda^2}\right)/A, \tag{4.1.26}$$

$$\cos\theta_0 = \left(\frac{1}{2\Lambda}\frac{\mathrm{d}}{\mathrm{d}t}\langle|x|^2\rangle\Big|_{t=0}\right)/A. \tag{4.1.27}$$

In the following, we analyze the solution (4.1.16) or equivalently (4.1.20) in the case that the spatial dimension is larger than or equal to two, namely $D \geq 2$.

1) $H \leq 0$ case

We consider the case that the total energy of the system H is less than or equal to zero. In this case, we show that the wavefunction surely collapses in a finite time.

From (4.1.21), $l(\theta_0)$ should be positive because of the positivity of $\langle|x|^2\rangle$ defined by (4.1.11), and therefore the constant A should satisfy

$$A > \left|\frac{H}{2\Lambda^2}\right| = -\frac{H}{2\Lambda^2}. \tag{4.1.28}$$

When (4.1.28) is satisfied, there exist two zero points of $l(\theta)$ which lie in $0 \leq \theta \leq \pi$. We write them as θ_+ and θ_- ($0 \leq \theta_- < \pi/2 < \theta_+ \leq \pi$). Explicitly, $\theta_\pm$ are given by

$$\theta_+ = \pi - \mathrm{Arcsin}\left(\frac{-H}{2\Lambda^2 A}\right), \tag{4.1.29}$$

$$\theta_- = \mathrm{Arcsin}\left(\frac{-H}{2\Lambda^2 A}\right). \tag{4.1.30}$$

Here and hereafter, the region (branch) of $\mathrm{Arcsin}\, x$ is defined to be $[-\pi/2, +\pi/2]$. Then, the constant θ_0 should be

$$\theta_- < \theta_0 < \theta_+. \tag{4.1.31}$$

Since the function $f(t)$ defined by (4.1.15) is larger than or equal to zero when $D \geq 2$, and $\sin[2\Lambda(t-u)]$ appearing in (4.1.16) is also larger than or equal to zero for $0 \leq t \leq \frac{\pi}{2\Lambda}$, we obtain an inequality,

$$\langle|x|^2\rangle \leq l(\theta(t)), \tag{4.1.32}$$

for $0 \leq t \leq \frac{\pi}{2\Lambda}$ or equivalently $\theta_0 \leq \theta \leq \theta_0 + \pi$. The function $l(\theta(t))$ becomes surely negative for some value of t which lies in $0 \leq t \leq \frac{\pi}{2\Lambda}$, when (4.1.28) and (4.1.31) are satisfied. Then, from the inequality (4.1.32), $\langle|x|^2\rangle$ should also be negative for some value of t, $0 \leq t \leq \frac{\pi}{2\Lambda}$. This contradicts to the definition of $\langle|x|^2\rangle$ (4.1.11) and implies the development of the singularity, characterized by the divergence of $\|\nabla\phi\|_2$, in a finite time defined as t_0. In fact, from the Cauchy-Schwarz inequality (4.1.9), we see that $\|\nabla\phi\|_2$ tends to infinity when $\langle|x|^2\rangle$ goes to zero. It is known that the instant t_0 may differ from the moment at which $\langle|x|^2\rangle$ vanishes, defined as t_c, and that t_0 is less than or equal to t_c, in general [85]. We call t_c the collapse-time in this paper.

We can show that $\sup_{x\in\mathbf{R}^D}|\phi(x,t)|$ tends to infinity when $\|\nabla\phi\|_2$ diverges. This problem has been discussed also in Refs. [79, 45]. For $g = -1$, the energy (4.1.4) with the harmonic

potential (4.1.2) is written as

$$\begin{aligned} H &= \int \left(|\nabla\phi|^2 + \sum_{n=1}^{D} \nu_n^2 x_n^2 |\phi|^2 - \frac{1}{2}|\phi|^4 \right) \mathrm{d}x \\ &= \|\nabla\phi\|_2^2 + \sum_{n=1}^{D} \nu_n^2 \|x_n\phi\|_2^2 - \frac{1}{2}\|\phi\|_4^4. \end{aligned} \tag{4.1.33}$$

Then, the following inequalities hold,

$$\begin{aligned} \|\phi\|_4^4 &= -2H + 2\|\nabla\phi\|_2^2 + 2\sum_{n=1}^{D} \nu_n^2 \|x_n\phi\|_2^2 \\ &\geq -2H + 2\|\nabla\phi\|_2^2 + 2\Lambda^2 \langle |x|^2 \rangle \\ &\geq -2H + 2\|\nabla\phi\|_2^2 + 2(\Lambda D N/2)^2 \|\nabla\phi\|_2^{-2}. \end{aligned} \tag{4.1.34}$$

In deriving the third line of (4.1.34), we have used (4.1.9). Further, combining an inequality

$$\|\phi\|_4^4 \leq \left(\sup_{x\in\mathbf{R}^D} |\phi(x,t)| \right)^2 \|\phi\|_2^2 = \left(\sup_{x\in\mathbf{R}^D} |\phi(x,t)| \right)^2 N, \tag{4.1.35}$$

with (4.1.34), we find that $\sup_{x\in\mathbf{R}^D} |\phi(x,t)|$ goes to infinity when $\|\nabla\phi\|_2$ diverges.

From the inequality (4.1.32), we see that $\langle |x|^2 \rangle$ vanishes before $l(\theta(t))$ reaches zero at $\theta = \theta_+$. Thus, by using (4.1.19), we can obtain an upper bound of the collapse-time, $t_{\mathrm{c},M}$,

$$t_{\mathrm{c},M} = \frac{1}{2\Lambda}(\theta_+ - \theta_0). \tag{4.1.36}$$

When $\theta_0 \leq \pi/2$, namely $\frac{\mathrm{d}}{\mathrm{d}t}\langle |x|^2 \rangle\Big|_{t=0} \geq 0$, from (4.1.26) we get

$$\theta_0 = \mathrm{Arcsin}\left(\frac{\langle |x|^2 \rangle|_{t=0}}{A} - \frac{H}{2\Lambda^2 A} \right). \tag{4.1.37}$$

Substituting (4.1.29) and (4.1.37) into (4.1.36), we have

$$\begin{aligned} t_{\mathrm{c},M} &= \frac{1}{2\Lambda}\left[\pi - \mathrm{Arcsin}\left(\frac{-H}{2\Lambda^2 A} \right) - \mathrm{Arcsin}\left(\frac{\langle |x|^2 \rangle|_{t=0}}{A} - \frac{H}{2\Lambda^2 A} \right) \right] \\ &= \frac{1}{2\Lambda}(\pi/2 + \mathrm{Arcsin}\,\xi), \end{aligned} \tag{4.1.38}$$

where ξ is defined as

$$\begin{aligned} \xi \equiv & \left[\left(\langle |x|^2 \rangle|_{t=0} - \frac{H}{2\Lambda^2} \right)^2 + \left(\frac{1}{2\Lambda} \frac{\mathrm{d}}{\mathrm{d}t}\langle |x|^2 \rangle\Big|_{t=0} \right)^2 \right]^{-1} \\ & \times \left[\frac{1}{2\Lambda} \frac{\mathrm{d}}{\mathrm{d}t}\langle |x|^2 \rangle\Big|_{t=0} \sqrt{ \langle |x|^2 \rangle|_{t=0} \left(\langle |x|^2 \rangle|_{t=0} - \frac{H}{\Lambda^2} \right) + \left(\frac{1}{2\Lambda} \frac{\mathrm{d}}{\mathrm{d}t}\langle |x|^2 \rangle\Big|_{t=0} \right)^2 } \right. \\ & \left. + \frac{H}{2\Lambda^2} \left(\langle |x|^2 \rangle|_{t=0} - \frac{H}{2\Lambda^2} \right) \right]. \end{aligned} \tag{4.1.39}$$

In deriving (4.1.38), we have used a formula,

$$\begin{aligned} &\mathrm{Arcsin}\,\eta - \mathrm{Arcsin}\,\zeta \\ &= \mathrm{Arcsin}\left(\eta\sqrt{1-\zeta^2} - \zeta\sqrt{1-\eta^2}\right), \end{aligned} \tag{4.1.40}$$

for $0 \leq \eta \leq 1$ and $0 \leq \zeta \leq 1$.

When $\theta_0 \geq \pi/2$ namely $\frac{\mathrm{d}}{\mathrm{d}t}\langle|x|^2\rangle\Big|_{t=0} \leq 0$, θ_0 becomes

$$\theta_0 = \pi - \mathrm{Arcsin}\left(\frac{\langle|x|^2\rangle|_{t=0}}{A} - \frac{H}{2\Lambda^2 A}\right), \tag{4.1.41}$$

instead of (4.1.37). In spite of this change, we obtain $t_{\mathrm{c},M}$ just the same as (4.1.38).

2) $H > 0$ case

For the $H \leq 0$ case, we have shown that the wavefunction surely collapses in a finite time, regardless of the initial condition on the wavefunction $\phi_0(x)$. Here we prove that even when the total energy H is positive, the collapse of wavefunction occurs in a finite time for a certain class of the initial conditions. We investigate such conditions according to the value of θ_0, as follows.

We first consider the case that $0 \leq \theta_0 \leq \pi/2$, which is equivalent to

$$\langle|x|^2\rangle|_{t=0} \geq \frac{H}{2\Lambda^2}, \qquad \frac{\mathrm{d}}{\mathrm{d}t}\langle|x|^2\rangle\Big|_{t=0} \geq 0. \tag{4.1.42}$$

As mentioned in the $H \leq 0$ case, $f(t)$ defined by (4.1.15) is larger than or equal to zero when $D \geq 2$, and $\sin[2\Lambda(t-u)]$ appearing in (4.1.16) is also larger than or equal to zero for $0 \leq t \leq \frac{\pi}{2\Lambda}$ or equivalently $\theta_0 \leq \theta \leq \theta_0 + \pi$. Then, if

$$l(\theta_0 + \pi) \leq 0, \tag{4.1.43}$$

$l(\theta(t))$ becomes negative for some value of t in an interval $0 \leq t \leq \frac{\pi}{2\Lambda}$, and thus due to (4.1.32) the collapse of the wavefunction happens. By use of (4.1.21) and

$$l(\theta_0 + \pi) = H/\Lambda^2 - l(\theta_0), \tag{4.1.44}$$

the condition (4.1.43) is rewritten as

$$\langle|x|^2\rangle|_{t=0} \geq H/\Lambda^2. \tag{4.1.45}$$

When the condition (4.1.45) is satisfied, there exist zero points of $l(\theta)$, of which we denote the positive and minimum one by θ_*. It is easily confirmed that θ_* lies in $\pi \leq \theta_* \leq 3\pi/2$. Considering $0 \leq \theta_0 \leq \pi/2$ and using (4.1.26), we get

$$\theta_0 = \mathrm{Arcsin}\left(\frac{\langle|x|^2\rangle|_{t=0}}{A} - \frac{H}{2\Lambda^2 A}\right). \tag{4.1.46}$$

Similarly, since $l(\theta_*) = 0$ and $\pi \leq \theta_* \leq 3\pi/2$, we have

$$\theta_* = \pi + \mathrm{Arcsin}\left(\frac{H}{2\Lambda^2 A}\right). \tag{4.1.47}$$

Then, from (4.1.46) and (4.1.47), we obtain the upper bound of the collapse-time $t_{c,M}$,

$$\begin{aligned} t_{c,M} &= \frac{1}{2\Lambda}(\theta_* - \theta_0) \\ &= \frac{1}{2\Lambda}(\pi/2 + \mathrm{Arcsin}\,\xi), \end{aligned} \tag{4.1.48}$$

with ξ being defined by (4.1.39).

Next, we consider the case that $\pi/2 < \theta_0 < 3\pi/2$, namely

$$\frac{\mathrm{d}}{\mathrm{d}t}\langle|x|^2\rangle\Big|_{t=0} < 0. \tag{4.1.49}$$

In this case, if

$$A \geq \frac{H}{2\Lambda^2}, \tag{4.1.50}$$

$l(\theta(t))$ becomes negative for some value of t which lies in $0 \leq t \leq \frac{\pi}{2\Lambda}$. Then, if (4.1.50) is satisfied, we see from (4.1.32) that ϕ collapses in a finite time, and the upper bound of the collapse time $t_{c,M}$ is calculated in the same way as (4.1.48).

We further investigate the collapse-condition (4.1.50). Substituting (4.1.25) into (4.1.50), we have

$$\left(\frac{1}{2\Lambda}\,\frac{\mathrm{d}}{\mathrm{d}t}\langle|x|^2\rangle\Big|_{t=0}\right)^2 \geq \langle|x|^2\rangle|_{t=0}\left(\frac{H}{\Lambda^2} - \langle|x|^2\rangle|_{t=0}\right). \tag{4.1.51}$$

When $H/\Lambda^2 \leq \langle|x|^2\rangle|_{t=0}$ which is equivalent to the collapse-condition for the $0 \leq \theta_0 \leq \pi/2$ case (4.1.45), the right hand side of (4.1.51) is negative. Then, regardless of the value of $\frac{1}{2\Lambda}\,\frac{\mathrm{d}}{\mathrm{d}t}\langle|x|^2\rangle\Big|_{t=0}$, (4.1.51) holds. When $H/\Lambda^2 \geq \langle|x|^2\rangle|_{t=0}$, the right hand side of (4.1.51) is positive. By taking the square roots of both sides of (4.1.51) and noting that $\frac{\mathrm{d}}{\mathrm{d}t}\langle|x|^2\rangle\Big|_{t=0}$ is negative, we get

$$\frac{\mathrm{d}}{\mathrm{d}t}\langle|x|^2\rangle\Big|_{t=0} \leq -2\sqrt{\langle|x|^2\rangle|_{t=0}\,(H - \Lambda^2\langle|x|^2\rangle|_{t=0})}. \tag{4.1.52}$$

The condition (4.1.52) can be regarded as an extention of the one obtained by Weinstein in the case (iii) of **Theorem 4.2** in Ref. [80], where the "free" or the conventional (i.e. without external potential) nonlinear Schrödinger field is considered. In fact, if $\nu_n = 0$ for all n, (4.1.52) becomes the same (apart from the discord of the factor, 2) as the one for the free nonlinear Schrödinger (NLS) field [80]. We note that, if

$$\nu_n = \nu \quad (\text{for all } n), \tag{4.1.53}$$

we have

$$H - \Lambda^2 \langle |x|^2 \rangle|_{t=0} = \|\nabla \phi_0\|_2^2 - \|\phi_0\|_4^4/2, \tag{4.1.54}$$

and thus the collapse-condition (4.1.52) becomes formally the same as in the free NLS field case.

Finally, we consider the case that $3\pi/2 \leq \theta_0 < 2\pi$, namely

$$\langle |x|^2 \rangle|_{t=0} < \frac{H}{2\Lambda^2}, \qquad \frac{\mathrm{d}}{\mathrm{d}t} \langle |x|^2 \rangle \Big|_{t=0} \geq 0. \tag{4.1.55}$$

From (4.1.21), $l(\theta_0)$ should be positive, yielding that the function $l(\theta)$ in (4.1.18) is always positive for $\theta_0 \leq \theta \leq \theta_0 + \pi$ or equivalently $0 \leq t \leq \frac{\pi}{2\Lambda}$. Then, we cannot see from (4.1.32) whether $\langle |x|^2 \rangle$ becomes negative for $0 \leq t \leq \frac{\pi}{2\Lambda}$. Further, for $t \geq \frac{\pi}{2\Lambda}$, the inequality (4.1.32) does not hold any more, because the integral

$$\int_0^t f(u) \sin[2\Lambda(t-u)] \mathrm{d}u, \tag{4.1.56}$$

appearing in the right hand side of (4.1.16) is not necessarily positive for $t \geq \frac{\pi}{2\Lambda}$. Accordingly, we cannot see whether $\langle |x|^2 \rangle$ becomes negative for $t \geq \frac{\pi}{2\Lambda}$, either. Therefore, in the case that $3\pi/2 \leq \theta_0 < 2\pi$, we cannot conclude that the wavefunction ϕ collapses in a finite time.

It is interesting to consider a special case that the space is two-dimensional ($D = 2$), and the constants $\{\nu_n\}$ satisfy (4.1.53). In this case, $f(t)$ defined by (4.1.15) is identically zero, and (4.1.16) reduces to

$$\langle |x|^2 \rangle = l(\theta(t)) = \frac{H}{2\nu^2} + A \sin(2\nu t + \theta_0). \tag{4.1.57}$$

Then, we can trace the exact time-evolution of $\langle |x|^2 \rangle$. If the collapse of ϕ happens which can be proved in the same manner as in the previous cases, the collapse-time t_{c} is equal to its upper bound $t_{\mathrm{c},M}$.

To conclude this sub-section, some comments are in order. First, what we have presented in this section is a sufficient condition for the collapse. There remains a possibility that, even when the collapse-condition in this section is not satisfied, the expectation value $\langle |x|^2 \rangle$ may go to zero after several damped oscillations, which is due to the effect of the negative non-homogeneous term $-f(t)$ ($D \geq 2$) in the ordinary differential equation (4.1.14). In this case, the upper bound of the collapse-time $t_{\mathrm{c},M}$ (4.1.48) will be replaced by larger ones. A quantitative analysis of $f(t)$ is required to make clear this damped-oscillating phenomenon, which will be a future problem.

Second, different from the discussion in the repulsive case ($g = +1$), we have not considered the case $D = 1$ here. If $D = 1$, the positivity of $f(t)$ defined by (4.1.15) is not guaranteed, and thus we cannot examine the stability of the wavefunction by using the above mentioned method. The one-dimensional and self-focusing NLS equation with no external potential is integrable and has stable solition solutions [74]. The external harmonic potentials destroy the integrability. However, since the equation has no singularity at the origin, we conjecture that the effect of the potentials is only a deformation of solitary waves.

4.2 Collapse of the condensate

We predict the collapse of the Bose-Einstein condensate in a magnetic trap where the atoms have a negative s-wave scattering length [41]–[43]. We prove that the singularity of wavefunction emerges in a finite time even when the total energy of the system is positive. In addition, we present a refined formula for a critical number of atoms above which the collapse of the condensate occurs. This number for ^{7}Li atoms can be the same as the one in the recent experiment.

4.2.1 Time-evolution of the condensate

We consider the Bose-Einstein condensate confined by magnetic fields and investigate the time evolution of wavefunction when the interactions between atoms are effectively attractive. Since the magnetic trap has an axial symmetry and the system is near the ground state, we assume that the wavefunction is axially symmetric. The axis of the symmetry is chosen to be the z-axis. Let t denote time and $r_\perp$ the radius of the projection of the position vector $\boldsymbol{r}$ on the xy-plane. Time-evolution of macroscopic wavefunction $\Psi(r_\perp, z, t)$ of the condensate at very low temperature is described by the Gross-Pitaevskii equation for the system [70]–[72],

$$\mathrm{i}\hbar\frac{\partial\Psi}{\partial t} = -\frac{\hbar^2}{2m}\frac{1}{r_\perp}\frac{\partial}{\partial r_\perp}\left(r_\perp\frac{\partial\Psi}{\partial r_\perp}\right) - \frac{\hbar^2}{2m}\frac{\partial^2\Psi}{\partial z^2} + \frac{1}{2}m\omega_\perp^2 r_\perp^2\Psi + \frac{1}{2}m\omega_z^2 z^2\Psi + \frac{4\pi\hbar^2 a}{m}|\Psi|^2\Psi. \quad (4.2.1)$$

Here m is the atomic mass, ω_z and $\omega_\perp$ are the trap (angular) frequencies along the z-axis and in the xy-plane, respectively, and a is the s-wave scattering length. We take a to be negative. By introducing a characteristic length r_0,

$$r_0 \equiv \left(\frac{\hbar}{2m\omega_\perp}\right)^{1/2}, \quad (4.2.2)$$

we prepare dimensionless variables,

$$\rho = r_\perp/r_0, \quad \xi = z/r_0, \quad \tau = \omega_\perp t, \quad \psi = r_0^{3/2}\Psi. \quad (4.2.3)$$

In terms of these variables, Eq. (4.2.1) is written in the dimensionless form

$$\mathrm{i}\frac{\partial\psi}{\partial\tau} = -\frac{1}{\rho}\frac{\partial}{\partial\rho}\left(\rho\frac{\partial\psi}{\partial\rho}\right) - \frac{\partial^2\psi}{\partial\xi^2} + \frac{1}{4}(\rho^2 + \delta^2\xi^2)\psi + c|\psi|^2\psi, \quad (4.2.4)$$

where

$$\delta \equiv \omega_z/\omega_\perp, \quad c \equiv 8\pi a/r_0. \quad (4.2.5)$$

Note that the constant c is dimensionless and negative. In the terminology of the soliton theory, we refer to Eq. (4.2.4) as axially symmetric attractive nonlinear Schrödinger (NLS) equation with harmonic potentials. The NLS equation (4.2.4) has two integrals of motion,

$$I_1 = 2\pi\int_{-\infty}^{\infty}\mathrm{d}\xi\int_0^\infty \rho\,\mathrm{d}\rho|\psi|^2, \quad (4.2.6)$$

$$I_2 = 2\pi \int_{-\infty}^{\infty} \mathrm{d}\xi \int_0^{\infty} \rho \, \mathrm{d}\rho \left[|\partial_\rho \psi|^2 + |\partial_\xi \psi|^2 + \frac{1}{4}(\rho^2 + \delta^2 \xi^2)|\psi|^2 + \frac{1}{2} c |\psi|^4 \right]. \tag{4.2.7}$$

The total number of atoms N and the total energy E are related to the constants I_1 and I_2 as

$$N = I_1, \quad E = \hbar \omega_\perp I_2. \tag{4.2.8}$$

By definition, I_1 is positive. We define

$$\langle \eta^2 \rangle = 2\pi \int_{-\infty}^{\infty} \mathrm{d}\xi \int_0^{\infty} \rho \, \mathrm{d}\rho (\rho^2 + \xi^2)|\psi|^2, \tag{4.2.9}$$

which measures the geometrical extent of the wavefunction ψ and plays a key role in the Zakharov's theory [77, 78].

Differentiating (4.2.9) by τ twice and using (4.2.4), we have

$$\frac{\mathrm{d}^2}{\mathrm{d}\tau^2} \langle \eta^2 \rangle = 8 I_2 - 4\Omega^2 \langle \eta^2 \rangle - f(\tau), \tag{4.2.10}$$

where Ω and $f(\tau)$ stand for

$$\Omega \equiv \min(1, \delta), \tag{4.2.11}$$

$$f(\tau) \equiv 4\pi \int_{-\infty}^{\infty} \mathrm{d}\xi \int_0^{\infty} \rho \, \mathrm{d}\rho [2(\delta^2 - 1)\xi^2 |\psi|^2 + |c||\psi|^4] \quad (\text{for } \delta > 1), \tag{4.2.12}$$

$$f(\tau) \equiv 4\pi \int_{-\infty}^{\infty} \mathrm{d}\xi \int_0^{\infty} \rho \, \mathrm{d}\rho [2(1 - \delta^2)\rho^2 |\psi|^2 + |c||\psi|^4] \quad (\text{for } 0 < \delta < 1). \tag{4.2.13}$$

A differential equation (4.2.10) for $\langle \eta^2 \rangle$ is readily solved to give

$$\langle \eta^2 \rangle = A \sin(2\Omega\tau + \theta_0) + \frac{2}{\Omega^2} I_2 - \frac{1}{2\Omega} \int_0^{\tau} f(u) \sin[2\Omega(\tau - u)] \mathrm{d}u. \tag{4.2.14}$$

Constants A and θ_0 are to be determined by the initial conditions on ψ. Without loss of generality, we assume A to be positive.

We first consider the case that I_2 and therefore the total energy of the condensate E are negative. Because $\langle \eta^2 \rangle$ is a positive quantity, the right hand side of (4.2.14) should also be positive for $\tau = 0$. Accordingly, θ_0 in (4.2.14) must be $0 < \theta_0 < \pi$. Let us define a function, $G(\tau)$, as

$$G(\tau) \equiv A \sin(2\Omega\tau + \theta_0) + \frac{2}{\Omega^2} I_2. \tag{4.2.15}$$

Since the function $f(\tau)$ is always positive and $\sin[2\Omega(\tau - u)]$ in (4.2.14) is positive for $0 \le \tau \le \pi/2\Omega$, the last term in (4.2.14) is negative for $0 \le \tau \le \pi/2\Omega$. We thus obtain an inequality,

$$\langle \eta^2 \rangle \ \le \ G(\tau), \tag{4.2.16}$$

for $0 \le \tau \le \pi/2\Omega$. From the definition (4.2.15), we see that $G(\tau)$ becomes negative for some value of τ which lies in $0 \le \tau \le \pi/2\Omega$, if $0 < \theta_0 < \pi$. Then, from the inequality (4.2.16), $\langle \eta^2 \rangle$ should become negative for some value of τ, $0 \le \tau \le \pi/2\Omega$. This contradicts to the definition of $\langle \eta^2 \rangle$ (4.2.9), which implies the development of the singularity. Thus,

when the total energy of the condensate E is negative, the wavefunction ψ surely collapses in a finite time, regardless of the initial condition on ψ.

Next, we prove that, even when the total energy E is positive, the collapse of wavefunction occurs in a finite time for a certain class of the initial conditions on ψ. Actually, in the experiments of the Bose-Einstein condensation under a magnetic trap, the total energy E and therefore I_2 are positive. We assume the initial shape of ψ to be gaussian,

$$\psi(\rho, \xi, \tau = 0) = \frac{(q^2 k \delta^{1/2} I_1)^{1/2}}{(2\pi)^{3/4}} \exp[-(q^2\rho^2 + \delta k^2 \xi^2)/4], \tag{4.2.17}$$

where q and k are positive parameters. From Eqs. (4.2.4), (4.2.9) and (4.2.17), we can show that

$$\frac{\mathrm{d}}{\mathrm{d}\tau}\langle\eta^2\rangle = 0 \quad (\text{for } \tau = 0), \tag{4.2.18}$$

which yields $\theta_0 = \pi/2$ or $\theta_0 = 3\pi/2$ in (4.2.14). Correspondingly, the solution (4.2.14) now yields

$$\langle\eta^2\rangle = \langle\eta^2\rangle_+ \equiv A\cos(2\Omega\tau) + \frac{2}{\Omega^2} I_2 - \frac{1}{2\Omega}\int_0^\tau f(u)\sin[2\Omega(\tau - u)]\mathrm{d}u, \tag{4.2.19}$$

when $\theta_0 = \pi/2$, and

$$\langle\eta^2\rangle = \langle\eta^2\rangle_- \equiv -A\cos(2\Omega\tau) + \frac{2}{\Omega^2} I_2 - \frac{1}{2\Omega}\int_0^\tau f(u)\sin[2\Omega(\tau - u)]\,\mathrm{d}u, \tag{4.2.20}$$

when $\theta_0 = 3\pi/2$. Substituting the initial shape (4.2.17) into $\langle\eta^2\rangle|_{\tau=0}$ and I_2, we get

$$\langle\eta^2\rangle|_{\tau=0} = (2q^{-2} + \delta^{-1}k^{-2})I_1, \tag{4.2.21}$$

$$I_2 = \left[\frac{1}{2}(q^2 + q^{-2}) + \frac{\delta}{4}(k^2 + k^{-2})\right] I_1 + \frac{cq^2 k\delta^{1/2}}{16\pi^{3/2}} I_1^2. \tag{4.2.22}$$

From Eq. (4.2.22), we see that I_2 is positive when

$$I_1 < I_{1,a}(q, k). \tag{4.2.23}$$

Here

$$I_{1,a}(q, k) \equiv \frac{4\pi^{3/2}}{|c|q^2 k\delta^{1/2}}[2(q^2 + q^{-2}) + \delta(k^2 + k^{-2})]. \tag{4.2.24}$$

On the other hand, Eqs. (4.2.21) and (4.2.22) give

$$\langle\eta^2\rangle|_{\tau=0} - \frac{2}{\Omega^2} I_2 = \frac{|c|q^2 k\delta^{1/2}}{8\pi^{3/2}\Omega^2} I_1(I_1 - I_{1,b}(q, k)), \tag{4.2.25}$$

where $I_{1,b}(q, k)$ is defined as

$$I_{1,b}(q, k) \equiv \frac{4\pi^{3/2}}{|c|q^2 k\delta^{1/2}} g(q, k), \tag{4.2.26}$$

with

$$g(q,k) \equiv 2[q^2 + (1-2\Omega^2)q^{-2}] + \delta[k^2 + (1-2\Omega^2/\delta^2)k^{-2}]. \tag{4.2.27}$$

Depending on whether I_1 is larger or smaller than $I_{1,b}(q,k)$, we can determine which of $\langle\eta^2\rangle_\pm$ should be chosen as the solution of Eq. (4.2.10). When $I_1 > I_{1,b}(q,k)$ ($I_1 < I_{1,b}(q,k)$), $\langle\eta^2\rangle_+$ ($\langle\eta^2\rangle_-$) is the solution of Eq. (4.2.10). Remark that the function $g(q,k)$ may take both positive and negative values, because $1-2\Omega^2 = -1 < 0$ for $\delta > 1$ and $1-2(\Omega/\delta)^2 = -1 < 0$ for $0 < \delta < 1$.

In the case that $g(q,k) > 0$ and therefore $I_{1,b}(q,k) > 0$, if $I_1 < I_{1,b}(q,k)$, $\langle\eta^2\rangle_-$ is an appropriate solution of Eq. (4.2.10) and satisfies

$$\langle\eta^2\rangle_- \ \leq \ -A\cos(2\Omega\tau) + \frac{2}{\Omega^2}I_2, \tag{4.2.28}$$

for $0 \leq \tau \leq \pi/2\Omega$. The right hand side of the inequality (4.2.28) is always positive because $A = \frac{2}{\Omega^2}I_2 - \langle\eta^2\rangle|_{\tau=0} < 2I_2/\Omega^2$. Then, we cannot see from (4.2.28) whether $\langle\eta^2\rangle_-$ surely becomes negative for $0 \leq \tau \leq \pi/2\Omega$. Further, for $\tau \geq \pi/2\Omega$, the inequality (4.2.28) does not hold any more, because the integral,

$$\int_0^\tau f(u)\sin[2\Omega(\tau-u)]\mathrm{d}u, \tag{4.2.29}$$

is not necessarily positive for $\tau \geq \pi/2\Omega$. Accordingly, we cannot see whether $\langle\eta^2\rangle_-$ becomes negative for $\tau \geq \pi/2\Omega$, either. Therefore, when $I_1 < I_{1,b}(q,k)$, we do not conclude that the wavefunction ψ collapses in a finite time. This conclusion is consistent with that in the case $3\pi/2 \leq \theta_0 < 2\pi$ in the sub-section 4.1.2. On the other hand, if $I_1 > I_{1,b}(q,k)$, the behavior of $\langle\eta^2\rangle$ may change drastically. As the solution of (4.2.10), $\langle\eta^2\rangle_+$ defined by (4.2.19) is appropriate and satisfies

$$\langle\eta^2\rangle_+ \ \leq \ A\cos(2\Omega\tau) + \frac{2}{\Omega^2}I_2, \tag{4.2.30}$$

for $0 \leq \tau \leq \pi/2\Omega$. Using (4.2.19) and (4.2.25), we have

$$A = \langle\eta^2\rangle|_{\tau=0} - \frac{2}{\Omega^2}I_2 = -\frac{1}{2\Omega^2}g(q,k)I_1 + \frac{|c|q^2k\delta^{1/2}}{8\pi^{3/2}\Omega^2}I_1^2. \tag{4.2.31}$$

Suppose that

$$A \geq 2I_2/\Omega^2, \tag{4.2.32}$$

which is possible as seen from (4.2.31). When the inequality (4.2.32) holds, the right hand side of (4.2.30) becomes negative for some value of τ which lies $0 \leq \tau \leq \pi/2\Omega$. Then, from (4.2.30), $\langle\eta^2\rangle_+$ also becomes negative for some value of τ, $0 \leq \tau \leq \pi/2\Omega$. This is contradictory to the positivity of $\langle\eta^2\rangle_+$, implying that the singularity of the wavefunction emerges in a finite time. In other words, the wavefunction ψ collapses in a finite time. Let us rewrite the condition (4.2.32) so as to make its physical significance clear. Substituting (4.2.22) and (4.2.31) into (4.2.32), we get

$$I_1 \geq I_{1,c}(q,k), \tag{4.2.33}$$

where

$$I_{1,c}(q,k) \equiv \frac{4\pi^{3/2}}{|c|q^2 k\delta^{1/2}} h(q,k), \tag{4.2.34}$$

with

$$h(q,k) \equiv 2[q^2 + (1-\Omega^2)q^{-2}] + \delta[k^2 + (1-\Omega^2/\delta^2)k^{-2}]. \tag{4.2.35}$$

Contrary to $g(q,k)$, the function $h(q,k)$ is always positive. From (4.2.24), (4.2.26) and (4.2.34), we find that

$$I_{1,b} < I_{1,c} < I_{1,a} \quad \text{(for all } q \text{ and } k\text{)}. \tag{4.2.36}$$

Therefore, if the initial shape of ψ is gaussian (4.2.17), the collapse occurs when $I_1 > I_{1,c}(q,k)$. The inequality (4.2.36) assures the consistency of the analysis.

In the case that $g(q,k) < 0$, and therefore $I_{1,b}(q,k) < 0$, $\langle\eta^2\rangle_+$ (4.2.19) is the only solution of (4.2.10) because I_1 should be positive. Except for this, the discussion for the collapse goes in the same manner for the $I_{1,b}(q,k) > 0$ case. Thus, we conclude that the solution of the NLS equation (4.2.4) with the initial condition (4.2.17) surely collapses in a finite time for $I_1 \geq I_{1,c}(q,k)$ even when the total energy is positive.

The above result predicts an interesting phenomenon, the collapse of the Bose-Einstein condensate, for the assembly of bosonic atoms with a negative s-wave scattering length. Using (4.2.5), (4.2.8) and (4.2.34) in (4.2.33), we obtain a critical number of atoms $N_{\rm c}$,

$$N_{\rm c}(q,k) = N_0 \frac{h(q,k)}{q^2 k}, \tag{4.2.37}$$

with

$$N_0 \equiv (\pi/\delta)^{1/2} r_0/(2|a|). \tag{4.2.38}$$

The collapse of the wavefunction occurs when the number of the trapped atoms, N, exceeds $N_{\rm c}(q,k)$. The formula (4.2.37) gives the critical number of atoms $N_{\rm c}$ as a function of two parameters q and k in (4.2.17). The extents of the initial wavefunction are proportional to q^{-1} for the ρ-direction and k^{-1} for the ξ-direction. When q and k equal 1, the initial wavefunction (4.2.17) represents the ground state for the Schrödinger equation under harmonic potentials,

$$\mathrm{i}\frac{\partial\psi}{\partial\tau} = -\frac{1}{\rho}\frac{\partial}{\partial\rho}\left(\rho\frac{\partial\psi}{\partial\rho}\right) - \frac{\partial^2\psi}{\partial\xi^2} + \frac{1}{4}(\rho^2 + \delta^2\xi^2)\psi. \tag{4.2.39}$$

It is interesting that the formula includes another anisotropy effect of the magnetic trap through $\Omega = \min(1, \delta \equiv \omega_z/\omega_\perp)$.

4.2.2 Application to ^{7}Li system

We estimate the critical number for the assembly of ^{7}Li atoms which have a negative s-wave scattering length. In order to apply the above discussion to this system, we first improve quantitatively the evaluation for $\langle\eta^2\rangle_+$ (4.2.30) as follows. If there exists a constant, $\bar{f}$, such that $0 < \bar{f} \leq f(\tau)$, the inequality (4.2.30) can be replaced by

$$\langle\eta^2\rangle_+ \;\leq\; \left(A + \frac{\bar{f}}{4\Omega^2}\right)\cos(2\Omega\tau) + \left(\frac{2}{\Omega^2}I_2 - \frac{\bar{f}}{4\Omega^2}\right), \tag{4.2.40}$$

for $0 \leq \tau \leq \pi/2\Omega$. Then, the condition for the collapse of ψ is modified as

$$A \geq \frac{2}{\Omega^2} I_2 - \frac{\bar{f}}{2\Omega^2}, \tag{4.2.41}$$

instead of (4.2.32). Here, we assume that the collapse of the wavefunction occurs without oscillations, which means that $\langle \eta^2 \rangle$ goes to zero monotonously and the integral,

$$2\pi \int_{-\infty}^{\infty} \mathrm{d}\xi \int_0^{\infty} \rho \, \mathrm{d}\rho |\psi|^4, \tag{4.2.42}$$

is a monotone increasing function of a (scaled) time τ. Under this assumption, from (4.2.12) or (4.2.13), we can estimate $\bar{f}$ as

$$\bar{f} = 4\pi |c| \int_{-\infty}^{\infty} \mathrm{d}\xi \int_0^{\infty} \rho \, \mathrm{d}\rho |\psi(\rho, \xi, \tau = 0)|^4. \tag{4.2.43}$$

Using the initial condition on ψ (4.2.17) in (4.2.43), we get

$$\bar{f} = I_1^2 k q^2 / N_0. \tag{4.2.44}$$

Thus, substituting (4.2.22), (4.2.31) and (4.2.44) into (4.2.41), we arrive at a renewed critical number of atoms, $N_{\mathrm{c,new}}$,

$$N_{\mathrm{c,new}} = N_0 \frac{h_{\mathrm{new}}(q,k)}{q^2 k}, \tag{4.2.45}$$

where

$$h_{\mathrm{new}}(q,k) \equiv \frac{2}{3} h(q,k). \tag{4.2.46}$$

Apparently, $N_{\mathrm{c,new}}$ is smaller than N_{c}.

In the experiment for ^{7}Li [12], the values of frequencies ω_z and $\omega_\perp$ were $\omega_z/2\pi = 117\,\mathrm{Hz}$ and $\omega_\perp/2\pi = 163\,\mathrm{Hz}$, which gives $\delta = 0.718$. The s-wave scattering length of ^{7}Li was observed to be $a = -27.3 a_0$ (a_0 : Bohr radius) [29]. Substituting these experimental values into (4.2.38) and (4.2.46), we get

$$N_{\mathrm{c,new}}(q,k)/N_0 = 4k^{-1}(1 + 0.485 q^{-4})/3 + 0.479 q^{-2} k, \tag{4.2.47}$$

with $N_0 = 1520$.

To fix a relation between q and k, we use the minimal condition for I_2 (4.2.22). From $\partial_q I_2 = 0$ and $\partial_k I_2 = 0$, we have

$$q^2 - q^{-2} = \delta(k^2 - k^{-2}), \tag{4.2.48}$$

which yields q as a function of k,

$$q = Q(k) \equiv \left[\delta(k^2 - k^{-2})/2 + \sqrt{1 + \delta^2 (k^2 - k^{-2})^2/4} \right]^{1/2}. \tag{4.2.49}$$

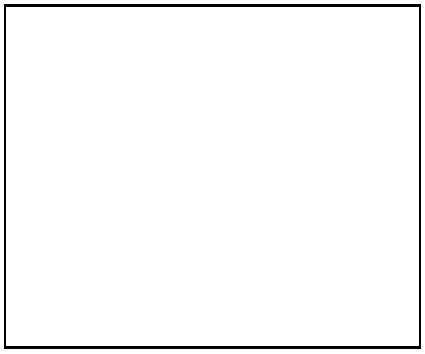

Figure 4.2.1: $N_{\rm c,new}/N_0$ as a function of k for the case that $\delta = 0.718$ [12].

Substitution of $\delta = 0.718$ into (4.2.49) gives

$$q = Q(k) \equiv \left[0.359(k^2 - k^{-2}) + \sqrt{1 + 0.129(k^2 - k^{-2})^2}\right]^{1/2}. \tag{4.2.50}$$

We plot $N_{\rm c,new}(Q(k), k)/N_0$ as a function of k for $\delta = 0.718$ (Fig. 4.2.1). The refined critical number $N_{\rm c,new}(Q(k), k)$ is a monotone decreasing function of k. This behavior is reasonable: For smaller (larger) k, the wavefunction is more spread (confined), and such configuration imposes more (less) severe restriction on the collapse. In what follows, we consider the case $k > 1$ since the gaussian wavefunction (4.2.17) with $q = k = 1$ does not include the effect of attractive inter-atomic interaction which makes the exact ground state more confined. This has been considered in the sub-section 3.1.3. For instance, in the case of almost spherical trap, the result (3.1.66) gives $k = 1.59$ and $q = 1.45$.

If we set $k = 1.20$, $Q(k)$ and $N_{\rm c,new}(Q(k), k)$ are calculated as $Q(1.20) = 1.14$ and $N_{\rm c,new}(Q(1.20), 1.20) = 2840$. In the case that $k = 2.20$, $Q(k)$ and $N_{\rm c,new}(Q(k), k)$ are estimated as $Q = 1.90$ and $N_{\rm c,new} = 1400$. The latter value of $N_{\rm c,new}$ agrees well with the one in the experiment, which is about 10^3 [13]. It is also consistent with the theoretical ones obtained by different approaches, which are $(1 \sim 3) \times 10^3$ [31]–[40], [45]–[51].

4.3 Summary

We have studied the dynamical properties of Bose-Einstein condensates. In Sec. 4.1, as a preliminary to the analysis of the collapse of the condensate, we have considered the stability of the wavefunction of the D-dimensional nonlinear Schrödinger equation (4.1.1) with harmonic potential terms (4.1.2), for both repulsive ($g = +1$) and attractive ($g = -1$) cases. This is an extention of the Zakharov's theory [77, 78]. In the repulsive case, we have shown that the solution of Eq. (4.1.1) is absolutely stable for any spatial dimension when confined in the harmonic potential. In the attractive case for $D \geq 2$, by solving the equation of motion for the expectation value of the square of the radius (4.1.14), we have investigated the time-evolution of the wavefunction ϕ. When the total energy of the system H is equal

to or less than zero, the wavefunction ϕ surely collapses in a finite time, regardless of the initial condition. On the other hand, when $H > 0$, we have obtained conditions that the collapse of the wavefunction occurs, according to the value of the constant θ_0 appearing in (4.1.16). When $0 \leq \theta_0 \leq \pi/2$ which is equivalent to (4.1.42), the collapse-condition is obtained as (4.1.45). When $\pi/2 < \theta_0 < 3\pi/2$, equivalent to (4.1.49), the collapse-condition is (4.1.52). This result is an extention of Weinstein's where the nonlinear Schrödinger (NLS) field without external potential, is considered [80]. We have also obtained an upper bound of the collapse-time of the wavefunction $t_{c,M}$, represented by the formula (4.1.38) with (4.1.39). In a special case that $D = 2$ and $\nu_n = \nu$, since the function $f(t)$ defined by (4.1.15) is identically zero, the time-evolution of $\langle |x|^2 \rangle$ can be traced exactly by (4.1.57), and therefore the collapse-time t_c is just equal to its upper bound $t_{c,M}$. Improvements of the collapse-conditions and the upper bound of the collapse-time require a more detailed analysis of $f(t)$. We, however, emphasize that the collapse time is the order of $1/\nu$.

In Sec. 4.2, we have considered the instability of the Bose-Einstein condensate with effectively attractive inter-atomic interactions under a magnetic trap. The Gross-Pitaevskii equation (4.2.1) for the system is essentially the same as the attractive nonlinear Schrödinger equation with harmonic potential terms (4.2.4). First, we have shown that the collapse of the wavefunction surely happens in a finite time when the total energy of the condensate E is negative. Second, by assuming the initial condition on the wavefunction to be gaussian (4.2.17) with two parameters q and k, we have proved that the collapse can happen even when E is positive. This situation corresponds to the experiments on the Bose-Einstein condensate. We have also proved that the condensate collapses when the number of atoms N exceeds N_c (4.2.37). Further, we have presented a refined formula for the critical number $N_{c,new}$ (4.2.45), which is smaller than N_c. Using a relation between q and k which is obtained from the minimal condition for the energy (4.2.49), we have plotted $N_{c,new}/N_0$ as a function of k for $\delta = 0.718$ (Fig. 4.2.1). Our estimated number for the assembly of ^{7}Li, which is about 1400 for $q = 1.90$ and $k = 2.20$, agrees well with the one in the experiment [13]. We have simplified the analysis by assuming (i) axial symmetry of the system, (ii) zero temperature and (iii) s-wave scattering. All the assumptions are more or less consistent in the sense that we only consider the properties of the dilute condensate at the very low energy region. In addition, we have not taken account (iv) three-body collisions and (v) the short-range repulsive part of the inter-atomic potential, which may play important roles at the final state of the collapse. Detail examinations of those neglected effects are left for future studies. On the other hand, it is extremely interesting to observe the time-development of the wavefunction near the collapse. The asymptotic analysis has been given in [87].

Chapter 5

Summary and Concluding Remarks

We have reviewed recent theoretical research on the properties of Bose-Einstein condensation, in particular, static and dynamical stabilities of Bose-Einstein condensates confined in magnetic trap. It has been shown that the variational approach and the analysis of the time-dependent nonlinear Schrödinger equation give significant information on the stability of the condensates.

Bose-Einstein condensation was discovered in liquid helium about 70 years ago, and has been "rediscovered" in alkali atomic gases confined in trap, due to the developments of technology in atomic physics. There are many advantages in experiments using atomic vapors under magnetic trap, which are summarized as follows.
1) The atom-atom interactions are weak (the s-wave scattering length is about 10^{-8}m, whereas at the required densities the inter-atomic spacing is about 10^{-6}m, for the ^{87}Rb case [11]). Therefore, the purely quantum-statistical nature of the BEC transition can be captured.
2) We can choose various species of bosonic (or fermionic) atoms and prepare even their mixtures with different number of each atoms.
3) We have controllable parameters such as density, temperature and the frequencies of the magnetic trap. In particular, the number of atoms and the temperature are now independent. This offers an idealistic situation to study the quantum statistical mechanics.
4) The interaction strength can be varied by use of the Feshbach resonance [88, 89]. The s-wave scattering length depends on the applied magnetic field and even the sign of it changes.
These new aspects give rich dynamical behaviors of the condensate at microscopic, mesoscopic and macroscopic levels. Understanding of those systems is fundamental in quantum statistical mechanics, condensed matter physics and atom optics. The trapped Bose-Einstein condensates may serve as a source of the coherent matter waves. In atom optics, we expect many applications such as atom holography [90, 91], atom interferometer [92] and atom laser [93]–[95]. In principle, Bose-Einstein condensation is expected to occur for all bosonic atoms and molecules with and without charges, and thus we believe that those studies will continue to be interesting in coming years.

Acknowledgements

One of the authors (MW) likes to thank V. E. Zakharov, L. P. Pitaevskii and Y. Kagan for useful comments. This work was partially supported by Grant-in-Aid for Scientific Research from the Ministry of Education, Science and Culture, Japan. One of the authors (TT) acknowledges JSPS Research Fellowships for Young Scientists.

Appendix A

Bose-Einstein Condensation of a Free Boson Gas Confined in Harmonic Potentials

We discuss the Bose-Einstein condensation of a free gas under harmonic potentials. The N-body Hamiltonian (first quantization) is

$$\begin{aligned} H &= \sum_{j=1}^{N} H_j \\ &= \sum_{j=1}^{N} \left[\frac{1}{2m} \left(p_{jx}^2 + p_{jy}^2 + p_{jz}^2 \right) + \frac{m}{2} \left(\omega_x^2 x_j^2 + \omega_y^2 y_j^2 + \omega_z^2 z_j^2 \right) \right], \end{aligned} \tag{A.1}$$

where $\boldsymbol{p}_j \equiv (p_{jx}, p_{jy}, p_{jz})$ is the momentum operator of particle-j, $\boldsymbol{p}_j \equiv -\mathrm{i}\hbar\partial/\partial \boldsymbol{r}_j$. Since there is no interaction between particles, the eigenstates are expressed as

$$\Psi(\boldsymbol{r}_1, \boldsymbol{r}_2, \cdots, \boldsymbol{r}_N) = \prod_{j=1}^{N} \phi(\boldsymbol{r}_j), \tag{A.2}$$

and a single-particle state $\phi(\boldsymbol{r})$ satisfies

$$\left[-\frac{\hbar^2}{2m} \left(\frac{\partial^2}{\partial x^2} + \frac{\partial^2}{\partial y^2} + \frac{\partial^2}{\partial z^2} \right) + \frac{m}{2} \left(\omega_x^2 x^2 + \omega_y^2 y^2 + \omega_z^2 z^2 \right) \right] \phi(\boldsymbol{r}) = \epsilon \phi(\boldsymbol{r}). \tag{A.3}$$

The eigenvalues of (A.3) is well-known;

$$\epsilon_{n_x n_y n_z} = \left(n_x + \frac{1}{2} \right) \hbar\omega_x + \left(n_y + \frac{1}{2} \right) \hbar\omega_y + \left(n_z + \frac{1}{2} \right) \hbar\omega_z, \tag{A.4}$$

where $n_x, n_y, n_z = 0, 1, 2, \cdots$.

We adopt the grand canonical ensemble. The total particle number N and the total energy E are given by

$$N = \sum_{n_x,n_y,n_z} \left[\exp\beta\left(\epsilon_{n_xn_yn_z} - \mu\right) - 1\right]^{-1}, \tag{A.5}$$

$$E = \sum_{n_x,n_y,n_z} \epsilon_{n_xn_yn_z} \left[\exp\beta\left(\epsilon_{n_xn_yn_z} - \mu\right) - 1\right]^{-1}, \tag{A.6}$$

where $\beta = (k_{\rm B}T)^{-1}$ and μ is the chemical potential. For later discussions, we shift the chemical potential as $\mu - \hbar\left(\omega_x + \omega_y + \omega_z\right)/2 \to \mu$. At very low temperature, (A.5) is written in the following form,

$$N = N_0 + N_1, \tag{A.7}$$

where

$$N_0 = 1/\left(e^{-\beta\mu} - 1\right), \tag{A.8}$$

$$N_1 = \sum_{n_x,n_y,n_z\neq 0} \left[\exp\beta\left(n_x\hbar\omega_x + n_y\hbar\omega_y + n_z\hbar\omega_z\right) - 1\right]^{-1}. \tag{A.9}$$

Discussions, here and in what follows, are essentially the same as those for a free boson gas in a box. The Bose-Einstein condensation is the situation where N_0 becomes macroscopic, that is, $N_0 \sim O(N)$. Equation (A.8) implies $\mu \leq 0$ and $-\beta\mu \sim O(1/N)$. We have set $\mu = 0$ in (A.9). Therefore, N_1 in (A.9) gives the maximum of the contribution from the cxcited states at low temperature.

We replace the summations in (A.9) by an integral over the single-particle energy ϵ with the density of states $D(\epsilon)$,

$$D(\epsilon)\mathrm{d}\epsilon = \frac{\epsilon^2}{2(\hbar\bar{\omega})^3}\mathrm{d}\epsilon. \tag{A.10}$$

The formula (A.10) can be derived as follows. We estimate the number of the states, $N(\epsilon)$, whose energies are smaller than ϵ, which is equivalent to the number of positive integer sets $\{n_x, n_y, n_z\}$ satisfying $0 < n_x\hbar\omega_x + n_y\hbar\omega_y + n_z\hbar\omega_z \leq \epsilon$. Geometrically, this corresponds to a volume, $(\epsilon/\hbar\omega_x)(\epsilon/\hbar\omega_y)(\epsilon/\hbar\omega_z)/6$. Therefore, we obtain $N(\epsilon) = \frac{1}{6}\epsilon^3/(\hbar\bar{\omega})^3$, where $\bar{\omega}^3 \equiv \omega_x\omega_y\omega_z$. A relation $D(\epsilon) = \mathrm{d}N(\epsilon)/\mathrm{d}\epsilon$ gives (A.10).

Using (A.10) to rewrite the summations in (A.9), we obtain

$$N_1 = \int_0^\infty \frac{D(\epsilon)\mathrm{d}\epsilon}{\exp(\beta\epsilon) - 1} = \left(\frac{k_{\rm B}T}{\hbar\bar{\omega}}\right)^3 \zeta(3), \quad T \leq T_{\rm c}, \tag{A.11}$$

where

$$\zeta(3) = \int_0^\infty \frac{x^2\mathrm{d}x}{e^x - 1} = 1.202\cdots. \tag{A.12}$$

The transition temperature is defined by

$$N = \zeta(3) \left(\frac{k_{\rm B} T_{\rm c}}{\hbar \bar{\omega}} \right)^3 . \tag{A.13}$$

For $T \leq T_{\rm c}$, we have

$$N = N_0 + \zeta(3) \left(\frac{k_{\rm B} T}{\hbar \bar{\omega}} \right)^3 , \tag{A.14}$$

and therefore

$$\frac{N_0}{N} = 1 - \left(\frac{T}{T_{\rm c}} \right)^3 , \quad T \leq T_{\rm c}. \tag{A.15}$$

The exponent is changed from 3/2 (confined in a box) to 3 (confined in harmonic potentials).

The total energy E in (A.6) is calculated in the thermodynamic limit [96]; $N \to \infty$, $\bar{\omega} \to 0$, $N\bar{\omega}^3 =$ fixed. The result is

$$\begin{aligned} E &= 3Nk_{\rm B}T \frac{g_4(z)}{g_3(z)}, \quad T > T_{\rm c}, \\ &= 3\frac{(k_{\rm B}T)^4}{(\hbar\bar{\omega})^3}\zeta(4), \quad T \leq T_{\rm c}, \end{aligned} \tag{A.16}$$

where with $z = \exp(\beta\mu)$

$$g_n(z) \equiv \sum_{l=1}^{\infty} \frac{z^l}{l^n}, \tag{A.17}$$

and $\zeta(4) = \pi^4/90 = 1.082\cdots$. The specific heat $C = {\rm d}E/{\rm d}T$ has a discontinuity, $\Delta C/Nk_{\rm B} = 9\zeta(3)/\zeta(2) = 6.6$. The transition is of second order. It is well-known that for a free boson in a box the derivative of the specific heat is discontinuous and the transition is of 3rd order (see for instance, Ref. [5]).

Appendix B

Pseudopotential

In this appendix, we give some details of deriving the pseudopotential. The argument follows Refs. [5, 73].

We consider the two-body problem. Each particle has the mass, m, and an inter-particle potential, $v(\boldsymbol{r})$, is the "hard-sphere" one,

$$v(\boldsymbol{r}) = \begin{cases} 0 & (r > a) \\ \infty & (r \leq a), \end{cases} \tag{B.1}$$

where a is the hard-sphere diameter with $\boldsymbol{r}$ the relative position vector between two particles and $r = |\boldsymbol{r}|$. The Schrödinger equation in the center-of-mass system is

$$\frac{\hbar^2}{2\mu}\left(\Delta + k^2\right)\psi(\boldsymbol{r}) = v(\boldsymbol{r})\,\psi(\boldsymbol{r}), \tag{B.2}$$

where μ means the reduced mass,

$$\mu = m/2. \tag{B.3}$$

Obviously, $\psi(\boldsymbol{r})$ is the wavefunction in the center-of-mass coordinate system, and $(\hbar k)^2/(2\mu)$ is the energy of the relative motion. Substituting (B.1) into (B.2), we have

$$\begin{aligned} \left(\Delta + k^2\right)\psi(\boldsymbol{r}) &= 0 \quad (r > a), \\ \psi(\boldsymbol{r}) &= 0 \quad (r \leq a). \end{aligned} \tag{B.4}$$

In terms of the spherical coordinate,

$$\boldsymbol{r} = (r\sin\theta\cos\phi, r\sin\theta\sin\phi, r\cos\theta)\,, \tag{B.5}$$

the solution of Eq. (B.4) for $r > a$ can be written as

$$\psi(\boldsymbol{r}) = \sum_{l=0}^{\infty}\sum_{m=-l}^{+l} Y_{lm}(\theta,\phi)A_{lm}\left(j_l(kr) - \tan\eta_l\, n_l(kr)\right), \tag{B.6}$$

with the boundary condition,

$$\psi(\boldsymbol{r})|_{r=a} = 0. \tag{B.7}$$

Here $Y_{lm}(\theta,\phi)$ is a normalized spherical harmonic function, $j_l(x)$ and $n_l(x)$ the spherical Bessel and Neumann functions respectively, and A_{lm} and η_l constants. We note that the constant η_l is determined by the condition (B.7) as

$$\tan\eta_l = j_l(ka)/n_l(ka). \tag{B.8}$$

The scattering length a_l for the partial l-wave is defined by

$$a_l \equiv -\lim_{k\to 0}\tan\eta_l(k)/k. \tag{B.9}$$

In what follows, we assume that the energy of the relative motion $(\hbar k)^2/(2\mu)$ is sufficiently small, and thus we consider a spherically symmetric (s-wave) solution,

$$\psi(\boldsymbol{r}) = A\left(j_0(kr) - \tan\eta_0\, n_0(kr)\right), \tag{B.10}$$

where

$$\begin{aligned} j_0(x) &= \sin x/x, & \text{(B.11)}\\ n_0(x) &= -\cos x/x, & \text{(B.12)}\\ A &\equiv A_{00}/\sqrt{4\pi}. & \text{(B.13)} \end{aligned}$$

From (B.8), (B.11) and (B.12), we have

$$\tan\eta_0 = -\tan(ka), \tag{B.14}$$

leading to

$$\eta_0 = -ka. \tag{B.15}$$

Thus, a is identified with the s-wave scattering length.

An idea of the pseudopotential is as follows: we find an equation with some "potential" such that (B.10) is the solution everywhere. For sufficiently small x, $j_0(x)$ and $n_0(x)$ behave like

$$j_0(x)\approx 1, \quad n_0(x)\approx -1/x \quad (x\ll 1). \tag{B.16}$$

Thus, from (B.10), for sufficiently small kr, we get

$$r\psi(\boldsymbol{r}) = A\left(r + \frac{\tan\eta_0}{k}\right), \tag{B.17}$$

which gives

$$A = \frac{\partial}{\partial r}\left(r\psi(\boldsymbol{r})\right). \tag{B.18}$$

Remark that the relation (B.18) is used only at $\boldsymbol{r}=0$. Because $j_0(x)$ is regular at $x=0$, $j_0(kr)$ satisfies

$$(\Delta + k^2)j_0(kr) = 0, \tag{B.19}$$

for all r. On the other hand, $n_0(x)$ is singular at $x = 0$. Then, we calculate

$$F_0(r) \equiv (\Delta + k^2) n_0(kr), \tag{B.20}$$

with care. We integrate $F_0(r)$ over a sphere V of radius ϵ about the origin. From (B.20), we have

$$\int_V \mathrm{d}^3\boldsymbol{r}\, F_0(r) = \int_V \mathrm{d}^3\boldsymbol{r}\, \Delta n_0(kr) + k^2 \int_V \mathrm{d}^3\boldsymbol{r}\, n_0(kr). \tag{B.21}$$

By applying the divergence theorem to the first term in the right hand side of Eq. (B.21), we get

$$\begin{aligned} \int_V \mathrm{d}^3\boldsymbol{r}\, \Delta n_0(kr) &= \int_{\partial V} \mathrm{d}\boldsymbol{S} \cdot \nabla n_0(kr) \\ &= 4\pi\epsilon^2 \left. \frac{\partial}{\partial r} n_0(kr) \right|_{r=\epsilon} \\ &= 4\pi\epsilon \sin(k\epsilon) + \frac{4\pi}{k} \cos(k\epsilon). \end{aligned} \tag{B.22}$$

The second term in Eq. (B.21) gives

$$\begin{aligned} k^2 \int_V \mathrm{d}^3\boldsymbol{r}\, n_0(kr) &= 4\pi \int_0^\epsilon r^2 \mathrm{d}r \left(\frac{-\cos(kr)}{kr} \right) \\ &= -4\pi\epsilon \sin(k\epsilon) - \frac{4\pi}{k} \cos(k\epsilon) + \frac{4\pi}{k}. \end{aligned} \tag{B.23}$$

Substituting (B.22) and (B.23) into (B.21), we obtain

$$\int_V \mathrm{d}^3\boldsymbol{r}\, F_0(r) = \frac{4\pi}{k}. \tag{B.24}$$

Noting that $F_0(r)$ is identically equal to zero for $r \neq 0$, we conclude from (B.24) that

$$F_0(r) = (\Delta + k^2) n_0(kr) = \frac{4\pi}{k} \delta(\boldsymbol{r}). \tag{B.25}$$

Using (B.14), (B.18), (B.19) and (B.25) in Eq. (B.10), we have an equation that the solution (B.10) satisfies everywhere,

$$(\Delta + k^2)\psi(\boldsymbol{r}) = \frac{4\pi}{k} \tan(ka)\, \delta(\boldsymbol{r})\, \frac{\partial}{\partial r} \left(r\psi(\boldsymbol{r}) \right). \tag{B.26}$$

For sufficiently small ka, we can replace $\tan(ka)$ by ka. Then, by dividing the both sides of Eq. (B.26) by $\hbar^2/(2\mu)$, we finally arrive at

$$-\frac{\hbar^2}{2\mu} \Delta\psi(\boldsymbol{r}) + \tilde{v}(\boldsymbol{r})\, \psi(\boldsymbol{r}) = \frac{\hbar^2}{2\mu} k^2 \psi(\boldsymbol{r}), \tag{B.27}$$

where

$$\tilde{v}(\boldsymbol{r}) \equiv \frac{4\pi\hbar^2 a}{m} \delta(\boldsymbol{r})\, \frac{\partial}{\partial r} \left(r\, \cdot \right). \tag{B.28}$$

The operator $\tilde{v}(\boldsymbol{r})$ (B.28) is known as the pseudopotential [5, 73]. We note that $\partial/\partial r\,(r\,\cdot)$ appearing in (B.28) is not a hermitian operator. But, if $\psi(\boldsymbol{r})$ is well behaved, namely differentiable at the origin, we can replace $\partial/\partial r\,(r\,\cdot)$ by unity. So far, we have considered a to be positive. In general, however, the "diameter" of the hard-sphere a can be extended to be negative. This occurs when we may replace the low energy scattering from an attractive inter-particle potential of finite range by that from a hard-sphere one, known as the "shape-independent approximation."

Appendix C

The Ground State Energy under the Thomas-Fermi Approximations

We give some details of calculations of the ground state energy of the condensate under the one-, two- and three-dimensional Thomas-Fermi approximations.

First, we consider the one-dimensional case. We start from the one-dimensional Ginzburg-Pitaevskii-Gross equation [69]–[72] with a harmonic potential term,

$$-\frac{\hbar^2}{2m}\frac{\partial^2\Psi}{\partial x^2}+\frac{m}{2}\omega^2x^2\Psi+g|\Psi|^2\Psi=\mu\Psi. \tag{C.1}$$

Here and hereafter, $g(>0)$ means the strength of the inter-atomic interaction, and μ is the chemical potential. In the Thomas-Fermi approximation, the first term (the kinetic term) in the left hand side of Eq. (C.1) is neglected, which gives the number density of the condensate, $|\Psi|^2$, as

$$|\Psi|^2=\frac{1}{g}\left(\mu-\frac{1}{2}m\omega^2x^2\right). \tag{C.2}$$

By integrating the density (C.2) in the interval $[-x_0,x_0]$, where $x_0\equiv\sqrt{2\mu/(m\omega^2)}$, we get the number of the particles N,

$$N=\int_{-x_0}^{x_0}\mathrm{d}x|\Psi|^2=\frac{4}{3g}\left(\frac{2}{m\omega^2}\right)^{1/2}\mu^{3/2}, \tag{C.3}$$

leading to

$$\mu=\left(\frac{3gN}{4}\right)^{2/3}\left(\frac{m\omega^2}{2}\right)^{1/3}. \tag{C.4}$$

Substituting (C.4) into the thermodynamic identity,

$$\mu=\frac{\partial E}{\partial N}, \tag{C.5}$$

we have the energy, E_{1D}, given by

$$E_{\mathrm{1D}}=\frac{3}{5}\left(\frac{3g}{4}\right)^{2/3}\left(\frac{m\omega^2}{2}\right)^{1/3}N^{5/3}. \tag{C.6}$$

Next, we consider the two-dimensional case. The two-dimensional equation is

$$-\frac{\hbar^2}{2m}\left(\frac{\partial^2}{\partial x^2}+\frac{\partial^2}{\partial y^2}\right)\Psi+\frac{m}{2}(\omega_x^2x^2+\omega_y^2y^2)\Psi+g|\Psi|^2\Psi=\mu\Psi. \tag{C.7}$$

According to the Thomas-Fermi approximation, we ignore the kinetic energy terms in the left hand side of (C.7) and get

$$|\Psi|^2=\frac{1}{g}\left(\mu-\frac{1}{2}m\omega_x^2x^2-\frac{1}{2}m\omega_y^2y^2\right). \tag{C.8}$$

By integrating (C.8) in the region $\mu-\frac{1}{2}m\omega_x^2x^2-\frac{1}{2}m\omega_y^2y^2>0$, we have the number of particles N,

$$N=\int_{-x_0}^{x_0}\mathrm{d}x\int_{-y_0}^{y_0}\mathrm{d}y|\Psi|^2, \tag{C.9}$$

where x_0 and y_0 are defined as

$$x_0\equiv\left(\frac{2\mu}{m\omega_x^2}\right)^{1/2},\quad y_0\equiv\left(\frac{2}{m\omega_y^2}\right)^{1/2}\left(\mu-\frac{1}{2}m\omega_x^2x^2\right)^{1/2}. \tag{C.10}$$

Substituting (C.8) and (C.10) into (C.9), we have

$$N=\frac{4}{3g}\left(\frac{2}{m\omega_y^2}\right)^{1/2}\left(\frac{2}{m\omega_x^2}\right)^{1/2}\frac{3\pi}{8}\mu^2, \tag{C.11}$$

from which we get

$$\mu=\left(\frac{3gN}{4}\right)^{1/2}\left(\frac{m\omega_x^2}{2}\right)^{1/4}\left(\frac{m\omega_y^2}{2}\right)^{1/4}\left(\frac{8}{3\pi}\right)^{1/2}. \tag{C.12}$$

Using (C.12) in (C.5), we obtain the energy in the two-dimensional case, E_{2D},

$$E_{\mathrm{2D}}=\frac{2}{3}\left(\frac{8}{3\pi}\right)^{1/2}\left(\frac{3g}{4}\right)^{1/2}\left(\frac{m\omega_x^2}{2}\right)^{1/4}\left(\frac{m\omega_y^2}{2}\right)^{1/4}N^{3/2}. \tag{C.13}$$

Finally, we consider the three-dimensional case. The three-dimensional equation is

$$-\frac{\hbar^2}{2m}\left(\frac{\partial^2}{\partial x^2}+\frac{\partial^2}{\partial y^2}+\frac{\partial^2}{\partial z^2}\right)\Psi+\frac{m}{2}(\omega_x^2x^2+\omega_y^2y^2+\omega_z^2z^2)\Psi+g|\Psi|^2\Psi=\mu\Psi. \tag{C.14}$$

As in the previous cases, we approximate the number density of the condensate as

$$|\Psi|^2=\frac{1}{g}\left(\mu-\frac{1}{2}m\omega_x^2x^2-\frac{1}{2}m\omega_y^2y^2-\frac{1}{2}m\omega_z^2z^2\right). \tag{C.15}$$

The number of particles N is given by

$$N=\int_{-x_0}^{x_0}\mathrm{d}x\int_{-y_0}^{y_0}\mathrm{d}y\int_{-z_0}^{z_0}\mathrm{d}z|\Psi|^2, \tag{C.16}$$

where x_0, y_0 and z_0 are defined as

$$\begin{aligned} x_0 &\equiv \left(\frac{2\mu}{m\omega_x^2}\right)^{1/2}, \quad y_0 \equiv \left(\frac{2}{m\omega_y^2}\right)^{1/2}\left(\mu - \frac{1}{2}m\omega_x^2 x^2\right)^{1/2}, \\ z_0 &\equiv \left(\frac{2}{m\omega_z^2}\right)^{1/2}\left(\mu - \frac{1}{2}m\omega_x^2 x^2 - \frac{1}{2}m\omega_y^2 y^2\right)^{1/2}. \end{aligned} \tag{C.17}$$

Substituting (C.15) and (C.17) into (C.16), we obtain

$$N = \frac{8\pi}{15g}\left(\frac{2}{m\omega_z^2}\right)^{1/2}\left(\frac{2}{m\omega_y^2}\right)^{1/2}\left(\frac{2}{m\omega_x^2}\right)^{1/2}\mu^{5/2}, \tag{C.18}$$

which gives

$$\mu = \left(\frac{15g}{8\pi}\right)^{2/5}\left(\frac{m\omega_x^2}{2}\right)^{1/5}\left(\frac{m\omega_y^2}{2}\right)^{1/5}\left(\frac{m\omega_z^2}{2}\right)^{1/5}N^{2/5}. \tag{C.19}$$

From (C.5) and (C.19), we have the energy in the three-dimensional case, denoted by $E_{3\mathrm{D}}$,

$$E_{3\mathrm{D}} = \frac{5}{7}\left(\frac{15g}{8\pi}\right)^{2/5}\left(\frac{m\omega_x^2}{2}\right)^{1/5}\left(\frac{m\omega_y^2}{2}\right)^{1/5}\left(\frac{m\omega_z^2}{2}\right)^{1/5}N^{7/5}. \tag{C.20}$$

To summarize, the ground state energy in the Thomas-Fermi approximation for the d-dimensional Ginzburg-Pitaevskii-Gross equation with harmonic potential terms has the particle number dependence as

$$E_{d\mathrm{D}} \sim N^{(d+4)/(d+2)}. \tag{C.21}$$

This N-dependence can be used to identify the effective dimensionality of the condensate under the anisotropic magnetic traps in the strongly repulsive case.

Bibliography

[1] S. N. Bose, *Z. Phys.* **26**, 178 (1924).

[2] A. Einstein, *Sitzungsber. Kgl. Preuss. Akad. Wiss.* **1924**, 261 (1924).

[3] A. Einstein, *Sitzungsber. Kgl. Preuss. Akad. Wiss.* **1925**, 3 (1925).

[4] A. Griffin, D. W. Snoke and S. Stringari, Eds., *Bose-Einstein Condensation* (Cambridge University Press, Cambridge, 1995).

[5] K. Huang, *Statistical Mechanics* (John Wiley & Sons, Inc., New York, 1963).

[6] A. Pais, *Subtle is the Lord, The Science and the Life of Albert Einstein* (Clarendon Press, Oxford, 1982) p. 432.

[7] W. H. Keesom, *Helium* (Elsevier, New York, 1942).

[8] F. London, *Nature (London)* **141**, 643 (1938).

[9] J. L. Lin and J. P. Wolfe, *Phys. Rev. Lett.* **71**, 1222 (1993).

[10] S. Chu, L. Hollberg, J. E. Bjorkholm, A. Cable and A. Ashkin, *Phys. Rev. Lett.* **55**, 48 (1985).

[11] M. H. Anderson, J. R. Ensher, M. R. Matthews, C. E. Wieman and E. A. Cornell, *Science* **269**, 198 (1995).

[12] C. C. Bradley, C. A. Sackett, J. J. Tollett and R. G. Hulet, *Phys. Rev. Lett.* **75**, 1687 (1995); *ibid.* **79**, 1170 (1997).

[13] C. C. Bradley, C. A. Sackett and R. G. Hulet, *Phys. Rev. Lett.* **78**, 985 (1997).

[14] K. B. Davis, M.-O. Mewes, M. R. Andrews, N. J. van Druten, D. S. Durfee, D. M. Kurn and W. Ketterle, *Phys. Rev. Lett.* **75**, 3969 (1995).

[15] A. S. Parkins and D. F. Walls, *Phys. Rep.* **303**, 1 (1998).

[16] F. Dalfovo, S. Giorgini, L. P. Pitaevskii and S. Stringari, *Rev. Mod. Phys.* **71**, 463 (1999).

[17] E. A. Cornell, J. R. Ensher and C. E. Wieman, *preprint* (cond-mat/9903109).

[18] W. Ketterle, D. S. Durfee and D. M. Stamper-Kurn, *preprint* (cond-mat/9904034).

[19] M. Inguscio, S. Stringari and C. Wieman, Eds., *Bose-Einstein Condensation in Atomic Gases, Proceeding of the International School of Physics "Enrico Fermi"* (IOS Press, Amsterdam, 1999).

[20] D. G. Fried, T. C. Killian, L. Willmann, D. Landhuis, S. C. Moss, D. Kleppner and T. J. Greytak, *Phys. Rev. Lett.* **81**, 3811 (1998).

[21] D. J. Han, R. H. Wynar, Ph. Courteille and D. J. Heinzen, *Phys. Rev.* **A57**, R4114 (1998).

[22] U. Ernst, A. Marte, F. Schreck, J. Schuster and G. Rempe, *Europhys. Lett.* **41**, 1 (1998).

[23] T. Esslinger, I. Bloch and T. W. Hänsch, *Phys. Rev.* **A58**, R2664 (1998).

[24] L. V. Hau, B. D. Busch, C. Liu, Z. Dutton, M. M. Burns and J. A. Golovchenko, *Phys. Rev.* **A58**, R54 (1998).

[25] J. R. Gardner, R. A. Cline, J. D. Miller, D. J. Heinzen, H. M. J. M. Boesten and B. J. Verhaar, *Phys. Rev. Lett.* **74**, 3764 (1995).

[26] H. M. J. M. Boesten, C. C. Tsai, J. R. Gardner, D. J. Heinzen and B. J. Verhaar, *Phys. Rev.* **A55**, 636 (1997).

[27] E. Tiesinga, C. J. Williams, P. S. Julienne, K. M. Jones, P. D. Lett and W. D. Phillips, *J. Res. Natl. Inst. Stand. Technol.* **101**, 505 (1996).

[28] D. G. Friend and R. D. Etters, *J. Low Temp. Phys.* **39**, 409 (1980).

[29] E. R. I. Abraham, W. I. McAlexander, C. A. Sackett and R. G. Hulet, *Phys. Rev. Lett.* **74**, 1315 (1995).

[30] P. Nozières and D. Pines, *The Theory of Quantum Liquids* (Addison-Wesley, Redwood City, 1990) Vol. 2.

[31] P. A. Ruprecht, M. J. Holland, K. Burnett and M. Edwards, *Phys. Rev.* **A51**, 4704 (1995).

[32] A. L. Fetter, *preprint* (cond-mat/9510037).

[33] G. Baym and C. J. Pethick, *Phys. Rev. Lett.* **76**, 6 (1996).

[34] L. P. Pitaevskii, *Phys. Lett.* **A221**, 14 (1996).

[35] Y. Kagan, G. V. Shlyapnikov and J. T. M. Walraven, *Phys. Rev. Lett.* **76**, 2670 (1996).

[36] F. Dalfovo and S. Stringari, *Phys. Rev.* **A53**, 2477 (1996).

[37] R. J. Dodd, M. Edwards, C. J. Williams, C. W. Clark, M. J. Holland, P. A. Ruprecht and K. Burnett, *Phys. Rev.* **A54**, 661 (1996).

[38] E. V. Shuryak, *Phys. Rev.* **A54**, 3151 (1996).

[39] M. Houbiers and H. T. C. Stoof, *Phys. Rev.* **A54**, 5055 (1996).

[40] H. T. C. Stoof, *J. Stat. Phys.* **87**, 1353 (1997).

[41] T. Tsurumi and M. Wadati, *J. Phys. Soc. Jpn.* **66**, 3031 (1997).

[42] T. Tsurumi and M. Wadati, *J. Phys. Soc. Jpn.* **66**, 3035 (1997).

[43] M. Wadati and T. Tsurumi, *Phys. Lett.* **A247**, 287 (1998).

[44] M. Wadati and T. Tsurumi, *J. Phys. Soc. Jpn.* **68**, 3840 (1999).

[45] K. Watanabe, T. Mukai and T. Mukai, *Phys. Rev.* **A55**, 3639 (1997).

[46] T. Bergeman, *Phys. Rev.* **A55**, 3658 (1997).

[47] V. M. Pérez-García, H. Michinel, J. I. Cirac, M. Lewenstein and P. Zoller, *Phys. Rev.* **A56**, 1424 (1997).

[48] M. Ueda and A. J. Leggett, *Phys. Rev. Lett.* **80**, 1576 (1998).

[49] M. Ueda and K. Huang, *Phys. Rev.* **A60**, 3317 (1999).

[50] J. A. Freire and D. P. Arovas, *Phys. Rev.* **A59**, 1461 (1999).

[51] Y. E. Kim and A. L. Zubarev, *Phys. Lett.* **A246**, 389 (1998).

[52] C. J. Myatt, E. A. Burt, R. W. Ghrist, E. A. Cornell and C. E. Wieman, *Phys. Rev. Lett.* **78**, 586 (1997).

[53] M. R. Matthews, D. S. Hall, D. S. Jin, J. R. Ensher, C. E. Wieman, E. A. Cornell, F. Dalfovo, C. Minniti and S. Stringari, *Phys. Rev. Lett.* **81**, 243 (1998).

[54] D. S. Hall, M. R. Matthews, J. R. Ensher, C. E. Wieman and E. A. Cornell, *Phys. Rev. Lett.* **81**, 1539 (1998).

[55] T.-L. Ho and V. B. Shenoy, *Phys. Rev. Lett.* **77**, 3276 (1996).

[56] B. D. Esry, C. H. Greene, J. P. Burke, Jr. and J. L. Bohn, *Phys. Rev. Lett.* **78**, 3594 (1997).

[57] Th. Busch, J. I. Cirac, V. M. Pérez-García and P. Zoller, *Phys. Rev.* **A56**, 2978 (1997).

[58] H. Pu and N. P. Bigelow, *Phys. Rev. Lett.* **80**, 1130 (1998); *ibid.* **80**, 1134 (1998).

[59] E. Timmermans, *Phys. Rev. Lett.* **81**, 5718 (1998).

[60] H. Morise, T. Tsurumi and M. Wadati, *J. Phys. Soc. Jpn.* **68**, 1871 (1999).

[61] D. M. Stamper-Kurn, M. R. Andrews, A. P. Chikkatur, S. Inouye, H.-J. Miesner, J. Stenger and W. Ketterle, *Phys. Rev. Lett.* **80**, 2027 (1998).

[62] J. Stenger, S. Inouye, D. M. Stamper-Kurn, H.-J. Miesner, A. P. Chikkatur and W. Ketterle, *Nature* **396**, 345 (1998).

[63] H.-J. Miesner, D. M. Stamper-Kurn, J. Stenger, S. Inouye, A. P. Chikkatur and W. Ketterle, *Phys. Rev. Lett.* **82**, 2228 (1999).

[64] T.-L. Ho, *Phys. Rev. Lett.* **81**, 742 (1998).

[65] T. Ohmi and K. Machida, *J. Phys. Soc. Jpn.* **67**, 1822 (1998).

[66] C. K. Law, H. Pu and N. P. Bigelow, *Phys. Rev. Lett.* **81**, 5257 (1998).

[67] T. Isoshima, K. Machida and T. Ohmi, *Phys. Rev.* **A60**, 4857 (1999).

[68] S.-K. Yip, *Phys. Rev. Lett.* **83**, 4677 (1999).

[69] V. L. Ginzburg and L. P. Pitaevskii, *Sov. Phys. JETP* **7**, 858 (1958).

[70] L. P. Pitaevskii, *Sov. Phys. JETP* **13**, 451 (1961).

[71] E. P. Gross, *Nuovo Cimento* **20**, 454 (1961).

[72] E. P. Gross, *J. Math. Phys.* **4**, 195 (1963).

[73] K. Huang and C. N. Yang, *Phys. Rev.* **105**, 767 (1957).

[74] V. E. Zakharov and A. B. Shabat, *Sov. Phys. JETP* **34**, 62 (1972).

[75] M. J. Ablowitz and H. Segur, *Solitons and the Inverse Scattering Transform* (SIAM, Philadelphia, 1981).

[76] T. Tsurumi and M. Wadati, *J. Phys. Soc. Jpn.* **68**, 1531 (1999).

[77] V. E. Zakharov, *Sov. Phys. JETP* **35**, 908 (1972).

[78] V. E. Zakharov and V. S. Synakh, *Sov. Phys. JETP* **41**, 465 (1975).

[79] R. T. Glassey, *J. Math. Phys.* **18**, 1794 (1977).

[80] M. I. Weinstein, *Commun. Math. Phys.* **87**, 567 (1983).

[81] E. A. Kuznetsov, A. M. Rubenchik and V. E. Zakharov, *Phys. Rep.* **142**, 103 (1986).

[82] S. K. Turitsyn, *Phys. Rev.* **E47**, R13 (1993).

[83] E. A. Kuznetsov, J. J. Rasmussen, K. Rypdal and S. K. Turitsyn, *Physica* **D87**, 273 (1995).

[84] P. M. Lushnikov, *JETP Lett.* **62**, 461 (1995).

[85] L. Bergé, *Phys. Rep.* **303**, 259 (1998).

[86] C. Sulem and P.-L. Sulem, *The Nonlinear Schrödinger Equation* (*Applied Mathematical Sciences* Vol. 139) (Springer-Verlag, New York, 1999).

[87] T. Tsurumi and M. Wadati, *J. Phys. Soc. Jpn.* **67**, 1197 (1998).

[88] S. Inouye, M. R. Andrews, J. Stenger, H.-J. Miesner, D. M. Stamper-Kurn and W. Ketterle, *Nature* **392**, 151 (1998).

[89] J. Stenger, S. Inouye, M. R. Andrews, H.-J. Miesner, D. M. Stamper-Kurn and W. Ketterle, *Phys. Rev. Lett.* **82**, 2422 (1999).

[90] F. Shimizu, *Mater. Sci. Eng.* **B48**, 7 (1997).

[91] O. Zobay, E. V. Goldstein and P. Meystre, *Phys. Rev.* **A60**, 3999 (1999).

[92] A. Lenef, T. D. Hammond, E. T. Smith, M. S. Chapman, R. A. Rubenstein and D. E. Pritchard, *Phys. Rev. Lett.* **78**, 760 (1997).

[93] M.-O. Mewes, M. R. Andrews, D. M. Kurn, D. S. Durfee, C. G. Townsend and W. Ketterle, *Phys. Rev. Lett.* **78**, 582 (1997).

[94] I. Bloch, T. W. Hänsch and T. Esslinger, *Phys. Rev. Lett.* **82**, 3008 (1999).

[95] E. W. Hagley, L. Deng, M. Kozuma, J. Wen, K. Helmerson, S. L. Rolston and W. D. Phillips, *Science* **283**, 1706 (1999).

[96] S. R. de Groot, G. J. Hooyman and C. A. ten Seldam, *Proc. Roy. Soc. (London)* **A203**, 266 (1950).

Table and Figure Captions

Table 1.1 Experimental values of parameters. a; s-wave scattering length, $T_{\rm c}$; critical temperature, $N_{\rm t}$; the total number of atoms in trap, ω; trap frequency. Note that the total number of the atoms is the sum of normal and condensed ones. The values of $T_{\rm c}$, $N_{\rm t}$ and ω are taken from the reference in the right most column.

Fig. 3.1.1 Approximations for the repulsive inter-atomic interaction: I. weak interaction case (3.1.24), II. strong interaction case (3.1.31), III. intermediate case-1 (3.1.40), IV. intermediate case-2 (3.1.52). The abscissa and ordinate represent the anisotropy of the trap, δ, and the strength of the interaction, $G_\perp$, respectively.

Fig. 3.2.1 Stability of the two-component condensate: $N_1 = N_2$ case for (a) $\alpha > 0$, (b) $\alpha < 0$. The boundaries of stable and unstable regions (the solid lines) are determined by Eqs. (3.2.9) and (3.2.10). The dashed lines are discussed in 3.2.4.

Fig. 3.2.2 Phase diagram for $\alpha_{11} = \alpha_{22} \equiv \alpha > 0$ and $\alpha_{12} < -\alpha$.

Fig. 3.2.3 Phase diagram for $\alpha_{11} = \alpha_{22} \equiv \alpha < 0$. (a) $\alpha_{12} > 0$, (b) $\alpha < \alpha_{12} < 0$, (c) $\alpha_{12} < \alpha < 0$.

Fig. 3.2.4 Function $\gamma(\beta)$ defined in (3.2.35). We set $\alpha_{11} : \alpha_{22} : \alpha_{12} = 1 : -4 : 2^{-\frac{3}{2}}$.

Fig. 3.2.5 $\lim_{N_1 \to \infty} f(N_1)/N_1$ as a function of $2^{\frac{5}{2}}\alpha_{12}/\alpha_{11}$. We set $\alpha_{11} : \alpha_{22} = 1 : -4$.

Fig. 3.2.6 Phase diagram for $\alpha_{11} > 0$ and $\alpha_{22} < 0$. (a) $\alpha_{12} > 2^{-\frac{5}{2}}\alpha_{11}$, (b) $0 < \alpha_{12} < 2^{-\frac{5}{2}}\alpha_{11}$, (c) $\alpha_{12} < 0$.

Fig. 4.2.1 $N_{\rm c,new}/N_0$ as a function of k for the case that $\delta = 0.718$ [12].

atom	a [m]	$T_{\rm c}$ [K]	$N_{\rm t}$	ω [Hz]	Reference
^{1}H	7.2×10^{-11}	5×10^{-5}	2×10^{10}	$\omega_x = 2\pi \times 3.90 \times 10^3$, $\omega_y = 2\pi \times 3.90 \times 10^3$, $\omega_z = 2\pi \times 10.2$	[20]
^{7}Li	-1.44×10^{-9}	3×10^{-7}	1×10^5	$\omega_x = 2\pi \times 150.6$, $\omega_y = 2\pi \times 152.6$, $\omega_z = 2\pi \times 131.5$	[13]
^{23}Na	2.75×10^{-9}	2×10^{-6}	7×10^5	$\omega_x = 2\pi \times 745$, $\omega_y = 2\pi \times 235$, $\omega_z = 2\pi \times 410$	[14]
^{87}Rb	5.77×10^{-9}	1.7×10^{-7}	2×10^4	$\omega_x = 2\pi \times 120/\sqrt{8}$, $\omega_y = 2\pi \times 120/\sqrt{8}$, $\omega_z = 2\pi \times 120$	[11]
^{87}Rb	5.77×10^{-9}	4.3×10^{-7}	1.5×10^6	$\omega_x = 2\pi \times 64$, $\omega_y = 2\pi \times 64$, $\omega_z = 2\pi \times 181$	[21]
^{87}Rb	5.77×10^{-9}	5.5×10^{-7}	1×10^6	$\omega_x = 2\pi \times 280$, $\omega_y = 2\pi \times 280$, $\omega_z = 2\pi \times 24$	[22]
^{87}Rb	5.77×10^{-9}	5×10^{-7}	5×10^5	$\omega_x = 2\pi \times 20$, $\omega_y = 2\pi \times 200$, $\omega_z = 2\pi \times 200$	[23]

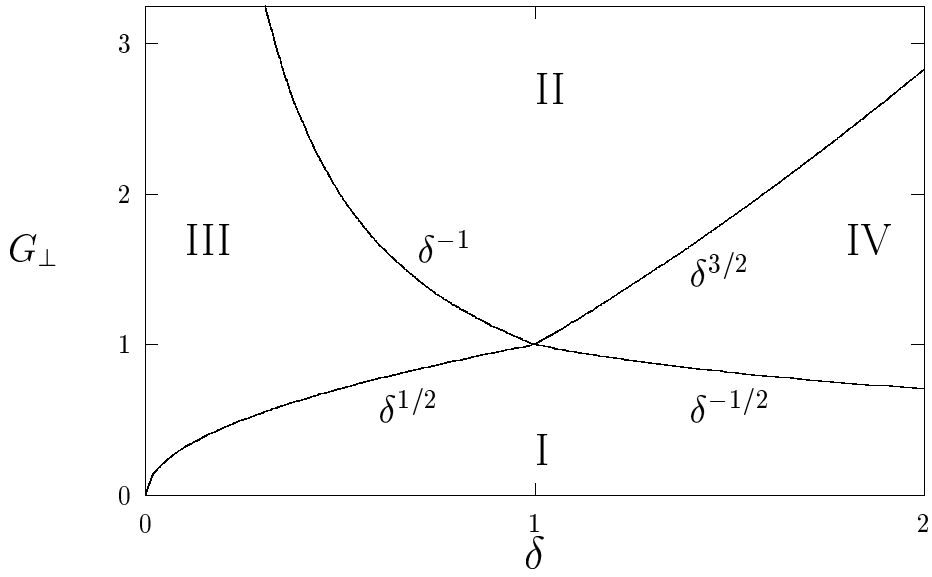
$G_\perp$
3
2
1
0
0
1
2
δ
II
III
IV
I
δ^{-1}
$\delta^{3/2}$
$\delta^{1/2}$
$\delta^{-1/2}$

This figure "fig3_2_1.gif" is available in "gif" format from:

http://arXiv.org/ps/cond-mat/9912470v1

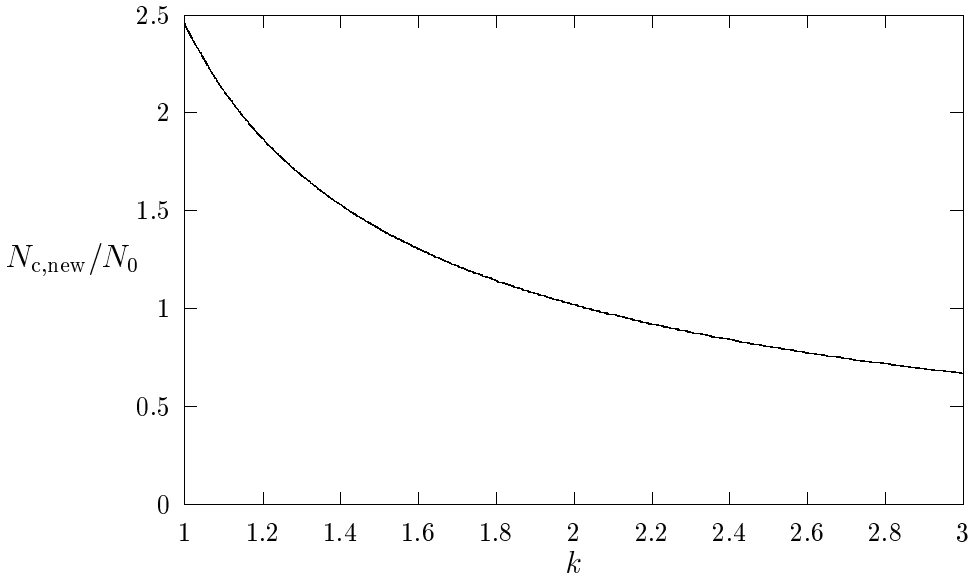
2.5
2
1.5
$N_{\mathrm{c,new}}/N_0$
1
0.5
0
1
1.2
1.4
1.6
1.8
2
2.2
2.4
2.6
2.8
3
k

This figure "fig3_2_2.gif" is available in "gif" format from:

http://arXiv.org/ps/cond-mat/9912470v1

This figure "fig3_2_3a.gif" is available in "gif" format from:

http://arXiv.org/ps/cond-mat/9912470v1

This figure "fig3_2_3b.gif" is available in "gif" format from:
http://arXiv.org/ps/cond-mat/9912470v1

This figure "fig3_2_3c.gif" is available in "gif" format from:

http://arXiv.org/ps/cond-mat/9912470v1

This figure "fig3_2_4.gif" is available in "gif" format from:

http://arXiv.org/ps/cond-mat/9912470v1

This figure "fig3_2_5.gif" is available in "gif" format from:

http://arXiv.org/ps/cond-mat/9912470v1

This figure "fig3_2_6a.gif" is available in "gif" format from:
http://arXiv.org/ps/cond-mat/9912470v1

This figure "fig3_2_6b.gif" is available in "gif" format from:
http://arXiv.org/ps/cond-mat/9912470v1

This figure "fig3_2_6c.gif" is available in "gif" format from:

http://arXiv.org/ps/cond-mat/9912470v1